USING ENZYME STRUCTURE-ENVIRONMENT-ACTIVITY RELATIONSHIPS TO ENHANCE BIOCATALYST UTILITY

by

Joel L. Kaar

B.S. Chemical Engineering, University of Pittsburgh, 2001

Submitted to the Graduate Faculty of

the School of Engineering in partial fulfillment

of the requirements for the degree of

Doctor of Philosophy

University of Pittsburgh

2007

UNIVERSITY OF PITTSBURGH

SCHOOL OF ENGINEERING

This dissertation was presented

by

Joel L. Kaar

It was defended on

September 11th, 2007

and approved by

Dr. Mohammad M. Ataai, Professor, Departments of Chemical Engineering and Bioengineering

Dr. Eric J. Beckman, Professor, Department of Chemical Engineering

Dr. Harry C. Blair, Professor, Departments of Pathology and Physiology and Cell Biology

Dr. Johnny Huard, Professor, Departments of Orthopaedic Surgery and Bioengineering

Dissertation Director: Dr. Alan J. Russell, Professor, Departments of Surgery and Chemical Engineering

USING ENZYME STRUCTURE-ENVIRONMENT-ACTIVITY RELATIONSHIPS TO ENHANCE BIOCATALYST UTILITY

Joel L. Kaar, PhD

University of Pittsburgh, 2007

The overall objective of this work was to probe the fundamental relationship between enzyme structure, environment, and activity. These relationships were in turn exploited as the basis for developing effective strategies for stabilizing and thus improving the efficiency of biocatalysts.

Initially, the utility of ionic liquids, which represent an environmentally green alternative to conventional solvents, as reaction media for anhydrous enzymatic reactions was explored. Solvatochromic and partition coefficient analysis suggest that ionic liquids are considerably more polar and hydrophilic than organic solvents. In model transesterification reactions, the enzyme lipase was found to be highly active in 1-butyl-3-methylimidazolium hexafluorophosphate, but inactive in more hydrophilic ionic liquids. Conventional approaches to preventing deactivating conformational changes in non-aqueous environments were ineffective in improving lipase activity in ionic liquids. Moreover, stability studies indicated that lipase are significantly more stable in ionic liquids compared to in organic solvents.

To effectively control the pH of essential enzyme-bound water molecules, which is critical even in anhydrous enzymology, a novel buffering approach was developed. This approach was based on the hypothesis that simultaneous biocatalytic reactions that produce acid and base will create a dynamic pH equilibrium. The concept of biocatalytic pH control was successfully demonstrated by employing urease-catalyzed urea hydrolysis, which forms

ammonia, to neutralize acid produced by the enzymatic degradation of organophosphorous toxins. Based on the pH-dependent activity profiles of the enzymes, the pH of the combined enzyme system is predictable and can be controlled by adjusting the relative ratio of enzyme activities.

Lastly, poly(ethylene glycol)-modification was investigated as a method of enhancing the stability of therapeutic proteases in *in vivo* settings. Matrix metalloproteinase-1 (MMP-1), which has considerable therapeutic potential in the treatment of fibrotic conditions, was employed as a model protease for these studies. Comparison of the efficacy of native full-length enzyme, the truncated active enzyme, and a poly(ethylene glycol)-modified form of the truncated active enzyme in a laceration model in mice showed that the truncated active enzyme produced the greatest reduction in interfibrillar collagen. Structural characterization of the modified enzyme suggests that site-specific modification are key to retaining activity and to improving the enzyme's stability.

DESCRIPTORS

Biocatalytic buffering

Bioremediation

Diisopropylfluorophosphatase

Green chemistry

Ionic liquids

Lipase

Matrix metalloproteinase-1

Muscle fibrosis

Nerve agents

Nonaqueous enzymology

Organophosphorous hydrolase

PEGylation

Transesterification

Urease

TABLE OF CONTENTS

LIST OF TABLES XII

LIST OF FIGURES XIII

NOMENCLATURE XVIII

PREFACE XIX

1.0 INTRODUCTION 1

2.0 BACKGROUND AND LITERATURE REVIEW 6

2.1 ANHYDROUS ENZYMOLOGY 6

2.1.1 Enzyme Structure in Anhydrous Solvents 7

2.1.2 Influence of Water on Enzyme Activity 8

2.1.3 Solvent Types 9

2.2 EFFECT OF pH ON ENZYME ACTIVITY AND STABILITY 12

2.3 PROTEASE STABILITY 15

2.4 STRATEGIES FOR ENZYME STABILIZATION 16

2.4.1 Chemical Additives 16

2.4.2 Chemical Modification 19

2.4.3 Immobilization 23

2.4.4 Protein Engineering 28

2.4.5 Directed Evolution 30

3.0 SPECIFIC AIMS 32
4.0 CHARACTERIZATION OF ENZYME ACTIVITY AND STABILITY IN IONIC LIQUIDS 35
4.1 INTRODUCTION 35
4.2 MATERIALS AND METHODS 38
4.2.1 Materials 38
4.2.2 Methods 39
4.2.2.1 Determination of Octanol-Water Partition Coefficients 39
4.2.2.2 Solvatochromic Characterization 40
4.2.2.3 Poly(Ethylene Glycol)-Modified Lipase Synthesis 41
4.2.2.4 Lipase-Containing Polyurethane Foam Synthesis 41
4.2.2.5 Lipase Stability in Ionic Liquids 41
4.2.2.6 Water Activity Measurements in Ionic Liquids Using Humidity Sensor 42
4.2.2.7 Water Transfer Measurements in Ionic Liquids 42
4.2.2.8 Lipase-Catalyzed Transesterification of Methyl Methacrylate and 2-Ethylhexanol 43
4.3 RESULTS AND DISCUSSION 44
4.3.1 Physical Characterization of Ionic Liquids 44
4.3.2 Lipase Activity in Ionic Liquids 48
4.3.3 Use of Modified and Immobilized Lipases in Ionic Liquids 51
4.3.4 Lipase Stability in Ionic Liquids 53
4.3.5 Controlled Water Activity in Ionic Liquids 56

4.3.6 Impact of Water Activity on Lipase Activity in Ionic Liquids 61
4.4 CONCLUSIONS 64
5.0 BIOCATALYTIC pH CONTROL IN ENZYMATIC REACTIONS 65
5.1 INTRODUCTION 65
5.2 THEORETICAL MODELING OF DYNAMIC pH EQUILIBRIUM IN OPH-UREASE COMBINED ENZYME SYSTEM 69
5.3 MATERIALS AND METHODS 71
5.3.1 Materials 71
5.3.2 Methods 72
5.3.2.1 OPH Activity Assay 72
5.3.2.2 Urease Activity Assay 72
5.3.2.3 Preparation of *Helicobacter Pylori* Urease 73
5.3.2.4 Fluoride Inactivation of Ureases 73
5.3.2.5 Use of Cationic Scavengers to Prevent Fluoride Inactivation of Urease 74
5.3.2.6 ADA Activity Assay 74
5.3.2.7 Measurement of Nerve Agent Conversion and pH in Dynamic pH Controlled Reactions 75
5.4 RESULTS AND DISCUSSION 76
5.4.1 Characterization of pH Buffering in OPH-Urease System and Experimental Validation of Predictive Model 76
5.4.2 Effect of Fluoride on Urease Activity 83
5.4.3 Solution to the Fluoride Problem 88

5.4.3.1 Impact of Urease Activity on Fluoride Inactivation of OPH-Urease Buffer 89
5.4.3.2 Cationic Fluoride Scavengers 91
5.4.3.3 Alternative Base-Producing Biocatalytic Reaction 93
5.5 CONCLUSIONS 98
6.0 REDUCING SCARRING IN LACERATED SKELETAL MUSCLE USING MATRIX METALLOPROTEINASE-1 99
6.1 INTRODUCTION 99
6.2 MATERIALS AND METHODS 102
6.2.1 Materials 102
6.2.2 Methods 102
6.2.2.1 PEGylation of rhMMP-1 102
6.2.2.2 Muscle Laceration Model 103
6.2.2.3 Histological Analysis 105
6.2.2.4 MMP-1 Activity Assay Using Thioester Substrate 107
6.2.2.5 Collagen Degradation Assay 108
6.2.2.6 Stability of Native and PEG-Modified rhMMP-1 108
6.2.2.7 Computation of Solvent Accessibilities of Lysines 108
6.2.2.8 Computation of Lysine pKa Values 109
6.2.2.9 SDS-PAGE of Native and PEG-Modified rhMMP-1 109
6.2.2.10 Matrix Assisted Laser Desorption/Ionization Time-of-Flight (MALDI-TOF) Mass Spectrometry 109

6.2.2.11 Analytical Ultracentrifugation Analysis of Native and PEG-Modified rhMMP-1 111
6.3 RESULTS AND DISCUSSION 111
6.3.1 Rapid Assessment of Potential Therapuetic Efficacy of proMMP-1, rhMMP-1, and PEG-rhMMP-1 in Laceration Model 111
6.3.2 Quantitative Comparison of Efficacies of Native and PEG-Modified rhMMP-1 in Reducing Muscle Scarring in Laceration Model 114
6.3.3 Effect of PEGylation on rhMMP-1 *In Vitro* Activity and Stability 118
6.3.4 Prediction of Reactivity of Modification Sites in rhMMP-1 122
6.4 CONCLUSIONS 130
APPENDIX 132
BIBLIOGRAPHY 135

LIST OF TABLES

Table 1. Log *P* and Reichardt's dye (E^N_T) polarity values for ionic liquids and select organic solvents. 46

Table 2. Initial rates of lipase-catalyzed transesterification of methyl methacrylate and 2-ethylhexanol in ionic liquids and organic solvents. All initial rates are reported in the units μM/hr/mg-enzyme. 50

Table 3. Water activities of [bmim][PF_6] containing salt hydrates at 25 °C measured using a humidity sensor. The values were compared to the water activity of salt hydrates in organic solvents, which were compiled from the literature. 58

Table 4. Kinetic parameters for native and PEG-modified rhMMP-1 catalyzed degradation of thioester peptide substrate. 118

Table 5. Theoretical pKa and solvent accessibility values of the N-terminal α-amino group and lysines in rhMMP-1. The residue number corresponds to that of the residue in the sequence of full-length proMMP-1 125

LIST OF FIGURES

Figure 1. Michaelis-Menten mechanism showing potential ionization steps.[44] 13

Figure 2. Enzyme stabilization by specific additive. The ligand binds specifically to the native conformation of the enzyme, thereby forcing the equilibrium of enzyme folding to favor the catalytically active native state. In the enzyme structure, the diamond-shaped binding pocket represents the active site. 17

Figure 3. Enzyme immobilization techniques: (A) entrapment, (B) adsorption, (C) conventional covalent immobilization, and (D) multipoint covalent immobilization into polymeric network. The blue spheres represent enzyme molecules. 24

Figure 4. Structure of ionic liquids. Anions available for X_1^- were hexafluorophosphate ($[PF_6]$), acetate ($[CH_3CO_2]$), nitrate ($[NO_3]$) and trifluoroacetate ($[CF_3CO_2]$). Anions available for X_2^- were hexafluorophosphate ($[PF_6]$), acetate ($[CH_3CO_2]$), nitrate ($[NO_3]$), trifluoroacetate ($[CF_3CO_2]$), trifluoromethylsulfonate ($[CF_3SO_3]$) and methanesulfonate ($[CH_3SO_3]$). 37

Figure 5. Lipase-catalyzed transesterification of methyl methacrylate and 2-ethylhexanol to 2-ethylhexyl methacrylate. 38

Figure 6. Reichardt's dye (2,6-diphenyl-4-(2,4,6-triphenylpyridinio)phenolate)..... 40

Figure 7. Solvatochromic probing of organic solvents (from left: tetrahydrofuran, acetonitrile, methanol, t-amyl alcohol and acetone) with Reichardt's dye. Differences in solvent polarity alter the absorption energy of the dye. These differences are reflected by the visible color of the dye-containing solutions. 47

Figure 8. Stability of Novozym 435 in ionic liquids ($[bmim][PF_6]$ (◇), $[bmim][NO_3]$ (□), $[bmim][CH_3CO_2]$ (Δ), $[mmep][NO_3]$ (■), $[mmep][CH_3CO_2]$ (▲) and $[mmep][CH_3SO_3]$ (●)). Error bars represent the standard deviation for two separate experiments. 55

Figure 9. Stability of Novozym 435 in organic solvents (butanol (◇), tetrahydrofuran (□), acetonitrile (▲), dimethyl sulfoxide (■) and hexane (◆)). Error bars represent the standard deviation for two separate experiments. 56

Figure 10. Progress curves for the transfer of water from salt hydrate pairs (Na_2HPO_4 12/7 (▲), Na_2HPO_4 7/2 (■), NaAc 3/0 (●), Na_2HPO_4 2/0 (Δ), $Na_4P_2O_7$ 10/0 (○), $CuSO_4$ 5/3 (□)) to [bmim][PF_6]. 60

Figure 11. Solubility of water at 25 °C in [bmim][PF_6] that contained salt hydrates (▲) and that was pre-equilibrated with saturated salt solutions in presence of substrates (methyl methacrylate (Δ), 2-ethylhexanol (◇)). Experimentally measured water solubilities were compared to data from the literature (●). 61

Figure 12. Initial rates of lipase-catalyzed transesterification of methyl methacrylate and 2-ethylhexanol in [bmim][PF_6] (○) and hexane (●) at fixed a_w. In dry* incubations, crushed molecular sieves were employed in place of salt hydrates in order to remove residual water from the solvent. 63

Figure 13. The pH dependence curves of two enzyme-catalyzed reactions depicting the concept of biocatlaytic pH control. The base-producing enzyme (black line) has a lower optimal pH than the acid-producing enzyme (gray line). When both enzymes are present, the pH should stabilize at the intersection point, which is termed the pH set-point..... 67

Figure 14. (A) OPH-catalyzed hydrolysis of paraoxon and (B) urease-catalyzed hydrolysis of urea at neutral pH. 69

Figure 15. pH-Dependence of (A) urease (jack bean) activity and (B) the kinetic parameters k_{cat} (◆) and K_M (■) for paraoxon hydrolysis by OPH. Error bars are representative of standard deviations from the mean. 77

Figure 16. Dynamic pH buffer created by the simultaneous biocatalytic hydrolysis of paraoxon and urea. The solid line and closed circles represent the measured pH and paraoxon conversion profile respectively in the presence of urease (jack bean) and urea. The dotted and dash-dotted lines correspond to the model predicted pH and paraoxon conversion profile also in the presence of urease and urea. The dashed line and closed diamonds refer to the measured pH and paraoxon conversion profile in the absence of urease. The pH set-point remained constant as long as the ratio of activities of the enzymes was unchanged (A) [urease] = 0.081 units/mL and [OPH] = 0.0026 units/mL ([urease]/[OPH] = 31) (B) [urease] = 0.49 units/mL and [OPH] = 0.016 units/mL ([urease]/[OPH] = 31). 79

Figure 17. pH Buffering of paraoxon hydrolysis by OPH employing a ratio of jack bean urease-to-OPH activities of 0.54. The actual activities of urease and OPH were 0.0025 U/mL and 0.0047 U/mL respectively, resulting in a pH set-point of 7.20. The solid line and closed circles represent the measured pH and paraoxon conversion profile respectively in the presence of urease and urea. 81

Figure 18. pH Buffering of paraoxon hydrolysis by OPH employing a ratio of jack bean urease-to-OPH activities of 0.30. The actual activities of urease and OPH were 0.0014 U/mL and 0.0048 U/mL respectively, resulting in a pH set-point of 6.71. The solid line and closed circles represent the measured pH and paraoxon conversion profile respectively in the presence of urease and urea. 82

Figure 19. The impact of the ratio of jack bean urease-to-OPH activities on the pH set-point in the combined enzyme system. 83

Figure 20. Chemical structures of organophosphate compounds that are degraded by hydrolysis of a P-F bond. 84

Figure 21. Mechanism of fluoride inhibition of urease. E and E* represent enzyme and a form of the enzyme that is missing a critical active site water molecule. Only E* can bind fluoride. 85

Figure 22. Fluoride inhibition of (A) jack bean urease, (B) *H. pylori* urease, (C) Roche liquid stable, industrial jack bean urease, and (D) *K. aerogenes* 9-1 mutant urease. The activity of the ureases in the presence of various concentrations of fluoride (denoted by the numbers in millimolar) was monitored by progress curves. 87

Figure 23. Simultaneous biocatalytic hydrolysis of DFP (0.5 mM) and urea by OPH and urease (*K. aerogenes* urease 9-1 mutant). The actual activities of urease and OPH were (A) [urease] = 0.15 units/mL and [OPH] = 0.1 μg/mL and (B) [urease] = 0.5 units/mL and [OPH] = 0.1 μg/mL. The solid line and closed circles represent the measured pH and conversion of DFP as a function of relative butyrlcholinesterase inhibition respectively. 90

Figure 24. Protection of *K. aerogenes* urease mutant (9-1) from fluoride inactivation by the addition of (A) calcium chloride, (B) lanthanum nitrate, and (C) nickel chloride. Urease activity was monitored by progress curves in the presence of various concentrations of the cationic fluoride scavengers. For each assay, the concentrations of fluoride and cationic scavenger are inidicated as the top and bottom concentrations respectively. 93

Figure 25. ADA-catalyzed hydrolysis of adenosine. 94

Figure 26. (A) pH-Dependence of ADA activity. (B) The effect of fluoride ions on ADA activity..... 95

Figure 27. Simultaneous biocatalytic hydrolysis of DFP (5mM) and adenosine by OPH and ADA. The actual activities of adenosine deaminase and OPH were 0.2 units/mL and 0.4 units/mL respectively. The solid line and closed circles represent the measured pH and DFP conversion profile respectively. 97

Figure 28. Specific activity of proMMP-1 upon activation of the full-length enzyme with varying mass ratios of trypsin-to-enzyme. When fully activated, proMMP-1 had a specific activity of 0.0047 units/μg-enzyme when assayed with a thioester substrate. 104

Figure 29. Histological analysis of muscle adjacent to the laceration site 14 d after treatment. (A) Images of tissue stained with picrosirius red acquired with a 4x objective. (B) Comparison of interfibrillar collagen in control and treatment groups ($* p < 0.05$). The boxed areas represent the fields in which the amount of connective collagen was quantified. Error bars represent the standard deviation from the mean for each treatment group. 113

Figure 30. (A) Brightfield image of blue tissue marking dye at laceration site acquired with 100x objective. The arrows indicate the presence of hemosiderin, the brown pigment, at the site of injury. (B) Fluorescent image of the equivalent field showing co-localization of green fluorescent microspheres with the tissue marking dye at the laceration site. The arrows point to examples of individual microspheres in the captured field. (C) Control image showing the size of the green fluorescent microspheres prepared on a blank glass slide at the same magnification. 115

Figure 31. Results of histological analysis from follow-up *in vivo* study at 11 d post-treatment of lacerated GMs with rhMMP-1 (0.8 mU) or PEG-rhMMP-1 (0.8 mU). (A) Images of unstained sections showing tissue marking dye at site of laceration and matching area in Masson's trichrome stained specimens (10x objective). (B) Selected fields from Masson's trichrome stained specimens used for quantification of interfibrillar collagen and below, corresponding thresholded areas. (C) Comparison of interfibrillar collagen in the left and right GMs of mice within the same treatment group ($* p < 0.05$). The level of fibrosis in the GMs of mice treated with buffer only and in the GM of uninjured mice are also shown. Error bars represent the standard deviation from the mean for each treatment group. 117

Figure 32. Degradation of lyophilized type I collagen scaffolds by native rhMMP-1 (▲), PEG-rhMMP-1 (■), and buffer (◆). Error bars represent the standard deviation from the mean for three separate experiments. 119

Figure 33. Thermostability of native (●) and PEGylated rhMMP-1 (■) at 65 °C. The stability of rhMMP-1 in the presence of 10 % (w/v) fully hydrolyzed PEG-SPA (M_w 5000) was also measured (○). Error bars represent the standard deviation from the mean for two separate experiments. 121

Figure 34. (A) Stability of native and PEGylated rhMMP-1 in the presence of trypsin at 50 °C. Native rhMMP-1 (closed symbols) and PEG-rhMMP-1 (open symbols) were incubated with varying amounts of trypsin (0.0 mg/mL (squares), 0.1 mg/mL (diamonds), 0.5 mg/mL (triangles), 1.0 mg/mL (circles)). (B) Stability of native and PEGylated rhMMP-1 in the presence of subtilisin Carlsberg at 37 °C. Native rhMMP-1 (closed symbols) and PEG-rhMMP-1 (open symbols) were incubated with varying amounts of substilisin (0.0 mg/mL (squares), 0.001 mg/mL (diamonds), 0.1 mg/mL (circles)). 122

Figure 35. Schematic of rhMMP-1 PEGylation with PEG-SPA. 123

Figure 36. Ribbon diagram of rhMMP-1 showing the most likely sites of PEG-attachment (red). The active site residues H_{218}ALGHSLGLSH (purple) and the enzyme-associated zinc (green) and calcium (black) ions are also highlighted..... 126

Figure 37. SDS-PAGE of native and PEGylated rhMMP-1. Lanes: (1) protein molecular weight markers, (2) native rhMMP-1 (0.5 μg), (3) PEG-rhMMP-1 (M_w 5000; 1 μg), and (4) PEG-rhMMP-1 (M_w 5000; 2 μg). 128

NOMENCLATURE

1-butyl-3-methylimidazolium hexafluorophosphate	[bmim][PF_6]
1-butyl-3-methylimidazolium acetate	[bmim][CH_3CO_2]
1-butyl-3-methylimidazolium nitrate	[bmim][NO_3]
1-butyl-3-methylimidazolium trifluoroacetate	[bmim][CF_3CO_2]
1-methyl-1-(-2-methoxyethyl)pyrrolidinium hexafluorophosphate	[mmep][PF_6]
1-methyl-1-(-2-methoxyethyl)pyrrolidinium acetate	[mmep][CH_3CO_2]
1-methyl-1-(-2-methoxyethyl)pyrrolidinium nitrate	[mmep][NO_3]
1-methyl-1-(-2-methoxyethyl)pyrrolidinium trifluoroacetate	[mmep][CF_3CO_2]
1-methyl-1-(-2-methoxyethyl)pyrrolidinium trifluoromethylsulfonate	[mmep][CF_3SO_3]
1-methyl-1-(-2-methoxyethyl)pyrrolidinium methanesulfonate	[mmep][CH_3SO_3]
adenosine deaminase	ADA
diisopropylfluorophosphate	DFP
gastrocnemius muscle	GM
organophosphorous hydrolase	OPH
poly(ethylene glycol)	PEG
recombinant full-length matrix metalloproteinase-1	proMMP-1
recombinant human active matrix metalloproteinase-1	rhMMP-1
water activity	a_w

PREFACE

There are many individuals to whom I am indebted for their guidance and support in completing this thesis. It is to them that I dedicate this thesis and any future success in my research endeavors.

First and foremost, I am especially grateful to my advisor Dr. Alan Russell, who has provided me with every possible opportunity to succeed as a graduate student and beyond. His creativity and enthusiasm for great science made working under him an exciting and motivating experience. Among other things, he has taught me to be confident in my work and to not be timid in the face of opposition (even if it means arguing against your advisor in lab meetings!). Over the last six years, he has become as much a friend as a mentor.

I would like to thank Drs. Géraldine Drevon, Jason Berberich, and Rick Koepsel for their technical assistance, helpful discussions, and proofreading of this and numerous other documents. Throughout my time in the lab, they have made themselves available as day-to-day mentors and, as a result, are largely responsible for my growth and development as a researcher. Their mentoring was particular vital in the early stages of my research when I was still learning basic laboratory skills, including enzyme assays, bioconjugation techniques, molecular biology protocols, and how to function independently in the lab. They too have been great friends along the way with whom I've shared many laughs and countless cups of coffee.

I wish to express my gratitude to my committee members, Drs. Mohammad Ataai, Eric Beckman, Harry Blair, and Johnny Huard, for their insightful comments and constructive

critisms, which helped to improve the overall quality of my thesis. Special thanks to Dr. Blair for his assistance with the histology component of this work and to Dr. Yong Li, although not officially part of my committee, for help with animal surgeries. Additionally, I would like to acknowledge Dr. William Federspiel as being an influential instructor, mentor, collaborator, and friend.

I am also thankful to the members of the Russell lab, past and present, for having made the lab an enjoyable place to work. In particular, I would like to thank Dr. Hiro Murata who, in addition to being a tremendous help with chemistry related problems, always managed to keep me sane through his friendship and hilarious sense of humor. Special thanks also to Dr. Marina Kameneva, whose lab was adjacent to ours. By making sure I had my fill of chocolates, she made the days, and weekends, manageable.

Lastly, I am eternally grateful for the unconditional support and encouragment of my caring parents, Gary and Fran (who hopefully after reading this finally realize I do not work with stem cells!), brother, Scott, and amazing girlfriend, Jill Landsbaugh. Jill, while going through the rigoros of graduate school herself, has been perhaps my biggest source of support. She has always been willing to do everything and anything to help me through the hardsphips and frustrations in the lab. And she did so, having to put up with my often unpleasant moods, with nothing but a smile and the utmost loyalty when anyone else would have quickly grown impatient with my ways.

1.0 INTRODUCTION

Enzymes are highly efficient biological catalysts that are responsible for accelerating the reactions inside of living systems (i.e. cells). On appropriate substrates, they can enhance reaction rates in excess of one million times over the corresponding uncatalyzed reaction. Perhaps the most remarkable attribute of enzymes is the striking selectivity with which they bind to target substrates. Enzymes can differentiate substrate molecules on the basis of chemical functionality (chemoselectivity), positioning of target functional groups (regioselectivity), and chirality (stereoselectivity). The selectivity of enzymes, which is conferred by their unique amino acid sequence and three-dimension structure, virtually eliminates the formation of waste products due to side reactions, permitting reaction efficiencies to approach 100 %.

Due to the extraordinary catalytic efficiency of nature's catalysts, their use in asymmetric chemical synthesis and biotechnology has immense implications[1-4]. The combination of high turnover rates and specificity offered by enzymes is unmatched by conventional chemical catalysts. Moreover, with the ability to convert nearly any substrate, including many synthetic and non-naturally occurring compounds, enzymes can in certain cases catalyze reactions that cannot be achieved through classic chemistry. Biocatalysis also offers the potential to greatly reduce the environmental impact of existing chemical processes. Enzymes are completely biodegradable and typically most active under mild reaction conditions including near neutral pH and ambient temperatures and pressures, thus decreasing energy costs and increasing safety.

Because biocatalytic reactions produce practically no waste products, product purification is in general simple and such reactions are less polluting than parallel chemical synthesis routes.

The breadth of feasible biotransformation has been further broadened by advances in the ability to rationally manipulate biocatalyst function. One can now alter, and even expand, an enzyme's reaction specificity by introducing site-directed (by protein engineering)[5] or random (by directed evolution)[6] mutations into the primary structure of the enzyme. The properties of biocatalysts may also be tailored by changing their environment. In non-aqueous media, including organic solvents[7-9], supercritical fluids[10], and more recently ionic liquids[11], biocatalysts were shown to accept different substrates and accelerate reactions that otherwise do not occur in water as a result of being thermodynamically or kinetically unfavorable. The practice of altering biocatalyst function in this way, which was pioneered by Alexander M. Klibanov in the 1980s, has been appropriately termed "solvent engineering".[12]

Cells must constantly modulate their internal environment and, therefore, must be able to tightly control the concentration and activity of enzymes. Consequently, enzymes, and proteins in general, have evolved to be highly unstable molecules. Most enzymes remain active for only minutes or hours under ambient conditions even when in water. Their inactivation can be induced by variations in pH, temperature, and pressure as well as exposure to chemical denaturants such as surfactants, organic chemicals, and chelators.[13] Enzyme activity may also be largely affected by oxidation, freezing, thawing, and radiation. The root cause of inactivation can be either global unfolding of the enzyme molecule, loss of active site structure, or chemical modification of one or more peptide bonds or critical residues with respect to enzyme mechanism. The loss of activity may or may not be reversible depending on the properties of the

enzyme as well as its concentration in solution. This inherent instability represents a key shortcoming in most biocatalytic processes.

Because the preparation and purification of enzymes can be costly, enzymes must be effectively stabilized to improve their overall utility. The primary goal of any stabilization strategy is to minimize the physiochemical reactions that can occur, which evoke the loss of enzyme activity. Understanding the fundamental relationship between enzyme, structure, function, and molecular microenvironment is a prerequisite for developing rational strategies for enzyme stabilization. Conventional strategies for enzyme stabilization include the use of chemical additives, which can interact with the enzyme directly or with the milieu of the enzyme, chemical modification, and immobilization, which may be covalent or non-covalent in nature.[13] Stabilization may also be achieved through "re-designing" enzymes using protein engineering and natural evolution techniques.[6, 14]

Herein, enzyme structure-environment-activity relationships were utilized as the basis for developing effective means of stabilizing enzymes, and thus improving biocatalyst efficiency. Initially, this rational approach to stabilization was applied the use of enzymes in non-aqueous reaction media. Ionic liquids, organic salts that are liquids over ambient temperatures, were explored as an alternative to conventional solvents, many of which inherently denature enzymes (**Specific aim 1**). The impact of ionic liquid physical properties on enzyme activity and stability was probed using lipase as a model enzyme. Several approaches to preventing deactivating conformational changes in harsh non-aqueous environments as well as methods of controlling the degree of enzyme hydration were investigated as means of improving lipase activity in ionic liquids.

Even in anhydrous enzymology, enzyme structure and function is largely dependent upon the presence of water. Water molecules associated with the enzyme act as a "molecular lubricant", allowing for conformational flexibility, which is required for catalytic activity.[15-18] On a molecular level, the water shields charged and polar groups on an enzyme's surface, thereby preventing electrostatic interactions that may trap the enzyme in a rigid state. The degree to which an enzyme must be hydrated in order to be catalytically active can vary greatly depending on the enzyme.[15, 16]

In enzymatic hydrolysis reactions, the essential enzyme-bound water is acidified, thereby reducing the pH of the enzyme's microenvironment. Because variations in pH alter the structure and function of enzymes, tight control of pH is required during such reactions. To this end, the second section of this thesis addresses the development of a novel approach to controlling the pH within the aqueous layer surrounding an enzyme (**Specific aim 2**). The basis for this approach is that acid generated by a hydrolysis reaction can be balanced by the simultanesous biocatalytic formation of base, essentially mimicking how a cell controls its internal pH. The ability to control pH in this way represents a means of overcoming the shortcomings of conventional buffers in many reaction systems, particularly those that are low-water environments.

Proteases, such as α-chymotrypsin and subtilisin Carlsberg, are among the most well characterized enzymes in anhydrous media. These enzymes naturally catalyze the hydrolysis of peptide bonds. However, in anhydrous environments, they are capable of accelerating a number of industrially relevant reactions including esterifications, the synthesis of sugar acrylates, and peptide synthesis.[3, 19] The use of proteases in anhydrous media effectively stabilizes them since removing water suppresses their hydrolytic activity, thereby preventing autolysis as well as their inactivation by other digestive enzymes. Consequently, due to enhanced stability, proteases are

of much greater utility in anhydrous media despite still being important catalysts in many aqueous processes.

To enhance the overall utility of proteases, methods to stabilize proteases when the aqueous content of the reaction medium is increased must be developed. Covalent modification of enzymes with synthetic polymers represents a promising technique for improving the stability of enzymes in aqueous environments. The last section of this thesis examines the impact of poly(ethylene glycol) (PEG)-modification on the aqueous stability of the protease matrix metalloproteinase-1 (MMP-1) (**Specific aim 3**). Because MMP-1 is of potential therapeutic use, changes in the stability of MMP-1 as a result of PEG-modification were correlated to the therapeutic effectiveness of the protease.

2.0 BACKGROUND AND LITERATURE REVIEW

2.1 ANHYDROUS ENZYMOLOGY

Despite the fundamental role of water in enzyme folding and mechanisms, enzymes are not constrained to use only in aqueous reactions. In fact, the longstanding belief that enzymes only function in water is a gross misconception. The reality is that enzymes do not need much water at all. They are surprisingly active in essentially anhydrous environments as long as there is enough water to hydrate the enzyme molecule. This activity has enabled the portfolio of feasible biotransformations to be greatly expanded as well as enhanced the industrial utility of enzymes.

The properties of enzymes may be markedly altered by the absence of water in ways that improve their catalytic efficiency and permit them to catalyze very different reactions. Among the properties of enzymes that are unique to their use in anhydrous solvents are enhanced thermostability, altered substrate and enantiomeric specificities, and molecular memory.[9, 15, 16, 19, 20] Replacement of water with anhydrous solvents can also shift the thermodynamic equilibrium of biocatalytic reactions, thereby facilitating the catalysis of reactions that otherwise would not occur in water as a result of being thermodynamically or kinetically limited.[12, 21] Moreover, the use of enzymes in anhydrous reaction media may enhance the solubility of hydrophobic

substrates, eliminate undesirable side reactions involving water, increase the ease of product recovery, and prevent microbial contamination.[9, 15, 19]

2.1.1 Enzyme Structure in Anhydrous Solvents

To understand how enzymes function in anhydrous solvents, it is critical to first examine how the solvent environment affects the structure of enzymes. Interestingly, in anhydrous solvents, it is the conformational mobility of an enzyme that is altered rather than its structure per se. Enzymes become highly rigid molecules that are seemingly locked in their native-like conformation.[9, 15, 17, 18] This is presumably a result of electrostatic interactions between charged and polar groups in the enzyme, which can only occur in the absence of water. In the presence of water, water molecules accumulate around these groups effectively shielding them from each other.[15, 16] Thus, the propensity for an enzyme molecule to denature is in essence suppressed due to the loss of flexibility. However, the complete loss of conformational mobility may negatively impact enzyme activity, since small structural changes are typically essential for catalysis.[15, 17]

Enzyme structure and dynamics in anhydrous solvents has been exhaustively studied. Such studies have involved the use of structural determination techniques such as nuclear magnetic resonance and X-ray crystallography. For instance, using X-ray crystallography, the three-dimensional structures of the proteases subtilisin Carlsberg and γ-chymotrypsin were shown to be virtually the same in acetonitrile and hexane respectively as in water.[22, 23] Information regarding the conformational mobility and structure of enzymes in the dry state has also been obtained by spectroscopic techniques and enzyme activity assays.[15] The results of these studies confirm that enzymes lose the necessary flexibility to unfold and consequently are structurally trapped in anhydrous solvents.

2.1.2 Influence of Water on Enzyme Activity

Enzyme hydration, which refers to the number of water molecules associated with an enzyme rather than the total amount of water in the reaction medium, is critical even in essentially anhydrous biocatalysis.[24] Water acts as a "molecular lubricant" to enhance the conformational mobility of enzymes.[9, 15] In order for catalysis to be possible, an enzyme must be able to undergo structural rearrangement such that its binding pocket is properly oriented to accept a substrate molecule. The mobility of an enzyme is particularly important in conversions involving bulky substrate molecules.[15] When an enzyme is completely dry, representing the most extreme case, it lacks the necessary flexibility to accommodate substrate binding and thus is inactive.

The addition of only a small number of water molecules per molecule of enzyme may be sufficient to activate enzymes in anhydrous solvents.[15, 16] Such is the case with lipases, for example. Other enzymes may require up to as much as a monolayer of water surrounding the enzyme molecule to be catalytically active.[15, 16] Although enzyme activity increases with hydration, there is, for a given enzyme, an optimal degree of hydration for which its catalytic activity in anhydrous solvents is greatest. Deactivation of enzymes above a critical hydration level can be attributed to the aggregation of enzyme molecules.[15]

The degree of enzyme hydration in anhydrous solvents can best be described by thermodynamic property water activity.[15, 18, 24] Under equilibrium conditions, it is by definition equal in the various components of a reaction system, namely the enzyme, substrates, products, solvents, and headspace above the reaction solution and thus accounts for the uneven distribution of water between the components. Water activity is a particularly useful measure of enzyme hydration when comparing the effects of different solvents on the activity of an enzyme. This is

because the amount of water adsorbed to the surface of an enzyme will differ depending on the hydrophibicity of the solvent (i.e. hydrophilic solvents tend to strip water from an enzyme more so than hydrophobic solvents). Because water activity is related to the relative humidity of the vapor headspace, it can easily be measured using a humidity probe.

Water activity in anhydrous solvents can be fixed by the direct addition of water, pre-equilibration of the various reaction components including the enzyme and substrates with saturated salt solutions, and the use of salt hydrates.[24-29] The use of salt hydrates provides a particularly effective means of controlling water activity since water activity equilibrium is established rapidly and is not subject to changes resulting from the adsorption or evaporation of water from the environment. Briefly, the principle behind water activity control using salt hydrates is the formation of dynamic water equilibrium by the interconversion of the salt between higher and lower hydration states. Water activity is controlled as long as residual amounts both of the solid salts are present. Different salt hydrate pairs have different intrinsic fixed water activity equilibrium.[26]

2.1.3 Solvent Types

The catalytic properties of enzymes in anhydrous enzymology are highly solvent-dependent. This is the result of the ability of a solvent to dramatically influence the nature of the aqueous microenvironment of an enzyme. One way a solvent may influence an enzyme's aqueous microenvironment is through interacting directly with the enzyme-bound water. This type of interaction is generally discussed in terms of the ability of a solvent to inactivate an enzyme by means of stripping the essential water from the enzyme's surface.[15, 30] The tendency of a solvent to compete for water from an enzyme increases with increasing solvent

hydrophilicity. Another way in which a solvent can alter the microenvironment of an enzyme is by influencing the local concentration of substrates and products.[15] Differences in substrate solvation in particular can have a significant impact on the apparent activity of an enzyme.

Solvent properties such as Hildebrandt solubility parameters (δ), dielectric constants (ε), and dipole moments (μ) may all be used as predictors of enzyme activity in anhydrous solvents. Octanol-water partition coefficients (log *P*), which indicate the solvent hydrophilicity, also correlate strongly with enzyme activity and are routinely used to assess the likelihood of solvents to support enzyme activity.[31] Enzymes generally are most active in solvents that have a log *P* of greater than four since such solvents are highly hydrophobic and thus tend not to strip an enzyme of its essential bound water. Solvatochromic parameters provide a measure of solvent polarity, which can be useful for solvent selection.[32]

Anhydrous biocatalysis has traditionally involved the use of organic solvents. Indeed, much of what we know about how enzymes behave in essentially anhydrous environments is from the study of enzymes in organic solvents. However, because organic solvents are detrimental to the environment, there has been a strong drive in recent years to find alternative cleaner reaction media.

An alternative class of solvents that have attracted considerable attention are supercritical fluids, which are substances with temperatures and pressures that exceed their critical points. Enzyme activity, stability, and even specificity in supercritical fluids is dependent upon the solvent's physical properties, which can be rationally modulated by altering temperature and pressure.[10] Additionally, the rates of enzymatic reactions may be greater in supercritical fluids that in organic solvents due to relatively lower mass transfer limitations. Supercritical carbon dioxide has received the most attention because it offers several environmental advantages over

conventional organic solvents. Such advantages include being environmentally benign, nontoxic, nonflammable, and highly available.

Ionic liquids have also emerged as an environmentally friendly solution to the threat posed by organic solvents. These are organic salts that exists as liquids over unusually large temperature ranges, which span ambient temperatures, and which are thermally stable and have practically no vapor pressure.[33, 34] Moreover, ionic liquids have exceptional solvent properties, including the ability to dissolve virtually any chemical compound. By substituting the cation, anion, or attached substituents, the solvent properties may be manipulated, allowing ionic liquids to be tailored for specific reaction systems.[34] Although it is still not yet fully understood how ionic liquids influence the catalytic properties of enzyme, enzymes are active and remarkably stable in select ionic liquids such as 1-butyl-3-methylimidazolium hexafluorophosphate.[11, 35-37]

Enzyme reactions may also be carried out in the absence of bulk solvent by using gas-phase substrates.[38-41] Such reactions generally involve flowing gaseous substrates through a fixed-bed reactor containing dry enzyme in either free or immobilized form. A major benefit of using gas-phase substrates is that mass transfer limitations are significantly lower in the gas-phase compared to the solution phase.[42] Thus, such as the case with supercritical fluids, reactions that are diffusionally controlled can proceed at higher rates in the gas-phase than in conventional organic solvents. Reaction products may also be more easily recovered in the gas-phase compared to in solution-phase reactions.[42, 43]

2.2 EFFECT OF pH ON ENZYME ACTIVITY AND STABILITY

A key determinant of enzyme structure and function is pH. The pH of the essential water layer surrounding an enzyme molecule influences the ionization state of residues with acidic and basic side chain groups. When the ionization state of a residue that is critical to the enzyme's catalytic mechanism is perturbed, such as, for example, an active site residue that participates in the binding of substrate, the enzyme will be inactivated.[44] Although enzymes can contain many ionizable residues, within an enzyme there are usually only one or two such residues that must be in the correct ionization state for catalysis. The dependency of enzyme activity on pH is thus defined by the pKa values of the side chain groups of these residues. An enzyme that has only one critical pKa will have sigmoidal-shaped pH-activity curve whereas the activity versus pH of an enzyme with two critical pKa values will follow a bell-shaped curve.

Catalytically essential residues are almost always in the active site of an enzyme. However, charged groups on an enzyme's surface may indirectly alter the apparent pKa of an enzyme. This can occur when surface charges stabilize a particular ionization state of a critical active site residue, which may be several angstroms away, through long range electrostatic interactions.[44] The pKa of a critical residue is increased by the stabilization of its positively charged state by interactions with negatively charged surface groups. Conversely, the pKa of a critical residues is decreased by the stabilization of its negatively charged state by interactions with positively charged surface groups. Long range electrostatic interactions that affect the pKa of ionizable groups in an enzyme may be introduced through chemical modification and protein engineering as a means of shifting the enzyme's pH-activity profile.[5] Furthermore, variations in pH can disrupt electrostatic interactions between residues far from the active site, which leads to the destabilization, and thus inactivation, of an enzyme.[44]

The influence of pH on enzyme activity can described through classical Michaelis-Menten kinetics by accounting for the potential protonation of the enzyme and enzyme-substrate complex (**Figure 1**). According to the expanded kinetic model, the enzyme (E) and enzyme-substrate complex (ES) may be protonated yielding HE and HES respectively. However, product (P) can only be formed from the ES complex. The Michaelis constant K_M represents the association constant of ES, and thus is a measure of substrate affinity, while the rate constant of the conversion of ES to free E and P is k_{cat}, which practically represents the rate of substrate turnover per unit mass of enzyme. $K_{a,E}$ and $K_{a,ES}$ are the ionization constants of E and ES respectively while K'_M is the dissociation constant of HES. In this model, it is assumed that the substrate molecule is not ionizable.

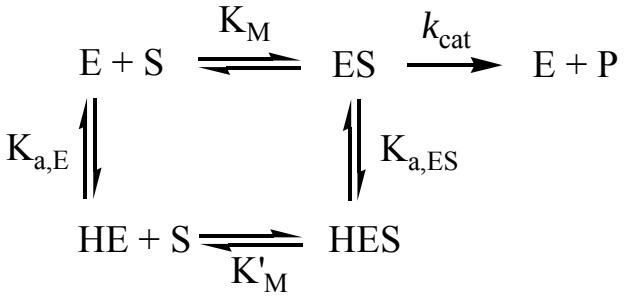

Figure 1. Michaelis-Menten mechanism showing potential ionization steps.[44]

Derivation of the steady-state rate expression (i.e. d[ES]/dt = 0) based on the proposed model yields (**Equation 1**):

$$v = \frac{k_{cat}[E]_{total}[S]}{K_M + [S]\left(1 + \frac{[H^+]}{K_{a,ES}}\right) + \left(\frac{K_M[H^+]}{K_{a,E}}\right)} \qquad \textbf{(Eq. 1)}$$

or

$$v = \frac{k_{cat}[E]_{total}[S]}{K_M + [S]\left(1 + \frac{10^{-pH}}{K_{a,ES}}\right) + \left(\frac{K_M(10^{-pH})}{K_{a,E}}\right)}$$

where v is the velocity of the reaction, $[E]_{total}$ is the total enzyme concentration. From the model of the Michaelis-Menten mechanism, it is clear that protonation of ES, and thus pH, will affect the apparent k_{cat} of an enzyme.[44] Solving for k_{cat}, which is equal to the maximum theoretical velocity (i.e. when [S] >>> K_M) of the enzyme reaction divided by $[E]_{total}$, indicates the apparent k_{cat} will vary with pH as (**Equation 2**):

$$(k_{cat})_{pH} = \frac{k_{cat}K_{a,ES}}{K_{a,ES} + 10^{-pH}} \qquad \textbf{(Eq. 2)}$$

Similarly, the apparent K_M of an enzyme will inherently be affected by the protonation of E and ES.[44] The dependency of the apparent K_M on pH can be described by (**Equation 3**):

$$(K_M)_{pH} = \frac{K_M K_{a,ES} + \left(\frac{K_M K_{a,ES}(10^{-pH})}{K_{a,E}}\right)}{K_{a,ES} + 10^{-pH}} \qquad \textbf{(Eq. 3)}$$

In the case that the substrate can also be protonated, the apparent K_M would be further affected by this ionization process. Given the relations of k_{cat} and K_M to pH, the dependence of the catalytic efficiency (k_{cat}/K_M) of an enzyme on pH is given by (**Equation 4**):

$$\left(\frac{k_{cat}}{K_M}\right)_{pH} = \frac{K_{a,E}\left(k_{cat}/K_M\right)}{K_{a,E} + 10^{-pH}} \qquad \textbf{(Eq. 4)}$$

2.3 PROTEASE STABILITY

Enzymes are readily inactivated through a variety of processes and as a result have extremely short catatlytic lifetimes, ranging typically from just a few minutes to hours. Inactivation of enzymes can largely be attributed to their intrinsic instability. The free energy barrier that prevents an enzyme molecule from unfolding is on the order of only 5 – 15 kcal/mol.[45] The drive to denature is even greater at elevated temperatures and pressures, extreme pH, and in the presence of denaturing agents. Depending on the size and concentration of the enzyme, the unfolding process, and thus inactivation, may be reversible or irreversible.[45] Inactivation can also result from irreversible covalent changes in the enzyme molecule, which may be caused by process such as oxidation, proteolysis, and radiation.[13]

Proteases, which are enzymes that catalyze the hydrolytic cleavage of proteins at specific sites, in particular, are inactivated rapidly even compared to most enzymes. In addition to other causes of inactivation, these enzymes can also autolytically degrade into inactive peptide fragments. The activities of proteases are greatest when the target peptide is denatured at the site of hydrolysis so as to make the cleavage site more accessible to the protease.[13] As a result, most proteases retain activity over the course of only minutes in aqueous solutions.

The stability of proteases may be markedly improved by engineering the reaction medium in which they are used. Proteases are generally stable in anhydrous solvents since they have very different activities in such media. Specifically, these enzymes, when in the dry state, catalyze synthesis reactions rather than digestive reactions, which cannot occur because water is not available to participate as a substrate. For instance, proteases are capable of catalyzing esterification reactions, peptide synthesis, and the synthesis of sugar acrylates in anhydrous

solvents.[3, 19] A prominent example of the use of proteases for industrial chemical synthesis is the production of aspartame catalyzed by the metalloendopeptidase thermolysin.[4]

One way in which the stability of proteases can be enhanced in aqueous and biphasic solutions is by covalent modification with PEG. PEG-attachment generally reduces the thermoinactivation of proteases in such environments by increasing the enzyme rigidity and by altering the enzyme's surface hydrophobicity.[40, 46-48] Moreover, proteases modified with PEG are more resistant to autolysis due to steric hinderance created by the PEG at cleavage sites in the protease molecule.[49] These same steric effects are also responsible for protecting PEG-protease conjugates from interaction with biomacromolecules, including proteins, other digestive enzymes, and antibodies.[50-53] Accordingly, PEGylation can reduce the *in vivo* clearance of proteases and thus increase the therapeutic effect of proteases, which are employed to treat many disease states.[54]

2.4 STRATEGIES FOR ENZYME STABILIZATION

2.4.1 Chemical Additives

Enzymes, and other proteins for that matter, can be effectively stabilized with a wide array of chemical additives.[13, 55] Such additives are generally soluble and can impact an enzyme's operational and storage stability. Furthermore, additives can increase the stability of enzymes against thermoinactivation (i.e. increase the melting temperature T_m of an enzyme) as well as chemical-induced denaturation. The enhancement in enzyme stability may result from interactions between the additive and the enzyme or the additive and medium of the enzyme.

Additives that interact directly with the enzyme are more generally referred to as specific additives, whereas those that induce solvent effects are referred to as non-specific additives. A third type of chemical additive that affords stability enhancements is those that compete with the enzyme for inactivating agents in the enzyme solution.

Stabilization by specific additives is a rather straightforward approach that is predicated on thermodynamic changes of enzyme folding upon ligand binding (**Figure 2**). Specific additives non-covalently bind to the enzyme in such a manner that is reversible and shifts the thermodynamics of folding of the enzyme to strongly favor the native conformation.[13, 55] In practice, specific additives may be substrate analogues, products, cofactors, salts, or ligands that bind to functional groups on the enzyme's surface. Because the stabilized enzyme should retain activity, it is critical that the additive not block substrate docking, which presumably may occur if substrate analogues or products are used as additives, or alter a site that is pertinent to the mechanism of catalysis.

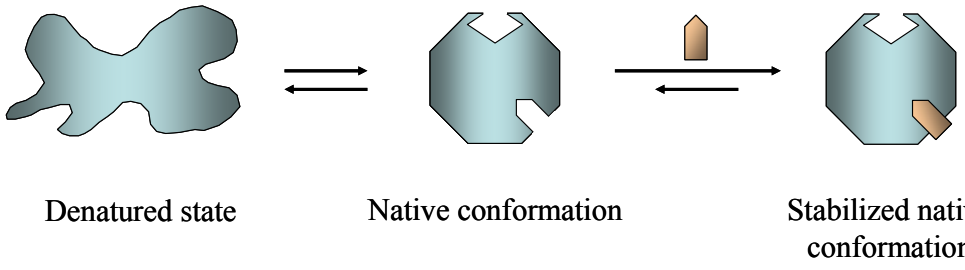

Figure 2. Enzyme stabilization by specific additive. The ligand binds specifically to the native conformation of the enzyme, thereby forcing the equilibrium of enzyme folding to favor the catalytically active native state. In the enzyme structure, the diamond-shaped binding pocket represents the active site.

Unlike specific additives, non-specifics additives do not interact with the enzyme directly, but rather stabilize the natively folded state of an enzyme through additive-medium interactions. Non-specific additives may be sugars, polyols, ionic and non-ionic surfactants, and synthetic polymers. The principal cause of stabilization is the result of either increases in surface tension of the enzyme solution or by solvophobic effects, both of which are associated with the preferentially hydration of the enzyme and thus preferential exclusion of the additive from the enzyme's aqueous microenvironment.[55-60] As the surface tension of an enzyme solution increases, the energetic cost associated with expanding the volume occupied by the enzyme also increases.[60] This ultimately makes unfolding thermodynamically unfavorable. Solvophobic effects arise from thermodynamically unfavorable interactions between the enzyme and additive.[55, 59, 60] In order to prevent for such interactions, an enzyme will adopt a state that minimizes its solvent accessible area. It is plausible that conformational changes due to solvophobic effects may instead lead to a loss of activity, thereby destabilizing the enzyme rather than stabilizing it. Steric exclusion, which also leads to preferential hydration, may also play a role in enzyme stabilization when large polymers such as PEG are used as non-specific additives.[60, 61] The principal of steric exclusion has to do with relative differences in the radii of water and that of the additive molecule. Assuming that the radius of the additive molecule is in fact larger that that of a water molecule, the volume surrounding the enzyme that is inaccessible to the additive (i.e. exclusion volume) will be larger than that which is inaccessible to water. Salts can also alter the solvation of enzymes, and thus may induce stabilization, through "salting out", which refers to the process of reducing the solubility of an enzyme.[55] The addition of salt in effect draws solvent away from the enzyme molecule. This in turn minimizes solvation of the

enzyme, particularly its hydrophobic pockets. Generally, kosmotropic salts, those to the left of the Hofmeister series, have a tendency to stabilize enzymes.

Chemical additives that serve to sequester inactivating agents represent a broad class of soluble stabilizers. Indeed, any chemical that inhibits the interaction between an enzyme and a molecule that inactivates it classifies as this type of stabilizing additives. Additives of this type may be used to scavenge oxidizing agents, metal ions, free radicals, and other various enzyme inhibitors.[13, 55]

2.4.2 Chemical Modification

Chemical modification is a technique whereby the structure of an enzyme is covalently altered either by the attachment of monofunctional reagents or chemical cross-linking. Enzymes are modified via the reaction between a modification reagent and accessible functional groups in the enzyme. The sulfhydryl group of cysteines and primary amines on the surface of an enzyme (i.e. ε-amine of lysines and the N-terminal α-amine) are ideal sites for modification since they are highly reactive under conditions that do not perturb enzyme structure, including near neutral pH.[62] Modification chemistries may, however, also be targeted to hydroxyl, carboxylic acid, guanidine, imidazole, and indole groups present in an enzyme.[62, 63]

In reality, when reacted with monofunctional or crosslinking reagents, only a fraction of the target functional groups in an enzyme are typically modified.[47] This stems from differences in the relative reactivity, which may arise from electrostatic interactions with neighboring residues, and accessibility of each potential modification site. For example, it is possible for a functional group to be buried in the inner core of an enzyme, and thus inaccessible, or be non-reactive due to electron withdrawing effects from other functional groups within close proximity.

Incomplete modification may also be due to the modification reaction becoming sterically hindered. Furthermore, chemical modification generally yields a heterogeneous mixture of enzyme with differing number of modifications. The properties of the modified enzyme may differ significantly depending on the number of modifications per enzyme molecule.[47] Thus, in order to discern the effects of modification, it is critical to separate the mixture of modified enzyme into populations with equal extents of modification. This is rarely done in practice though, as the effects of modification on enzyme properties are in most cases determined as an ensemble effect.

Enzyme stability may be significantly enhanced by covalent chemical modification. Although there are reports of the use of modification to minimize inactivation by pH[64], solvents[65], and even photooxidation[66], enzymes are, by far, most commonly modified for the purposes of thermostabilization and the prevention of proteolysis. Consequently, this section will focus solely on the impact of modification on the thermal denaturation of enzymes and their susceptibility to proteolytic digestion. It is important to note, however, that, with few exceptions, the basic principles involved in the stabilization of enzymes against heat and proteases by chemical modification also apply to the stabilization of enzymes from other modes of inactivation.

The effect of modification on the thermostability of enzymes may result from changes in an enzyme's surface properties and conformational rigidity.[47] In the case of monofunctional regents, thermostabilization may be increased by altering surface hydrophobicity, although there does not appear to be a consistent relationship between stability and the hydrophobicity (or hydrophilicity) of enzymes. The attachment of hydrophobic and hydrophilic acylating and alkylating reagents has been reported to increase thermostability.[47] Moreover, conjugation of

enzymes with PEG, which is amphiphilic in nature, also has been shown to improve the thermostability of enzymes.[46, 48] Therefore, the selection of modification reagent on the basis of hydrophobicity must be considered depending on the enzyme of interest, with every enzyme having a different degree of surface hydrophobicity for which its thermostability is maximal.[47] Altering the amino acid makeup of an enzyme's surface may also impart thermostability. Specifically, resistance to thermal denaturation has been shown to be markedly improved by the conjugation of guanidine groups to an enzyme's surface.[47, 67] This effect can be explained by relating the surface of guanidine-modified enzymes to that of thermophilic enzymes. Interestingly, the ratio of arginines-to-lysines is generally greater on the surface of thermophilic enzymes than on that of mesophilic enzymes.[68] Thus, it is likely that the attachment of guanidine groups may enhance thermostability by making the surface of mesophilic enzymes more thermophilic-like. In the case of enzyme intra- and intermolecular crosslinking, thermostabilization is due to increases in conformational rigidity.[13, 47, 59] The attachment of monofunctional reagents may also increase slightly the rigidity of an enzyme molecule, however, as might be expected, to a much lesser degree than crosslinking.[48]

Modification of enzyme structure may prevent interactions with biomacromolecules and thus afford stability against proteolysis. One way modification may prevent proteolysis is through steric effects. The attachment of large molecules, such as soluble polymers, to the surface of an enzyme may sterically block proteases from attacking it.[13] This is the rationale for enzyme PEGylation. The PEG chains form a cage-like structure around the enzyme molecule, thereby sterically inhibiting enzyme-proteins interactions.[69] PEGylated enzymes are hence less immunogenic and less susceptible to clearance by plasma proteins than free enzymes.[51-53, 70, 71] Another way modification can prevent proteolysis and even autolysis when the target enzyme is

itself a protease by altering positively charged residues.[13, 72] This is because many proteases cleave polypeptides following positively charged residues and eliminating positive charges in the polypeptide makes potential cleavage sites unrecognizable. If a positively charged residue is modified with a negatively charged reagent such as a dicarboxylic acid anhydride, additional electrostatic effects may be introduced.[13, 72] For instance, the accumulation of negative charge on the surface of the enzyme can cause the enzyme to repel proteases that also have a net negative charge. Since enzymes are more accessible to proteolytic digestion when unfolded, increases in enzyme rigidity, which can be achieved through crosslinking, may also minimize proteolysis under denaturing conditions.[13]

Increased stability as a result of chemical modification is usually accompanied by changes in the catalytic properties of an enzyme. The activity of an enzyme is almost always altered by modification. Such changes are dependent upon the extent and site(s) of modification. Modification of a residue that is critical to the catalytic mechanism of an enzyme will result in at least partial inactivation. Complete loss of activity is most often associated with the modification of residues in or near the active site. The modification of active site residues, which is likely to block substrate binding, can be prevented by adding a competitive inhibitor, substrate, or substrate-analogue to the modification reaction.[47, 73] By and large, modification to the surface of an enzyme will have minimal impact on activity. However, the greater the number of modifications per enzyme molecule, the more drastic the activity loss one can expect. Although far less common, there have been reported instances in which modification has led to enzyme activation.[65] Changes in enzyme activity are reflected in the Michaelis-Menten kinetic parameters k_{cat} and K_M. The k_{cat} and K_M of an enzyme generally decrease and increase respectively upon modification, resulting in an overall reduction in catalytic efficiency (k_{cat}/K_M).

Apparent inactivation may not necessarily be due to a reduction in catalytic efficiency but rather to changes in the pH-dependent activity of the enzyme.[47] The addition or removal of charge groups on the surface of an enzyme by chemical modification can influence the pKa of residues in the enzyme's active site, which are involved in catalysis.[74] Enzyme specificity may also change upon chemical modification.[75]

2.4.3 Immobilization

Immobilization, in its broadest sense, involves the fixation of an enzyme to an insoluble support. This fixation may be covalent or non-covalent in nature or neither, as the enzyme may instead be confined within a permeable support. Generally, enzymes are remarkably more stable in an immobilized state versus in a free state.[13, 76-78] There are many techniques for immobilizing enzymes including entrapment, physical adsorption, ionic adsorption, and single or multipoint covalent attachment, each of which stabilize enzymes in a different manner.

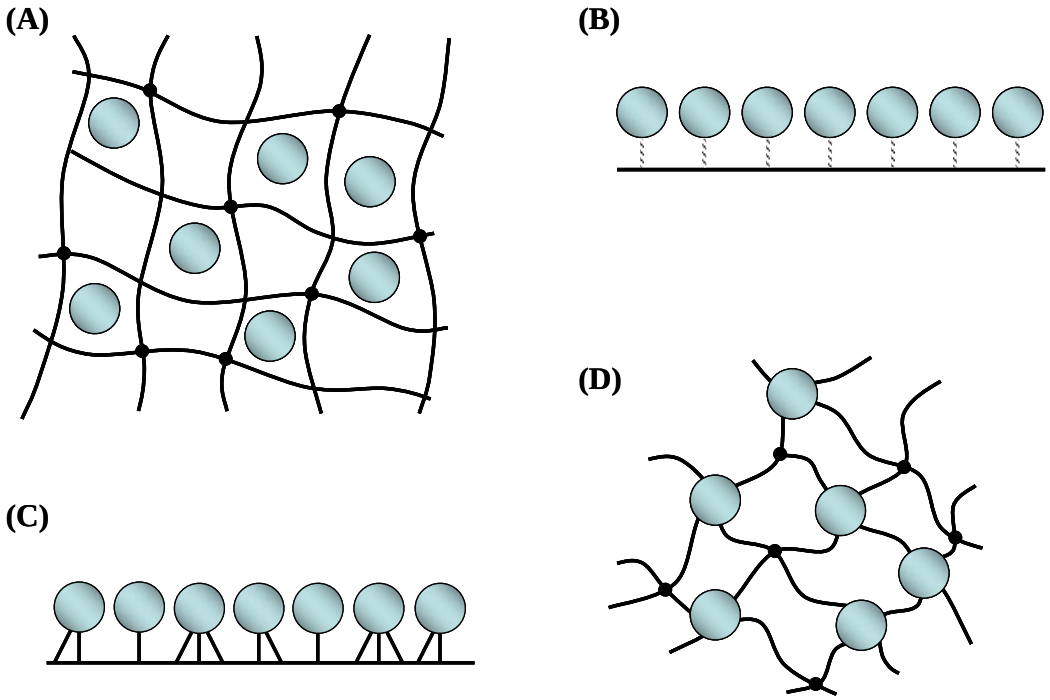

Figure 3. Enzyme immobilization techniques: (A) entrapment, (B) adsorption, (C) conventional covalent immobilization, and (D) multipoint covalent immobilization into polymeric network. The blue spheres represent enzyme molecules.

Enzyme immobilization by entrapment refers to the retention of an enzyme by a porous matrix, membrane or gel-like material based on differences between the size of the enzyme molecule and that of the pores.[77, 79] Entrapment occurs when the enzyme cannot leach from the framework of the support, as a result of having an effective radius greater than that of the pores, whereas reaction substrates and products can diffuse freely in and out (**Figure 3A**). Because the enzyme does not interact with the support directly, enzymes immobilized in this way are typically not subjected to conformational changes that may alter their activity. The encapsulation of enzymes within the lumen of a hollow membrane such as lipsomes, micelles, or rigid microspheres is a form of entrapment.[76] An entrapped enzyme may be stabilized as a result

of restricted conformation motion, which has the same effect as increasing enzyme rigidity. As such, entrapment may prevent thermal, pH, or chemical denaturation. Entrapment may also lead to stability enhancements as a result of influencing the microenvironment of an enzyme.[13] The intrinsic properties of the support, such as charge and hydrophobicity, may cause partitioning of denaturants or even ions between the microenvironment of the enzyme and bulk reaction media. It is thus feasible that, depending on the support, entrapment could result in the exclusion of an inactivating agent from the immediate vicinity of an enzyme. Similarly, the concentration of substrate in the microenvironment of an enzyme may be less than that in the bulk media due to partitioning. The observed activity of the entrapped enzyme will as a result be less than that of the free enzyme. Furthermore, the entrapment of an enzyme may prevent proteolysis as well as interactions with large macromolecules, which cannot diffuse into the framework of the support.

Enzymes that are immobilized by adsorption are bound to a support by non-covalent, ionic, or affinity interactions (**Figure 3B**).[77] In the case of physical adsorption, an enzyme may be immobilized through any one or combination of hydrogen bonding, hydrophobic interactions, or Van der Waals forces. Adsorption by affinity interactions provides a greater degree of specificity between the enzyme and support than other means of adsorption. Thus, there is generally less non-specific binding of reaction substrates, products, or additives to the support, which may displace the enzyme. The strongest interactions are formed through electrostatic interactions between an enzyme and charged support.[77] Compared to other immobilization techniques, adsorption is relatively simple in practice and does not require sophisticated chemistries. Adsorption, like entrapment, may increase the conformational rigidity, particularly when there are multiple interactions between an enzyme molecule and the support, and alter the properties of an enzyme's microenvironment.[76, 77] However, relative to other immobilization

techniques, the strength of interactions between an enzyme and support by adsorption are relatively weak. Changes in pH and ionic strength can disrupt such interactions, making the enzyme prone to leaching. Moreover, adsorption can lead to inactivation of an enzyme if a buried region or motif interacts with the support in a manner that induces unfolding. Inactivation may also occur as a result of adsorption interactions involving active site residues.

The covalent immobilization of an enzyme is achieved by the reaction of functional groups on the enzyme's surface with a solid support (**Figure 3C**).[76, 77, 79] As is the case in chemical modification, chemistries that are specific for the reactive groups on the side chains of lysine, cysteine, arginine, aspartic acid, glutamic acid, histidine, tyrosine, methionine, and tryptophan residues may be used.[62] In certain cases, it may be necessary to initially introduce functional groups onto the support using surface modification techniques such as radio frequency glow discharge. Depending on the number of accessible reactive groups on the enzyme surface, an enzyme may be bound to the support at more than one site. The formation of covalent linkages from the enzyme increases its conformational rigidity in a manner that is similar to chemical crosslinking.[76, 77] The greater the number of covalent linkages between the enzyme and surface, the greater the extent to which the enzyme's rigidity is increased. Comparatively, covalent immobilization can lead to much greater thermostability enhancements than entrapment or adsorption.[77] As is to be expected anytime the structure of an enzyme is modified, covalent immobilization may have deleterious effects on enzyme activity. The basis for this effect is analogous to that described for the loss of activity by chemical modification.

Combining the power of biology and the sophistication of polymers presents considerable opportunities. Enzyme-containing polymers are prepared by reacting a prepolymer with an enzyme, resulting in multipoint covalent attachment of the enzyme directly into the polymer

network (**Figure 3D**).[77, 80, 81] In this way, the enzyme plays the role of a monomer in the polymerization reaction. Multipoint covalent attachment ensures retention of the enzyme in the polymeric material and typically results in exceptional stability enhancements. Polyurethanes are ideal matrices for enzymes due to their ease of preparation and the tunability of their properties. While studying the effects of multipoint covalent immobilization on the stability of organophosphrous hydrolase, LeJeune and co-workers[80] described the first successful irreversible incorporation of an enzyme into a polyurethane polymer.

The characterization of immobilized enzymes is usually complicated by the existence of diffusional limitations.[13, 76] Diffusional limitations, which affect the apparent activity of an immobilized enzyme, may be external or internal with respect to the surface of the immobilized enzyme. The activity of an immobilized enzyme is limited by external diffusion when the rate of substrate diffusion from the bulk solution to the immobilized enzyme's surface is limiting (or when the rate of product diffusion from the immobilized enzyme's surface to the bulk solution is limiting). Conversely, the activity of an immobilized enzyme is limited by internal diffusion when the rate of substrate (or product) diffusion within the porous immobilized enzyme particle is limiting. Generally, the immobilization of enzymes by entrapment and multipoint covalent incorporation into a polymer matrix leads to both external and internal diffusional limitations whereas enzymes that are adsorbed or covalently attached to the surface of a support are only affected by external diffusional limitations. The existence of diffusional limitations can be confirmed experimentally by assaying enzyme activity as a function of the amount of immobilized enzyme. If the activity of the immobilized enzyme is diffusionally controlled, the relationship between activity and enzyme loading will be nonlinear. As a result of limited substrate diffusion, the apparent stability of an immobilized enzyme can significantly differ from

that of its true stability.[13] An immobilized enzyme may even have a greater apparent than intrinsic stability. The effects of diffusional limitations on the activity and stability of an immobilized enzyme may be reduced by decreasing the size, and thus increasing the net surface area, of the support-bound enzyme.

2.4.4 Protein Engineering

Advances in recombinant protein technology have dramatically increased the ease with which proteins may be produced at sizeable quantities and of high purities. This, combined with the advent of site-directed mutagenesis, a technique that allows one to alter the amino acid code of proteins, has provided the necessary tools to rationally engineer proteins. Protein engineering has emerged as a particularly useful technique for the study of enzyme mechanisms. By selectively mutating specific residues in an enzyme and correlating the mutations to activity and specificity, the precise role of these residues in catalysis can be elucidated.[14, 82, 83] Moreover, through protein engineering, it is now possible to re-design enzymes to have radically different catalytic properties. One of the early uses of protein engineering in this way was reported by Russell and Fersht[5], who demonstrated that the pH-activity profile and specificity of subtilisin could be altered via introducing mutations that change the enzyme's surface charge.

The three-dimensional arrangement of a polypeptide is stabilized by non-covalent interactions between amino acid residues, as well as between amino acid residues and water, and occasional disulfide bridges. Thus, it is logical that rationally introducing interactions of these types into an enzyme molecule by means of engineering its structure will have stabilizing effects. This approach has been successfully applied to the stabilization of enzymes against thermal and chemical denaturation by engineering sites for disulfide bridge formation.[59, 84, 85] In some cases,

only a single amino acid in the enzyme was converted to a cysteine, thereby introducing a site that could potentially form a disulfide linkage with a cysteine that is naturally found in the enzyme. In other cases, cysteines were substituted at two positions in the enzyme, enabling the potential for a disulfide bridge to be formed between the engineered sites. The thermal and chemical denaturation of enzymes has also been prevented by amino acid substitutions that provide sites for hydrophobic, electrostatic and Van der Waals interactions.[59, 78, 84, 85]

Inactivation as a result of covalent modifications of enzyme structure may further be prevented through protein engineering. For example, an enzyme may be engineered to be resistant to oxidation by mutating the one or more residues that are prone to being oxidized.[59, 86] In much the same way, proteolysis may be prevented by mutating the primary cleavage site or sites. This rationale is also effective in minimizing autolysis of proteases.[86]

The stabilization of enzymes through protein engineering has several distinct disadvantages relative to other stabilization techniques. The primary disadvantage associated with protein engineering is that a detailed structural understanding of the enzyme of interest is a prerequisite. Molecular modeling may assist in the identification of possible mutation sites. However, in many cases, detailed structural data is unavailable, thus making it practically impossible to rationally alter the enzyme's structure. The process of producing and purifying a recombinant enzyme can also be time consuming. For comparison, most chemical reactions that involve altering the surface of enzymes can be done in a matter of just minutes to at most hours whereas the time required to obtain a single purified mutant is on the order of days or weeks. Additionally, altering the structure of an enzyme may have a wide range of consequences with respect to its catalytic properties including many of which are unexpected. Thus, it may take

several rounds of introducing a mutation and analyzing its effects before obtaining an enzyme with the desired properties.

2.4.5 Directed Evolution

Directed evolution provides another pathway for developing enzymes with desired catalytic properties and stabilities. Although there may be many subtle variations, the general strategy of directed evolution is to construct a library of variants of the same enzyme and to subsequently selectively screen the library for variants that have the target functionality.[59, 87-91] To construct the library of variants, random mutations are typically introduced into the DNA coding sequence of the enzyme by means of chemical mutagenesis, error-prone polymerase chain reaction, and DNA shuffling. The process of introducing random mutations and screening for improved function is generally carried out several times, each time using the mutants that have the most improved function as the parental genes (i.e. the starting point) for the next cycle. Since the identification of improved mutant enzymes is based on the screening step, it is of critical importance that the assay used to measure the target function is both sensitive and not easily interfered with. Interferences, if not detected, can result in the selection of "junk", which are mutant enzymes that are of little or no use.

The use of directed evolution has proved to be an effective technique for generating robust enzymes. Enzymes have been evolved to have improved thermostability as well as increased pH stability and stability against oxidation, organic solvents, and surfactants.[59, 89, 91] Directed evolution may even be employed in conjunction with rational protein engineering to yield enzymes with improved stabilities.[92] In such cases, the enzyme is typically mutated first by site-directed mutagenesis and then by directed evolution.

Processes like evolution afford the opportunity to drastically alter enzyme stability without knowing anything about the enzyme's structure. This represents a considerable advantage over rational protein engineering, to which directed evolution is commonly compared to, which is based on the ability to predict a priori the effect of structural changes on enzyme function. However, directed evolution has its pitfalls as well. For example, in order for directed evolution to yield improvements of any kind, these improvements must be evolutionarily feasible in the first place. When this is not the case, it can lead one down a fruitless path. Additionally, while directed evolution may lead to stability enhancements, it may at the same time result in a dramatic loss of activity. The loss of activity in many cases may outweigh the benefit of stabilization. It is also possible for directed evolution to produce to a series of neutral mutations, which are those that do not improve or worsen enzyme stability. Furthermore, like rational protein engineering, the improvement of enzyme stability by directed evolution is a very long process, which can take upwards of weeks or months.

3.0 SPECIFIC AIMS

The overall objective of this research was to utilize fundamental relationship between enzyme structure, function, and environment to improve biocatalyst efficiency. The first aim of this thesis was to mediate solvent-enzyme interactions in anhydrous enzymology by engineering the physical properties of the reaction solvent. Because water is required for enzyme catalysis, even in anhydrous media, the properties of this essential water, such as pH, represent a key determinant of enzyme activity and stability. Thus, as a natural extension to the first aim, a novel approach to controlling pH within the aqueous microenvironment of an enzyme, for which purposes conventional buffers have limited utility, was investigated. Lastly, covalent modification with PEG was explored as method of enhancing the stability of proteases as the aqueous content of the reaction medium was increased. The purpose of this last section is to enhance the overall utility of proteases by making them more amenable to aqueous reactions.

Specific Aim 1: Determine the Impact of Ionic Liquid Physical Properties on Lipase Activity and Stability.

Ionic liquids are molten organic salts that have remarkable solvent properties and non-existent vapor pressures. Recently, their potential use as a "green" alternative to conventional solvents in non-aqueous biocatalysis has been met with great enthusiasm. To fully understand their utility in biocatalytic reactions, we have: 1) investigated how the physical properties of

ionic liquids vary with structure through solvatochromic probing and determination of partition coefficients, 2) measured lipase activity and stability in ionic liquids, 3) employed common methods of enzyme stabilization including adsorption, PEG-modification and multipoint covalent immobilization to enhance lipase activity in ionic liquids and 4) determined the degree to which lipase was irreversible inactivated in the ionic liquids. Additionally, we have examined the control of water activity in ionic liquids using salt hydrates and compared the effect of salt hydrates on lipase activity in ionic liquids and organic solvents.

Specific Aim 2: Demonstrate Dynamic pH Control in Nerve Agent Detoxification Using Competing Acid-Base Enzyme Reactions.

Hydrolytic reactions such as the enzymatic detoxification of nerve agents, if allowed to approach completion, can generate large amounts of acidic products, requiring effective pH buffering. To overcome buffering limitations of standard biological buffers in such reactions, we proposed a novel method of pH control based on the hypothesis that opposing acid and base forming enzyme reactions would create a dynamic pH equilibrium, essentially mimicking how cells manipulate their internal pH. This hypothesis was tested by employing urease-catalyzed hydrolysis of urea to buffer the degradation of the nerve agent mimic paraoxon by organophosphorous anhydrolase. The pH and conversion of paraoxon in the OPH-urease system was modeled using enzyme kinetic rate equations and experimentally verified. The extent to which ureases are inhibited by fluoride, a hydrolysis product of several G-type nerve agents, was also assessed. In order to improve the resistance of ureases, and thus biocatalytic pH control, to fluoride, the use of fluoride scavengers were explored. Alternative base-producing biocatalytic

reactions to be used in place of or in addition to urease to circumvent fluoride inactivation of the buffer were also identified.

Specific Aim 3: PEGylate Matrix Metalloproteinase-1 (MMP-1) and Characterize the Impact of PEG-Attachment on the Therapeutic Benefit Towards Reversing Scarring.

The effectiveness of enzyme therapies is limited by rapid clearance of the enzyme via proteolytic digestion, non-specific binding and immunogenic responses. Therapeutic enzymes that are digestive enzymes may have even shorter active lifetimes due to autolytic degradation. In this section, we investigated the use of PEGylation as a means of regulating biological interactions *in vivo* that impact the active lifetime of MMP-1, a zinc-containing endopeptidase that has considerable therapeutic potential in reversing the effects of scarring. PEG-MMP-1 was synthesized and characterized by protein electrophoresis and mass spectrometry analysis of the peptide fingerprint of tryptic digests of the modified protein. Additionally, residual MMP-1 activity after PEGylation was measured and thermal stability and resistance of the modified enzyme to proteolytic digestion were determined. The impact of PEGylation on the ability of MMP-1 to degrade pre-existing scar tissue was assessed in a muscle laceration model in mice.

4.0 CHARACTERIZATION OF ENZYME ACTIVITY AND STABILITY IN IONIC LIQUIDS

4.1 INTRODUCTION

Thermal stability and the non-existence of vapor pressure, which eliminates volatile organic compound (VOC) emissions, make ionic liquids an environmentally attractive alternative to conventional organic solvents. Recoverability and recyclability also render ionic liquids a practical solution to industrial environmental concerns.[33, 93] That said, little is known about the biological consequences of increased concentrations of ionic liquids in the environment.

As solvents for chemical processing, ionic liquids exhibit excellent properties including extremely high boiling points and the capacity to dissolve polar and non-polar, inorganic, and polymeric compounds.[33, 34] The chemical and physical nature of ionic liquids may be modified by exchanging the cation, anion, and attached substituents. This feature plays a key role in manipulating the solvent properties of an ionic liquid, thus enabling ionic liquids to be rationally designed for specific reaction systems.[34]

Replacement of organic solvents with ionic liquids in biocatalytic processes has recently gained much attention. Cull et al.[35] employed the ionic liquid 1-butyl-3-methylimidazolium hexafluorophosphate ([bmim][PF_6]) for the two-phase biotransformation of 1,3-dicyanobenzene

to 3-cyanobenzamide and 3-cyanobenzoic acid using the nitrile hydratase from *Rhodococcus* R312. This work estabilished ionic liquids as a potential alternative to organic solvents for multiphase biotransformations. The first reported enzymatic reaction in an ionic liquid, performed in our laboratory, involved the thermolysin-catalyzed synthesis of *Z*-aspartame in [bmim][PF_6].[11] In this report, it was shown that enzyme activity approached that observed in conventional organic solvents and that the enzyme was highly stabile in the ionic liquid. Since this work, there have been many reports of enzymatic catalysis in ionic liquids including the anhydrous transesterification of ethyl butanoate and butanol catalyzed by *Candida antarctica* lipase type B (CALB) in 1-butyl-3-methylimidazolium paired with hexafluorophosphate and tetrafluoroborate anions[36] and the α-chymotrypsin-catalyzed transesterification of *N*-acetyl-L-phenylalanine ethyl ester with 1-propanol in 1-butyl-3-methylimidazolium and 1-octyl-3-methylimidazolium hexafluorophosphate.[37]

Almost all enzymatic reactions performed to date have been in ionic liquids comprised of dialkylimidazolium cations and the hexafluorophosphate and tetrafluoroborate anions. Only recently have other cations and anions begun to be studied.[94-96] In this chapter, the viability of replacing conventional biocatalytic solvents with ionic liquids consisting of combinations of dialkylimidazolium and N-methyl-N-(-2-methoxyethyl) pyrolidinium cations with a broad range of anions including hexafluorophosphate, acetate, nitrate, methanesulfonate, trifluoroacetate and trifluoromethylsulfonate was investigated, with the interest of expanding the portfolio of potential solvent systems (**Figure 4**).

Herein, the first attempt of enzyme catalysis with pyrolidinium cations is described. The lipase-catalyzed transesterificataion of methyl methacrylate and 2-ethylhexanol was used as a model reaction for determining enzyme activity as a function of ionic liquid physical properties

(**Figure 5**). The polarity and hydrophobicity of ionic liquids as determined via solvatochromic and octanol-water partition coefficient analysis respectively is also compared to those of organic solvents commonly employed in biocatalytic reactions. Additionally, the use of salt hydrates to control the thermodynamic water activity (a_w), which may impact enzyme activity, specificity and hydrolytic equilibria, in ionic liquids and their effect on lipase catalysis in ionic liquids was explored.

1-Butyl-3-methylimidazolium [bmim]

1-methyl-1-(-2-methoxyethyl)pyrrolidinium [mmep]

Figure 4. Structure of ionic liquids. Anions available for X_1^- were hexafluorophosphate ($[PF_6]$), acetate ($[CH_3CO_2]$), nitrate ($[NO_3]$) and trifluoroacetate ($[CF_3CO_2]$). Anions available for X_2^- were hexafluorophosphate ($[PF_6]$), acetate ($[CH_3CO_2]$), nitrate ($[NO_3]$), trifluoroacetate ($[CF_3CO_2]$), trifluoromethylsulfonate ($[CF_3SO_3]$) and methanesulfonate ($[CH_3SO_3]$).

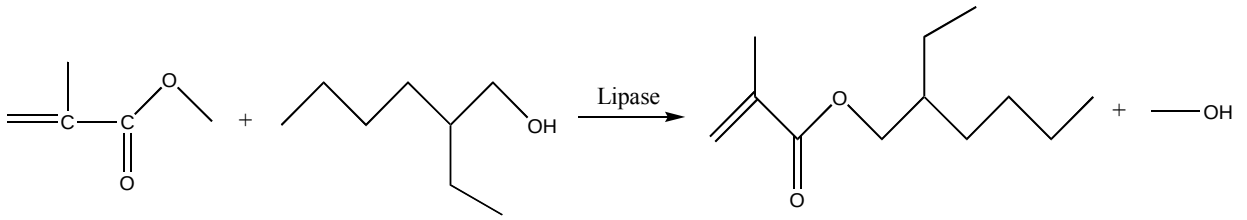

Methylmethacrylate **2-Ethyl-1-hexanol** **2-Ethylhexylmethacrylate** **Methanol**

Figure 5. Lipase-catalyzed transesterification of methyl methacrylate and 2-ethylhexanol to 2-ethylhexyl methacrylate.

4.2 MATERIALS AND METHODS

4.2.1 Materials

Lipase L-1754 (*Candida rugosa*) and Chirazyme L-2, carrier-fixed, C2, lyophilizate (*Candida antarctica* type B) were purchased from Sigma (St. Louis, MO) and BioCatalytics (Pasadena, CA) respectively. Novozym 435 was obtained as a gift from Novo Nordisk (Bagsvaerd, Denmark). All enzymes were used without further purification. Hypol 3000 was purchased from Hampshire Chemical (Lexington, MA). L-62 Pluronic was generously supplied by BASF (Parsippany, NJ). The 1-butyl-3-methylimidazolium hexafluorophosphate ([bmim][PF_6]) employed in water activity and water transfer experiments as well as in transesterification reactions with salt hydrates was purchased from Solvent Innovations GmbH (Cologne, Germany). Ionic liquids employed in all other experiments, including [bmim][PF_6], were synthesized and purified by SACHEM Inc. (Austin, TX) and used as supplied. All other reagents were purchased from Aldrich (St. Louis, MO) and were of the highest purity available.

4.2.2 Methods

4.2.2.1 Determination of Octanol-Water Partition Coefficients

Partition coefficients for ionic liquids were determined as a ratio of ionic liquid concentration in the octanol phase to that in the aqueous phase (**Equation 5**). The logarithm of the partition coefficient is referred to as the log *P* value.

$$\text{Partition Coefficient } (P) = \frac{[\text{solute}]_{\text{Octanol Phase}}}{[\text{solute}]_{\text{Aqueous Phase}}} \qquad \textbf{(Eq. 5)}$$

The "shake flask" method was employed for the determination of all log *P* values.[97] The imidazolium ring present in the dialkylimidazolium-containing ionic liquids absorbs strongly at approximately 211 nm and can be quantified by UV spectrometry.[98] Water-saturated octanol and octanol-saturated water were used in all experiments. For each ionic liquid, the maximum wavelength (λ_{max}) due to absorbance of the imidazolium ring was verified in both phases. The volume ratio of the octanol to aqueous phases was varied in an attempt to determine the necessary ratio to force the solute into the hydrophobic octanol phase to a detectable level. A 100:1 volume ratio was employed for the portioning of all ionic liquids.

In a 200-mL separatory funnel, ionic liquid was added to the saturated phases such that its final concentration did not exceed 10 mM in either phase. Inversion of the separatory funnel was carrier out at room temperature for 5 min at an approximate rate of 20 inversions/min. The phases were subsequently recovered and centrifuged to eliminate emulsions formed during partitioning. The absorbance at λ_{max} was measured in both phases using a Perkin-Elmer (Wellesley, MA) Lambda 45 UV/VIS spectrophotometer. Standard curves of concentration in both phases were prepared for all ionic liquids.

4.2.2.2 Solvatochromic Characterization

Polarity values (E^{N}_{T}) of ionic liquids and organic solvents were measured as described previously by Fletcher and co-workers.[99] Reichardt's dye was dissolved in the solvent and centrifuged to remove any residual dye particulates (**Figure 6**). The visible spectrum of the dye-containing solvents was scanned to determine the absorption band, which was subsequently correlated to an E^{N}_{T} value (**Equations 6 and 7**).

$$E_T(\text{solvent})[\text{kcal/mol}] = \frac{28591}{\lambda_{max}[\text{nm}]} \qquad \textbf{(Eq. 6)}$$

$$E^{N}_{T} = \frac{E_T(\text{solvent}) - 30.7}{32.4} \qquad \textbf{(Eq. 7)}$$

The normalized polarity scale ranges from water being the most polar (λ_{max} = 453 nm, E^{N}_{T} = 1.0) to tetramethylsilane being the least polar (λ_{max} = 925 nm, E^{N}_{T} = 0.0). All ionic liquids were dried in a vacuum oven (26 in Hg) at 70 °C for several days prior to analysis.

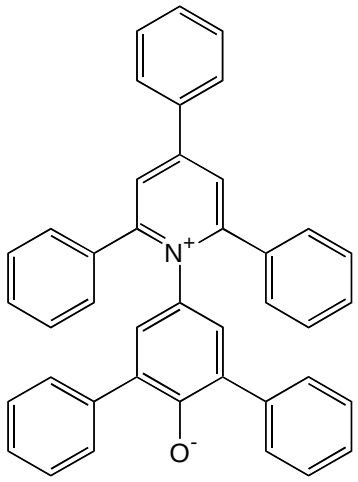

Figure 6. Reichardt's dye (2,6-diphenyl-4-(2,4,6-triphenylpyridinio)phenolate).

4.2.2.3 Poly(Ethylene Glycol)-Modified Lipase Synthesis

Free lipase (*Candida rugosa*) was dissolved in aqueous buffer (10 mM Tris, 5 mM calcium chloride, pH 7.5) at a concentration of 1 mg/mL. Poly(ethylene glycol)-monoisocyanate (PEG-NCO) was added in excess to the lipase solution at a 100:1 molar ratio of PEG-to-lipase. The reaction mixture was vigorously mixed at room temperature of 30 min and subsequently lyophilized.[100] No further purification such as the removal of unreacted PEG was attempted. The freeze-dried enzyme was employed in all experiments its crude form.

4.2.2.4 Lipase-Containing Polyurethane Foam Synthesis

The synthesis of lipase (*Candida rugosa*)-containing polyurethane foam was carried out using the procedure described by LeJeune and Russell.[80] Briefly, lipase (1 g) was added to aqueous buffer (2.5 mL; 50 mM Bis-Tris propane, 5 mM calcium chloride, pH 7.5) containing 1 %(w/w) L-62 Pluronic surfactant. Hypol 3000 (2.5 g), a toluene diisocyanate based pre-polymer, was added to the aqueous lipase solution and vigorously mixed for 30 s and 2500 rpm using a hand drill. The lipase-immobilized polyurethane foam was cured overnight at ambient temperature and pressure and subsequently stored at 4 °C. In preparation for use in transesterification reactions, the foam was ground into small particles using a drill fitted with a handmade bit wrapped in sandpaper (grit no. 180). The drill was set at a low rpm setting and the drill speed was kept constant to obtain a constant particle size.

4.2.2.5 Lipase Stability in Ionic Liquids

Lipase was incubated in organic solvent or ionic liquid (1 mL) at a specified temperature (30 or 50 °C) for various lengths of time. The enzyme solution was agitated at 300 rpm in a constant temperature shaker. The solvent then extracted and lipase activity was assayed using

the Sigma (St. Louis, MO) lipase diagnostic kit, which measures the rate in which the lipase catalyzes the conversion of olive oil triglycerides to fatty acids in buffer. The amount of fatty acids generated was measured via titration with sodium hydroxide (0.5 N).

4.2.2.6 Water Activity Measurements in Ionic Liquids Using Humidity Sensor

Salt hydrate (0.2 g/mL) and the ionic liquid [bmim][PF_6] were added to a glass test tube to which a HY-CAL Engineering (Elmonte, CA) Ultra-HTM humidity sensor was tightly sealed. The test tube and sensor were housed in a 25 °C constant temperature air bath in which all relative humidity measurements were recorded. Prior to all experiments, the sensor was calibrated with dry nitrogen, deionized water, and saturated salt solutions of lithium chloride, potassium carbonate, and sodium chloride. The sensor was allowed to equilibrate to in the sample to obtain a stable reading, which typically required less then 12 hr. In all experiments, only the higher hydrate of a salt hydrate pair was added to the test tube. Water is released by the salt to the sample resulting in the formation of the lower salt hydrate, thus creating an equilibrium state between the higher and lower hydrates. Salt hydrate pairs are referred in shorthand notation by stating the salt followed by the number of associated water molecules in the higher and lower hydrate. For example, NaI 2/0 refers to a mixture of NaI•$2H_2O$ and NaI•$0H_2O$.

4.2.2.7 Water Transfer Measurements in Ionic Liquids

The ionic liquid [bmim][PF_6] (10 g), which contained less than 0.1 % (w/w) water, was added to a 20-mL glass vial containing salt hydrate (0.2 g/mL). In all cases, only the higher hydrate of a salt hydrate pair was added. The salt hydrate-containing ionic liquid solutions were incubated at 25 °C while agitated at 300 rpm in a constant temperature shaker. Samples were

withdrawn periodically, filtered and assayed for water content using a Mettler Toledo (Columbus, OH) DL31 Karl Fischer (KF) titrator. In KF titration, the amount of water in a solvent is determined by consumption of the water when reacted with methanol, an alkyl imidazole reagent and iodine in the presence of excess sulfur dioxide. Because the water and iodine react in a 1:1 stoichiometry, the water content is directly proportional to the amount of iodine consumed, which is measured potentiometrically.[101]

4.2.2.8 Lipase-Catalyzed Transesterification of Methyl Methacrylate and 2-Ethylhexanol

The substrates methyl methacrylate and 2-ethylhexanol were dissolved separately in solvent at a concentration of 200 mM. Reactions were initiated by the addition of substrate stock solutions (1 mL) to lipase in a 5-mL glass vial. The enzyme suspension was sonicated for approximately 15 s to achieve a homogeneous distribution of the enzyme. The reaction vials where then immediately placed in a constant temperature shaker set at 30 °C and 300 rpm. Samples were withdrawn periodically and assayed for 2-ethylhexyl methacrylate formation via gas chromatography.[25, 102] When performing reactions in organic solvents, aliquots (1.0 μL) were removed from the reaction using a 1-μL Hamilton (Reno, NV) syringe. When performing reactions in ionic liquids, 2-ethylhexyl methacrylate was recovered via liquid extraction into hexane. All GC measurements were made with a Perkin-Elmer (Wellesley, MA) Autosystem GC fitted with an Alltech (Deerfield, IL) EC-1000 capillary column (30 m × 0.53 mm × 1.0 μm). A 1:4 split ratio using helium as the carrier gas was employed and the injector and detector temperatures were set to 300 °C. The oven program consisted of an initial temperature of 100 °C, which was maintained for 2 min. The temperature was then ramped to 160 °C at a rate of 25 °C /min and held for 3 min. Using these conditions, the retention time of 2-ethylhexyl

methacrylate was 5.1 min. A calibration curve of peak area versus concentration of 2-ethylhexyl methacrylate in the presence of the substrates was prepared for each organic solvent and ionic liquid. No internal standard was used; however, the GC was calibrated daily.

In transesterification reactions at controlled water activities, all components were pre-equilibrated with the salt hydrates for 1 h at 30 °C and 300 rpm prior to initiating the reaction. Typically, lipase and salt hydrate (0.4 g) were added to 2-ethyhexanol (200 mM) in a 5-mL glass vial. The same salt hydrate was added to methyl methacrylate (200 mM) in a separate vial. After equilibration, reactions were started by the addition of methyl methacrylate (1 mL) to the solution of 2-ethylhexanol (1 mL) containing enzyme and salt hydrate at a 1:1 (v/v) ratio. Crushed molecular sieves were substituted for salt hydrate in "dry" reactions.

4.3 RESULTS AND DISCUSSION

4.3.1 Physical Characterization of Ionic Liquids

Solvent selection for enzymatic reactions can be severely constrained due to the inherent deactivating effects of many solvents, which is particularly problematic with hydrophilic solvents. This ultimately limits the scope of biocatalytic reactions that can be performed in non-aqueous media. Hildebrandt solubility parameters (δ), dielectric constants (ε), and dipole moments (μ) may be employed to predict enzyme activity in solvent systems. However, the most common method of predicting enzyme activity is through the use of octanol-water partition coefficients.[31, 103] Solvatochromic parameters provide a simple and rapid means of assessing solvent polarity.[31]

A partition coefficient, which is often reported as a logarithmic value (log *P*), measures how a solvent distributes between an aqueous (water) and organic (1-octanol) phase, thus indicating solvent hydrophobicity. Laane et al.[31] reported that solvents with a log *P* less than two are considered hydrophilic in nature and tend to be unfavorable for enzymatic reactions. In contrast, solvents with a log *P* of greater than four generally support enzyme activity. Although log *P* analysis is a frequently employed method for gauging biocompatibility, it is important to note that this method is not always an accurate predictor of enzyme activity.[31, 103]

To our knowledge, these results are the first determinations of log *P* values for ionic liquids. Huddleston and colleagues[104] recently reported the existence of a distinct correlation between the partitioning of several substituted-benzene derivatives in a [bmim][PF_6]/water system. However, the authors do not explicitly measure, calculate, or approximate the log *P* of [bmim][PF_6] in an 1-octanol-water or any other biphasic system.

The experimentally measured log *P* for the ionic liquids investigated ranged from -2.39 to -2.90 (**Table 1**). For comparison, the reported log *P* for hexane, acetonitrile and tetrahydrofuran are 3.5, -0.33 and 0.49 respectively.[31] Based on the guidelines detailed by Laane and co-workers, this would indicate that the ionic liquids are highly hydrophobic and would likely inactivate enzymes. Because UV spectra of the pyrrolidinium-containing ionic liquids did not yield any characteristic absorption peaks, the log P for these ionic liquids could not be determined.Because the pyrrolidinium-containing ionic liquids did not absorb light in the UV region, their respective log *P* values could not be determined.

Table 1. Log *P* and Reichardt's dye (E^N_T) polarity values for ionic liquids and select organic solvents.

Solvent	E^N_T	log *P*
1-Butyl-3-methylimidazolium acetate	0.57	-2.77 ± 0.11
1-Butyl-3-methylimidazolium nitrate	0.65	-2.90 ± 0.01
1-Butyl-3-methylimidazolium trifluoroacetate	0.63	-
1-Butyl-3-methylimidazolium hexafluorophosphate	0.67	-2.39 ± 0.27
1-Methyl-1-(-2-methoxyethyl)pyrrolidinium acetate	0.52	-
1-Methyl-1-(-2-methoxyethyl)pyrrolidinium nitrate	0.84	-
1-Methyl-1-(-2-methoxyethyl)pyrrolidinium trifluoroacetate	0.37	-
1-Methyl-1-(-2-methoxyethyl)pyrrolidinium trifluoromethylsulfonate	0.91	-
1-Methyl-1-(-2-methoxyethyl)pyrrolidinium methanesulfonate	0.78	-
Hexane	0.009	3.5
Tetrahydrofuran	0.207	0.49
Acetonitrile	0.47	-0.33

The polar nature of ionic liquids was determined via measuring the solvatochromic parameter E^N_T, which is a normalized dimensionless value obtained from the shift of the charge-transfer absorption band of the solvatochromic probe Reichardt's dye in a solvent. Changes in the position of the charge-transfer absorption band within the visible spectrum result from hydrogen bonding between the solvent and the phenoxide oxygen atom present in the dye. An E^N_T value is determined spectroscopically as a function of the band shift (**Figure 7**).[32, 105]

Figure 7. Solvatochromic probing of organic solvents (from left: tetrahydrofuran, acetonitrile, methanol, t-amyl alcohol and acetone) with Reichardt's dye. Differences in solvent polarity alter the absorption energy of the dye. These differences are reflected by the visible color of the dye-containing solutions.

There are only a few reported cases of the solvatochromic characterization of ionic liquids.[99, 105-109] Results of the solvatochromic probing of [bmim][PF_6] with Reichardt's dye reported in the literature indicate that the dry ionic liquid has an E^N_T value very similar to that of ethanol (E^N_T = 0.67) and other short chain primary alcohols.[95, 99, 105, 106, 109] This value is sensitive to the water content of the ionic liquid.[106, 107] Muldoon and colleagues[105] suggest E^N_T's for ionic liquids are dependent upon the strength of hydrogen bonding between the cation of the ionic liquid and the phenoxide group in Reichardt's dye. A high E^N_T indicates that strong hydrogen bonding forces are present within the ionic liquid-dye complex. Hydrogen bonding with solvent molecules may perturb enzyme structure, leading to lose of function.

Results of solvatochromic analysis of [bmim][PF_6] in this study closely match the reported E^N_T (**Table 1**). Replacement of the [PF_6] anion with [CH_3CO_2], [NO_3] and [CF_3CO_2]

yielded E^N_T's of 0.57, 0.65 and 0.63 respectively. This small change in the polarity series is consistent with previous work.[105] The ionic liquids [mmep][CH_3CO_2], [mmep][NO_3], [mmep][CF_3CO_2], [mmep][CF_3SO_3] and [mmep][CH_3SO_3] have E^N_T's of 0.52, 0.84, 0.37, 0.91 and 0.78 respectively. Based on these results, the polarity of pyrrolidinium-containing ionic liquids appears to be strongly dependent on the anion. With the exception of [mmep][CF_3CO_2], the E^N_T's for all ionic liquids studied were greater than those of acetonitrile and other organic solvents commonly employed in non-aqueous biocatalysis.[32] Nonetheless, the polar nature of ionic liquids constitutes an ideal reaction media for biotransformations involving highly polar substrates such as carbohydrates, which contain multiple hydroxyl functionalitites and are not miscible in conventional solvents such as hexane.

4.3.2 Lipase Activity in Ionic Liquids

To determine impact of ionic liquids on enzyme activity, initial reaction rates of the lipase-catalyzed transesterification of methyl methacrylate and 2-ethylhexanol were measured in several ionic liquids and compared to rates observed in organic solvents. Our experience with this reaction system, combined with an extensive data set, made this an ideal model enzymatic reaction. The selection of lipase for these experiments was based on prior work in which several lipases including Amano lipases G (*Penicillium camembertii*), AY (*Candida rugosa*), AK (*Pseudomonas fluorescens*), MAP (*Mucor javanicus*), FAP (*Rhizopus oryzae*), PS (*Pseudomonas cepacia*) and Sigma lipases L1754 (*Candida rugosa*), L0763 (*Chromobacterium viscosum*), L3001 (wheat germ) were screened for activity in hexane using the same reaction.[25, 102] Reaction conditions of the transesterifications, 30 ºC and 300 rpm, were equivalent to those employed in this study, eliminating any potential temperature or mixing effects on lipase activity. Results of

the lipase screen indicated that *Candida rugosa* lipase was the most active and thus was selected as the model enzyme for this study.

In [bmim][PF_6], free lipase catalyzed the transesterification at an initial rate of 6.75 μM/hr/mg-enzyme, 1.5 times faster than the reaction in hexane (3.90 μM/hr/mg-enzyme; **Table 2**). Although [bmim][PF_6] showed promise as an effective solvent for the transesterification, the enzyme was inactive in all other ionic liquids investigated ([bmim][CH_3CO_2], [bmim][NO_3], [bmim][CF_3CO_2], [mmep][CH_3CO_2], [mmep][NO_3], [mmep][CH_3SO_3], [mmep][CF_3CO_2] and [mmep][CF_3SO_3]). No lipase activity was observed in the more polar organic solvents tetrahydrofuran or acetonitrile.

Table 2. Initial rates of lipase-catalyzed transesterification of methyl methacrylate and 2-ethylhexanol in ionic liquids and organic solvents. All initial rates are reported in the units μM/hr/mg-enzyme.

Solvent	Free Lipase (*Candida Rugosa*)	Novozym 435 (*Candida antarctica*)	Lipase-Immobilized Polyurethane Foam (*Candida rugosa*)	PEG-Lipase (*Candida rugosa*)
[bmim][CH_3CO_2]	0	0	0	-
[bmim][NO_3]	0	0	0	0
[bmim][PF_6]	6.75	15.8	0.93	0
[bmim][CF_3CO_2]	0	-	-	-
[mmep][CH_3CO_2]	0	0	0	0
[mmep][NO_3]	0	0	-	-
[mmep][CH_3SO_3]	0	0	0	-
[mmep][CF_3CO_2]	0	-	-	-
[mmep][CF_3SO_3]	0	-	-	-
Hexane	3.90	3.68	-	0.75
Tetrahydrofuran	0	0	-	-
Acetonitrile	0	8.85	-	-

Water was added to ionic liquids, 25 to 100 μL H_20/mL-ionic liquid, in attempt to activate free lipase in [bmim][NO_3] and [mmep][CH_3CO_2]. However, hydration of the enzyme failed to improve activity in either of the ionic liquids, making stripping of essential water molecules from the enzyme by the ionic liquids an unlikely mechanism of deactivation. Moreover, addition of the hydrophilic ionic liquids [bmim][NO_3] and [bmim][CH_3CO_2] as co-solvents to [bmim][PF_6] was also investigated as a means of supporting enzyme activity while increasing the overall polarity of the reaction media. The amount of the hydrophilic ionic liquids was varied such that the final concentration of [bmim][PF_6] in the bmim][NO_3]/[bmim][PF_6] and

[bmim][CH_3CO_2]/[bmim][PF_6] mixtures was 25, 50, or 75 % (v/v). Despite the use of [bmim][PF_6] as a co-solvent, no lipase activity was observed in any of the mixed ionic liquid mixtures, indicating [bmim][PF_6] did not prevent inactivation of the enzyme.

Our results suggest enzyme activity in ionic liquids is anion dependent. Anions such as [NO_3], [CH_3CO_2] and [CF_3CO_2] are more nucleophilic than [PF_6] and may coordinate more strongly to positively charged sites in lipase's structure causing conformation changes.[110] Similar results observed with [mmep][NO_3], [mmep][CH_3CO_2], [mmep][CF_3CO_2], [mmep][CF_3SO_3] and [mmep][CH_3SO_3] in which all anions are strong nucleophiles further supports the notion that nucleophilicity is critical to enzyme activity. However, due to little work with pyrrolidinium-containing ionic liquids, the possibility that the pyrrolidinium cation inhibits enzyme activity must not be ruled out. This new data calls into question the broad utility of ionic liquids as solvents for biocatalysis unless the deactivating mechanism can be understood and reversed.

4.3.3 Use of Modified and Immobilized Lipases in Ionic Liquids

Having shown free lipase to be inactive in all ionic liquids with the exception of [bmim][PF_6], several methods of enzyme stabilization were investigated in attempt to improve lipase activity in the ionic liquids. Adsorption, PEG-modification, and multipoint covalent immobilization in polyurethane foam are techniques that prevent deactivating conformational changes in harsh environments and enhance enzyme activity.[80, 111, 112] The effectiveness of these stabilization methods on lipase activity in ionic liquids was determined by employing the various lipase forms to catalyze the transesterification reaction.

Using *Candida antarctica* lipase, type B adsorbed onto a macroporous acrylic support (Novozym 435), initial rates of 3.68 and 8.85 μM/hr/mg-enzyme were observed in hexane and acetonitrile respectively while no activity was detected in tetrahydrofuran (**Table 2**). In all of the ionic liquids screened ([bmim][PF_6], [bmim][CH_3CO_2], [bmim][NO_3], [mmep][CH_3CO_2], [mmep][NO_3] and [mmep][CH_3SO_3]), Novozym 435 was only activity in [bmim][PF_6] (15.8 μM/hr/mg-enzyme).

Modification with PEG, in addition to its stabilizing effects, greatly enhances the solubility of enzymes in non-aqueous media and in turn, as a result of reduced mass transfer limitations, may have activating effects.[112] Although PEG-modified *Candida rugosa* lipase catalyzed the transesterification reaction in hexane (0.75 μM/hr/mg-enzyme), no improvement in lipase activity relative to that of free lipase was detected in [bmim][PF_6], [bmim][NO_3] or [mmep][CH_3CO_2] as a result of PEGylation (**Table 2**).

Multipoint covalent immobilization was considered by incorporating lipase (*Candida rugosa*) into the preparation of waterborne polyurethane foam. Reactive residues on the surface of the enzyme are conjugated to the polymer backbone during synthesis, thus making the enzyme a monomer in the polymerization step. Drevon and Russell[113] reported the irreversible immobilization of the nerve-agent degrading enzyme diisofluorophosphatase in polyurethane foam. Upon thorough rinsing with water, less than 1 % (w/w) enzyme leached from the enzyme-containing polyurethane. Additionally, the immobilized enzyme retained 67 % activity relative to the native enzyme. The transesterification catalyzed by polyurethane-immobilized lipase yielded an initial rate of 0.93 μM/hr/mg-enzyme (**Table 2**). However, no detectable activity was observed [bmim][CH_3CO_2], [bmim][NO_3], [mmep][CH_3CO_2] or [mmep][CH_3SO_3] thereby indicating immobilization was ineffective in activating lipase in the ionic liquids.

Sheldon and co-workers[110] reported similar results using immobilized forms of *Candida antarctica* lipase type B. Conversions of less than 5 % in a 24 hr period were measured in the transesterification of phenylglycine methyl ester using cross-linked enzyme crystals and cross-linked enzyme aggregates. The lack of immobilized lipase activity when employing a different lipase than that used in this work supports our conclusion that the described activating techniques would most likely prove ineffective in enhancing the activity of lipases from other sources in the ionic liquids as well. Clearly, for the broad range of ionic liquids tested, ionic liquids are not the panacea for non-aqueous biocatalysis that we had hoped.

4.3.4 Lipase Stability in Ionic Liquids

The stability of Novozym 435 in ionic liquids was explored to determine if lipase inactivation in the ionic liquids was permanent (i.e. irreversible). Novozym 435 was incubated in the ionic liquid for a specific period of time after which the enzyme was recovered via extraction of the ionic liquid, diluted with water, assayed for hydrolytic activity. The ionic liquid was extracted using pipette with care taken to minimize enzyme loss. The relative activity results indicate the fraction of lipase irreversibly inactivated as a result of incubation in the ionic liquid. However, these experiments as performed do not represent the stability of lipase in catalyzing a reaction.

Upon incubation in [bmim][PF_6] for 24 hr at 30 ºC, Novozym 435 retained 96 % of its initial activity (**Figure 8**). Unlike in [bmim][PF_6], the enzyme was considerably less stable in the other ionic liquids [mmep][NO_3] and [bmim][NO_3] at the same temperature and over the same time period. However, incubation in [mmep][CH_3SO_3], [bmim][CH_3CO_2] and [mmep][CH_3CO_2] resulted in marked increases in enzyme activity once re-suspended in water.

Relative activities after removal from [mmep][CH_3CO_2], [bmim][CH_3CO_2] and [mmep][CH_3SO_3] were 297, 202 and 176 % respectively. For comparison, at the same conditions, no activity loss was observed when incubated in hexane, whereas Novozym 435 was completely inactivated after incubation in butanol (**Figure 9**). Relative activity retentions of 73, 68 and 55 % respectively were measured after incubation in tetrahydrofuran, acetonitrile and dimethyl sulfoxide.

Interestingly, although the ionic liquids [mmep][CH_3SO_3], [bmim][CH_3CO_2] and [mmep][CH_3CO_2] do not support lipase activity, they cause irreversible activation of the adsorbed enzyme. One plausible explanation for the activation effect is that these ionic liquids swell the acrylic resin on which the enzyme is adsorbed, causing previously inaccessible enzyme to be accessed once returned to water. While seemingly less likely, it also cannot be ruled out that the ionic liquid exposed enzyme has a modified tertiary structure with increased activity in water. Further elucidation of enzyme structure in these ionic liquids via spectroscopic techniques such as circular dichroism is required to fully explain this data set.

Sheldon et al.[110] recently studied the stability of free lipase (*Candida antarctica*), Novozym 435, cross-linked lipase crystals and cross-linked lipase aggregates in several ionic liquids. The authors reported that after 100 hr of incubation in [bmim][PF_6] at 80 °C, an increase (120 %) in free lipase activity was observed. Similarly, results indicated an increase (350 %) in Novozym 435 activity after 40 hr incubation in [bmim][PF_6] at the same temperature. It is suggested that the ionic liquid coated and thus protected the layer of essential water surrounding the free and adsorbed lipases, but it is hard to explain the increases in activity through a merely protective mechanism. We believe that one must invoke a permanent activating conformational change or an increase in active site concentration to explain this unusual data.

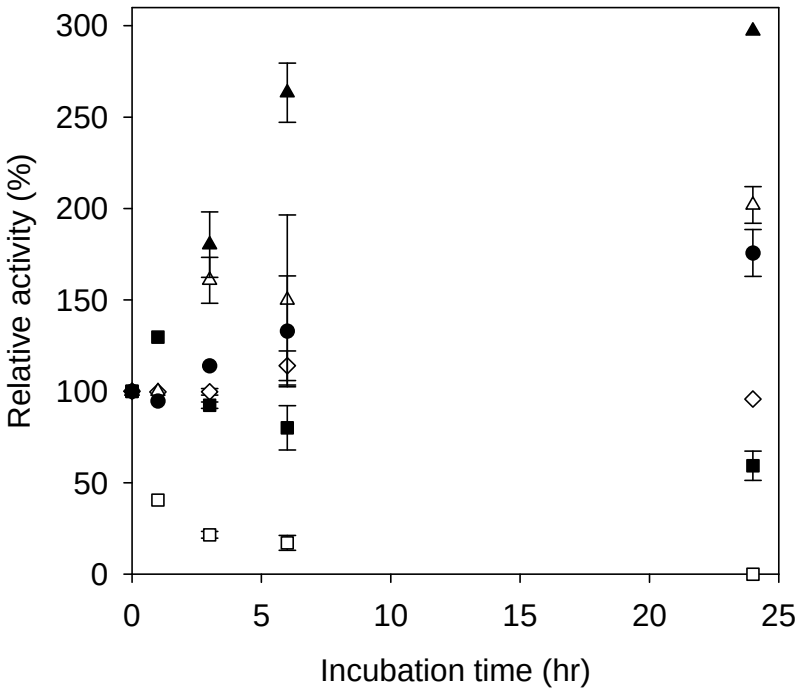

Figure 8. Stability of Novozym 435 in ionic liquids ([bmim][PF_6] (◇), [bmim][NO_3] (□), [bmim][CH_3CO_2] (Δ), [mmep][NO_3] (■), [mmep][CH_3CO_2] (▲) and [mmep][CH_3SO_3] (●)). Error bars represent the standard deviation for two separate experiments.

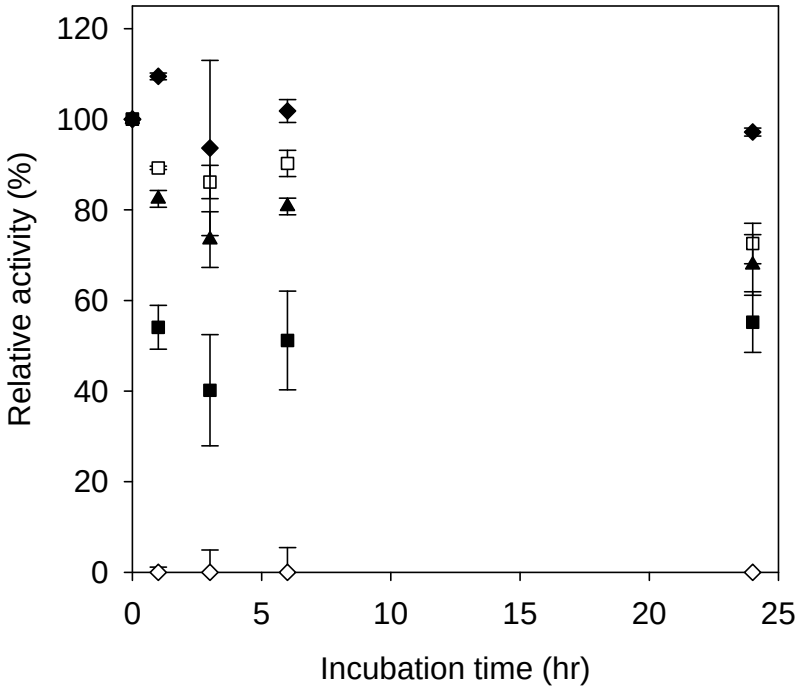

Figure 9. Stability of Novozym 435 in organic solvents (butanol (◇), tetrahydrofuran (□), acetonitrile (▲), dimethyl sulfoxide (■) and hexane (◆)). Error bars represent the standard deviation for two separate experiments.

4.3.5 Controlled Water Activity in Ionic Liquids

The degree of enzyme hydration is a critical parameter in non-aqueous or gas phase biocatalytic reactions.[24, 38, 39, 96, 114] In addition to its effects on enzyme activity, thermodynamic water activity (a_w), which describes the amount of water available to the enzyme, may also impact enzyme specificity and shift the reaction equilibrium thereby defining the efficiency of the desired reaction.[24] Because solvent properties influence enzyme activity, true comparison of enzyme reaction rates in different mediums can only be obtained at controlled a_w. In the case of

ionic liquids, a_w control is particularly critical since ionic liquids are hygroscopic and can absorb considerable amounts of water. Hence, in order to realize the absolute effect of ionic liquids on enzyme activity and stability, methods of controlling a_w in ionic liquids must be explored.

Common methods for controlling a_w in organic solvents include pre-equilibration with saturated salt solutions and the addition of various amounts of water to the reaction system.[24] These methods, although simple and effective, are subject to adsorption or evaporation of water to or from the environment and thus are only applicable for initial rate measurements and are not practical for large scale reactions. Furthermore, pre-equilibration typically requires lengthy time periods on the order of days to weeks. Salt hydrates may also be employed to control a_w in solvent systems.[24-29] Through the inter-conversion of the salt between higher and lower hydration states, a dynamic water equilibrium is established that tightly controls a_w in the reaction medium. Each salt hydrate pair has an intrinsic fixed a_w equilibrium and as long as residual amounts of the solid salts are present, a_w remains constant.[26]

To date, there have been only a few reports on the control of a_w in ionic liquids, all of which have involved pre-equilibration of the ionic liquid with a saturated salt solution.[96, 114] In this study, salt hydrate control of a_w in the ionic liquid [bmim][PF_6] is investigated.

Initially, the a_w of [bmim][PF_6] with several salt hydrates was determined by measuring the humidity, which is equal to a_w at equilibrium, of the gas headspace above the ionic liquid. Eckstein et al.[114] recently reported that ionic liquids have high salt hydrate solubilities, indicating a_w control using salt hydrates in ionic liquids was not feasible. However, our results indicate otherwise as of the seven salt hydrates investigated, a_w was controlled in the ionic liquid with all but one (NaI). All measured a_w values for the salt hydrates closely match reported literature values with the exception of NaI, which partially dissolved in the ionic liquid (**Table 3**).

Although partial dissolution of a salt hydrate should not prevent a_w control, the salt ions may, in the case of a biocatalytic reaction, adversely impact enzyme activity. For example, the salt may bind to the enzyme surface thereby inducing conformational changes. The solubility of the salt hydrate $CuSO_4$•5H2O in other ionic liquids was also screened. The salt hydrate did not dissolve in [mmep][CH_3SO_3] or [mmep][CF_3SO_3], whereas it was soluble in [bmim][NO_3], [bmim][CH_3CO_2], [mmep][CF_3CO_2] and [mmep][CH_3CO_2].

Table 3. Water activities of [bmim][PF_6] containing salt hydrates at 25 °C measured using a humidity sensor. The values were compared to the water activity of salt hydrates in organic solvents, which were compiled from the literature.

	a_w		
Salt Hydrate Pairs	**Halling[27]**	**Zacharis et al.[29]**	**[bmim][PF_6]**
NaI 2/0	0.12	0.07	0.17
Na_2HPO_4 2/0	0.16	-	0.17
NaAc 3/0	0.28	0.34	0.28
$CuSO_4$ 5/3	0.32	0.42	0.42
$Na_4P_2O_7$ 10/0	0.49	0.47	0.47
Na_2HPO_4 7/2	0.61	0.61	0.63
Na_2HPO_4 12/7	0.80	0.79	0.78

Controlled a_w in [bmim][PF_6] was also verified by assaying the water content of the salt hydrate containing ionic liquids over time via KF titration. The salt hydrates were categorized as quick or slow based on the length of time required to approach the equilibrium a_w (**Figure 10**). Equilibrium a_w was obtained rapidly in the ionic liquid containing Na_2HPO_4 2/0, Na_2HPO_4 7/2,

Na_2HPO_4 12/7 and NaAc 3/0. Slow salt hydrates included $Na_4P_2O_7$ 10/0 and $CuSO_4$ 5/3. Similar results were reported by Zacharis et al.[29] in which the rate of water transfer to isopropyl ether was rapid with Na_2HPO_4 12/7, Na_2HPO_4 7/2 and NaAc 3/0 and slow with $Na_4P_2O_7$ 10/0. The similar trends in water transfer rates in [bmim][PF_6] and isopropyl ether suggest that salt hydrate properties are comparable in ionic liquids and conventional organic solvents.

The correlation between equilibrium water content and a_w in [bmim][PF_6] containing salt hydrates and in [bmim][PF_6] subjected to vapor-phase pre-equilibration with saturated salt solutions was compared (**Figure 11**). Results indicate the methods of a_w control yield identical trends and closely match the data reported by Anthony et al.[98], who measured the water content in [bmim][PF_6] using a gravimetric microbalance over a range of water vapor pressures.

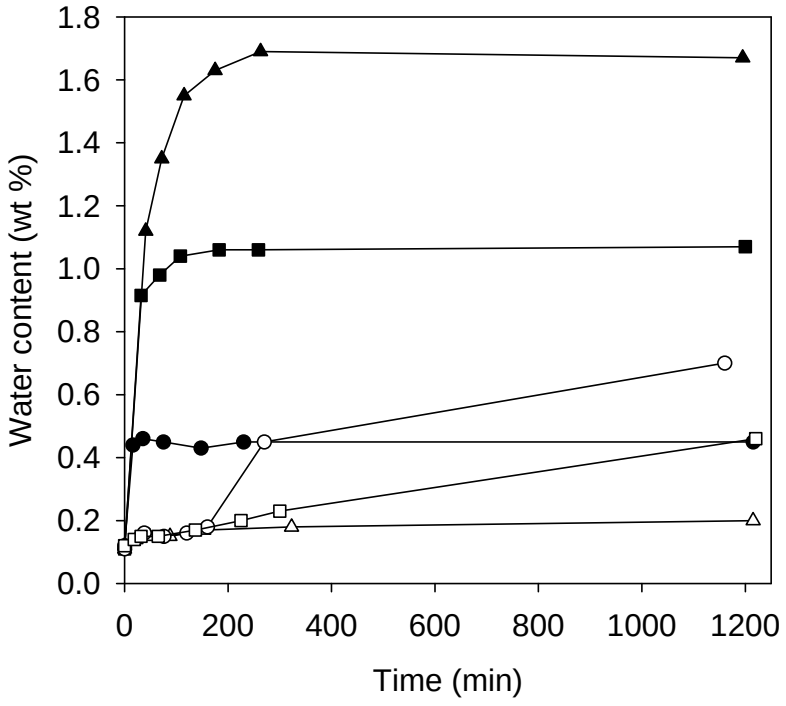

Figure 10. Progress curves for the transfer of water from salt hydrate pairs (Na_2HPO_4 12/7 (▲), Na_2HPO_4 7/2 (■), NaAc 3/0 (●), Na_2HPO_4 2/0 (Δ), $Na_4P_2O_7$ 10/0 (○), $CuSO_4$ 5/3 (□)) to [bmim][PF_6].

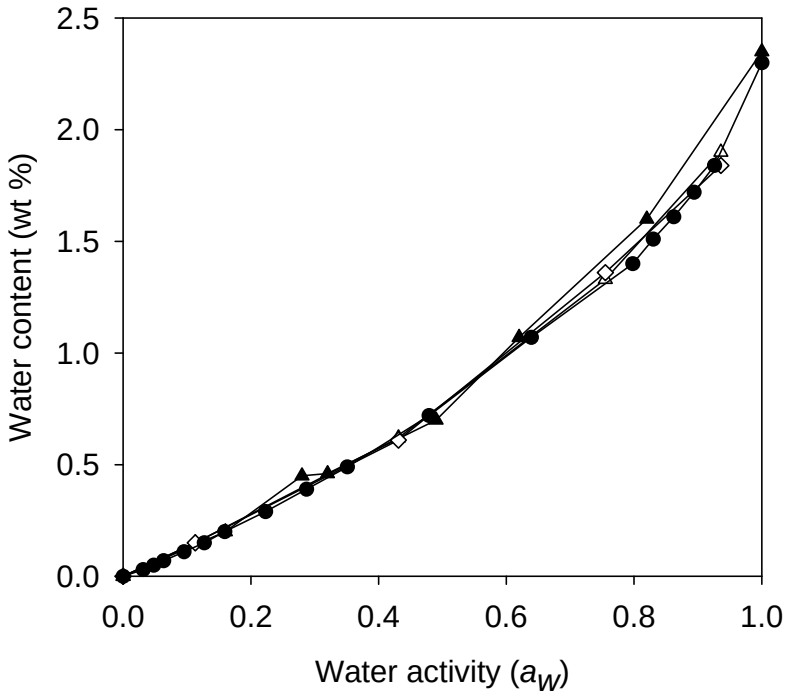

Figure 11. Solubility of water at 25 °C in [bmim][PF_6] that contained salt hydrates (▲) and that was pre-equilibrated with saturated salt solutions in presence of substrates (methyl methacrylate (Δ), 2-ethylhexanol (◇)). Experimentally measured water solubilities were compared to data from the literature (●).

4.3.6 Impact of Water Activity on Lipase Activity in Ionic Liquids

Using salt hydrates to control a_w in [bmim][PF_6], the activity of *Candida antarctica* lipase type B adsorbed to an acrylic support (Chirazyme L-2, carrier-fixed, C2) in the ionic liquid as a function of a_w was determined. The lipase-catalyzed transesterification of methyl methyacrylate and 2-ethylhexanol was employed as a model reaction for measuring initial rates

over a range of fixed a_w. Prior to initiating the reaction, the substrates and enzyme were pre-equilibrated with the salt hydrates in the ionic liquid for 1 hr.

The initial rate activity of the lipase increased non-linearly with decreasing a_w in [bmim][PF_6] and hexane (**Figure 12**). In both solvents, the enzyme is inactive at high a_w (a_w = 1). Chamouleau et al.[115] reported a similar trend in initial rate activity as a function of a_w for the esterification of fructose in 2-methyl-2-butanol catalyzed by immobilized *Candida antarctica* lipase type B. At high a_w, the hydrolytic reaction was preferred over ester synthesis. Furthermore, it is suggested that the decrease in initial rate at high a_w may be a result of limited transport of the hydrophobic substrates from the solvent through the water layer surrounding the enzyme.

In "dry" conditions, in which case molecular sieves were substituted for salt hydrate, the initial rate in hexane (523 mM/hr/g-enzyme) was considerably larger than that in [bmim][PF_6] (41 mM/hr/g-enzyme). This is most likely due to more efficient drying in hexane than in the ionic liquid, which resulted in a substantial difference in the actual a_w's in the two mediums. The high viscosity of the ionic liquid prohibited the complete removal of the crushed molecular sieves, which is necessary to measure and directly compare the water content in the two solvents.

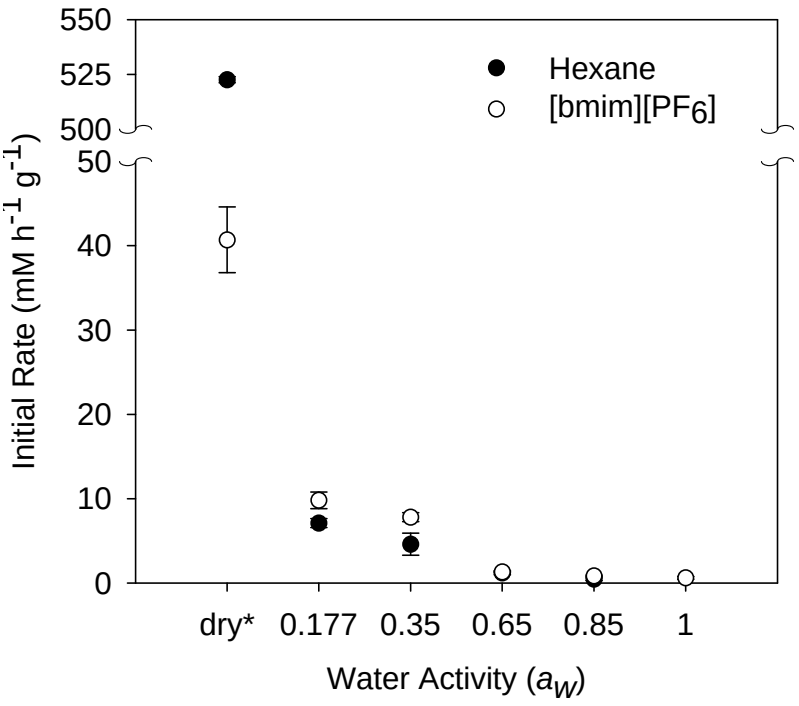

Figure 12. Initial rates of lipase-catalyzed transesterification of methyl methacrylate and 2-ethylhexanol in [bmim][PF_6] (○) and hexane (●) at fixed a_w. In dry* incubations, crushed molecular sieves were employed in place of salt hydrates in order to remove residual water from the solvent.

4.4 CONCLUSIONS

The objective of this work was to investigate the impact of ionic liquid physical properties on enzyme activity and stability. Solvatochromic studies and partition coefficient determinations suggest ionic liquids are highly polar and hydrophilic in nature in comparison to organic solvents such as hexane, acetonitrile and tetrahydrofuran. In the lipase-catalyzed transesterification of methyl methacrylate and 2-ethylhexanol, the initial rate activity of free lipase (*Candida rugosa*) in [bmim][PF_6] was greater than that in hexane. However, no enzyme activity was observed when the reaction was carried out in the other ionic liquids. Conventional methods of enzyme stabilization including adsorption, PEG-modification and multipoint covalent immobilization in polyurethane foams proved ineffective in improving enzyme activity in the all hydrophilic ionic liquids. Stability studies indicated that reversible inactivation of lipase is observed when the enzyme was suspended in [bmim][CH_3CO_2], [mmep] [CH_3CO_2] and [mmep][CH_3SO_3], whereas incubation in [bmim][NO_3] and [mmep][NO_3] irreversibly inactivated the enzyme. To use hydrophilic ionic liquids as solvents for biocatalytic transformations, the mechanism of inactivation must be more clearly understood.

Salt hydrate pairs were also employed to facilitate a_w control in the ionic liquid [bmim][PF_6]. The salt hydrates, with the exception of NaI, had low solubilities in the ionic liquid and behave similarly in the ionic liquid as in organic solvents. Initial rates of the *Candida antarctica* lipase-catalyzed transesterification of methyl methacrylate and 2-ethylhexanol over a range of a_w's showed comparable profiles in [bmim][PF_6] and hexane containing salt hydrate pairs, indicating the salts do not associate with the ionic liquid in such a way that might alter enzyme activity. These findings will enable direct comparison of enzyme activity and specificity within ionic liquids as well as between ionic liquids and various organic solvents.

5.0 BIOCATALYTIC pH CONTROL IN ENZYMATIC REACTIONS

5.1 INTRODUCTION

Biocatalysis represents a highly efficient method for neutralizing the threat of organophosphorous (OP) nerve agents and pesticides. Enzymes are capable of catalyzing the hydrolysis of a broad range of OP substrates at striking rates, which approach the diffusion-controlled limit in certain reactions.[116-119] Moreover, the activities of OP hydrolyzing enzymes are not dependent on cofactors and are stable in mild reaction conditions including near neutral pH and ambient temperatures.[120] Accordingly, biocatalytic decontamination can minimize the environmental impact of existing decontamination methods, including incineration and the use of materials that are corrosive, toxic, and persistent pollutants in the environment.[42, 120-122]

Despite the potential utility of enzymes in our defensive arsenal, there remains many barriers that limit their use. One of the major challenges in using OP hydrolyzing enzymes is controlling the environmental conditions of the enzyme, namely the reaction pH. The hydrolysis of OP substrates yields as many as two moles of acid per mole of substrate degraded. Thus, the reaction pH must be effectively buffered to prevent inactivation of the OP hydrolyzing enzyme prior to complete conversion of the agent. This challenge becomes exceedingly difficult in large-scale decontamination and is further amplified in low-water environments, such as foams and emulsions, where the concentration of agent can reach 0.5 M based on the chemical agent

challenge issued by the U.S. National Research Council Division of Military Science and Technology (10 g nerve agent per m^2).[123] At this agent concentration, the level of conventional buffer required to reach complete hydrolysis would be greater than 28 % (w/v), which exceeds the solubility of many buffer salts (the solubility of HEPES is 26 % (w/v)). Furthermore, at this concentration of buffer, the ionic strength of the reaction solution will be significantly altered, which can inhbit the OP hydrolyzing enzyme. Consequently, the buffering requirement of biocatalytic decontamination is such that more efficient means of controlling pH must be developed before the full promise of enzymes can be realized.

An alternative approach to pH control in hydrolysis reactions is to balance the production of acid with the biocatalytic generation of base, or vice versa. In this way, a dynamic pH equilibrium is created between the opposing reactions, essentially mimicking how cells manipulate their intracelluar pH (**Figure 13**). This approach can be conceptually described by considering an unbuffered aqueous solution containing an OP degrading enzyme and its substrate. The generation of acid as a result of enzymatic hydrolysis will cause a rapid drop in the solution pH, which ultimately will reach a point at which the enzyme is no longer active. By supplementing the reaction solution with a second hydrolytic enzyme and its substrate that is converted to a base, the acid may be neutralized. The solution pH will in theory settle at the point (pH set-point) at which the rates of acid and base formation are equivalent. Because the generation of base is catalytic, and the base-producing enzyme presumably has a pH-optimum lower than that of the acid-producing enzyme, base would be produced only in response to a decrease in pH. One would predict that the pH set-point would remain unchanged as long as the concentration of each substrate remained above the K_M of its respective enzymes. Furthermore, the pH set-point should be controllable by altering the ratio of activities of the two enzymes.

Gestrelius et al.[124] previously reported the pH optima for the coupled enzyme reaction involving amyloglucosidase and glucose oxidase is within the range bound by the optimal pH of each enzyme. It was demonstrated that the pH optima is a function of the ratio of the enzyme concentrations. However, the enzymes in this case were not catalyzing opposing acid-base reactions and the authors make no mention of biocatalytic buffering.

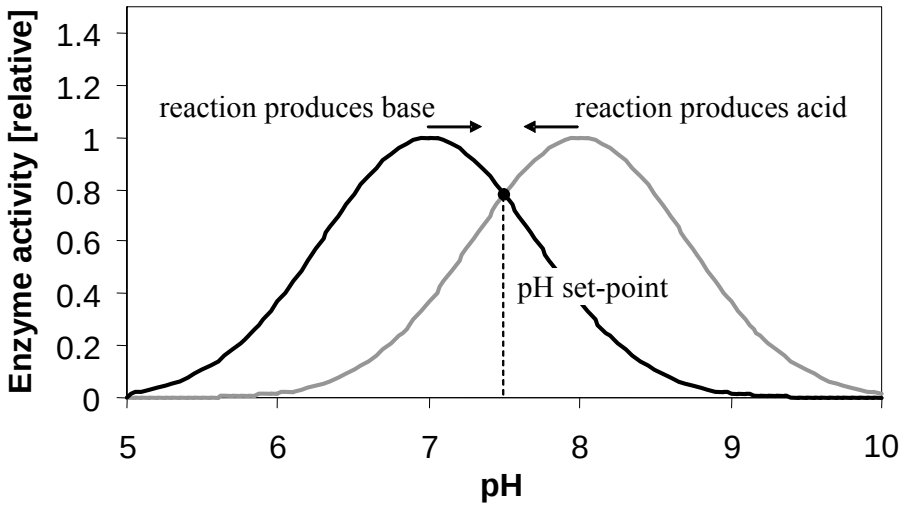

Figure 13. The pH dependence curves of two enzyme-catalyzed reactions depicting the concept of biocatlaytic pH control. The base-producing enzyme (black line) has a lower optimal pH than the acid-producing enzyme (gray line). When both enzymes are present, the pH should stabilize at the intersection point, which is termed the pH set-point.

Urea hydrolysis catalyzed by the enzyme urease is an ideal biocatalytic pH buffering agent. Hydrolysis yields two ammonia molecules and a single carbonic acid.[125-128] At neutral pH, dissociation of the carbonic acid and protonation of the ammonia cause the reaction pH to increase. Urea is highly soluble (up to 16.65 M) and environmentally safe. The molecular mass of urea is also considerably less than that of conventional buffer salts. Therefore, substantially

less urea is required to neutralize a given amount of acid, which equates to a higher buffering capacity per unit mass. This is of particular importance in considering the logistics associated with transporting decontaminant materials.

In this chapter, we investigated the feasibility of controlling pH during the hydrolysis of the model OP compound paraoxon, catalyzed by the enzyme organophosphorous hydrolase (OPH), with only the biocatalytic conversion of urea (**Figure 14**). The products of paraoxon conversion are *p*-nitrophenol and diethylphosphoric acid, which are partially and fully dissociated respectively at neutral pH. Initially, the impact on pH resulting from the addition of urease and urea to a solution containing OPH and paraoxon was determined. The predictability of the system was then ascertained by modeling the pH and conversion of paraoxon as a function of enzyme activities and substrate concentrations using Michaelis-Menten rate equations. The theoretical results were validated against experimental data. After exploring the fundamental theory of biocatalytic buffer, the key question of to what extent product inhibition impacts biocatalytic pH control was addressed. Fluoride, which is a common product in the hydrolysis of many nerve agents, is a strong inhibitor of ureases. The extent to which fluoride impacts the pH equilibrium in the OPH-urease combined enzyme system was determined. Moreover, the use of cationic fluoride scavengers and alternative base-producing biocatalytic reactions, including the adenosine deaminase (ADA)-catalyzed hydrolysis of adenosine, were investigated as potential strategies for improving the resistance of such systems to fluoride.

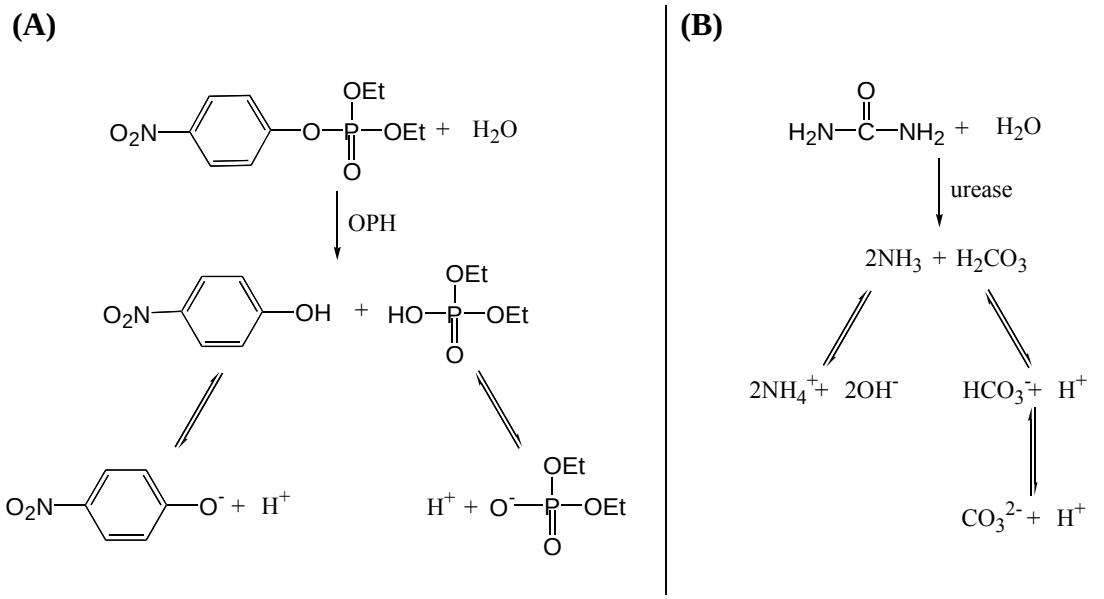

Figure 14. (A) OPH-catalyzed hydrolysis of paraoxon and (B) urease-catalyzed hydrolysis of urea at neutral pH.

5.2 THEORETICAL MODELING OF DYNAMIC pH EQUILIBRIUM IN OPH-UREASE COMBINED ENZYME SYSTEM

The pH in the OPH-urease system was described as a function of reaction time by a proton concentration balance (**Equation 8**), where V_{H^+} and V_{OH^-} represent the rate of formation of acid and base respectively. Using the correlation between proton concentration and pH, the rate of change in proton concentration can be expressed in terms of pH (**Equation 9**).

$$\frac{d[H^+]}{dt} = V_{H^+} - V_{OH^-} \qquad \textbf{(Eq. 8)}$$

$$\frac{dpH}{dt} = \frac{1}{(-\ln(10))(10^{-pH})}\left(\frac{d[H^+]}{dt}\right) = \frac{1}{(-\ln(10))(10^{-pH})}\left(V_{H^+} - V_{OH^-}\right) \qquad \textbf{(Eq. 9)}$$

The rates at which protons and hydroxide ions are formed in the combined enzyme system are described by the rates of paraoxon and urea hydrolysis and the dissociation constants of the hydrolysis products. The pH-dependence on the dissociation of *p*-nitrophenol (pKa, PNP[129]) and diethylphosphoric acid (pKa, DPA[130]) formed during paraoxon hydrolysis was related by the proportionality factor P_{H^+} (**Equation 10**). Similarly, the proportionality factor P_{OH^-} relates the overall release of hydroxide ions from the conversion of urea to the dissociation of ammonia and carbonic acid, which is in equilibrium with bicarbonate and carbonate, as a function of pH (**Equation 11**).

$$P_{H^+} = \frac{1}{1+10^{(pKa,PNP-pH)}} + \frac{1}{1+10^{(pKa,DPA-pH)}} \qquad \textbf{(Eq. 10)}$$

$$P_{OH^-} = \frac{2}{1+\frac{Ka,\,NH_4^+}{10^{-pH}}} - \left[\frac{1}{1+10^{pKa,H_2CO_3-pH}} - \left(\frac{10^{pH-pKa,HCO_3^-}}{1+10^{pKa,H_2CO_3-pH}}\right)\left(\frac{1}{1+10^{pH-pKa,HCO_3^-}}\right)\right] \qquad \textbf{(Eq. 11)}$$

$$-2\left[\left(\frac{10^{pH-pKa,HCO_3^-}}{1+10^{pKa,H_2CO_3-pH}}\right)\left(\frac{1}{1+10^{pH-pKa,HCO_3^-}}\right)\right]$$

Substitution of OPH (V_{OPH}) and urease (V_{urease}) activity and P_{H^+} and P_{OH^-} into the proton balance yields (**Equation 12**):

$$\frac{dpH}{dt} = \frac{1}{(-\ln(10))(10^{-pH})}\left(P_{H^+}V_{OPH} - P_{OH^-}V_{urease}\right) \qquad \textbf{(Eq. 12)}$$

$$V_{OPH} = \frac{-d[paraoxon]}{dt} = \frac{k_{cat}[OPH][paraoxon]}{K_M + [paraoxon]} \qquad \textbf{(Eq. 13)}$$

where the kinetics of OPH activity were computed using the Michaelis-Menten rate equation (**Equation 13**). Because the concentration of urea is such that urease is substrate-saturated

([urea] >>> K_M) for the full duration of the reaction, urease activity is assumed to be maximum (V_{max}) at all times. The pH and extent of paraoxon conversion at any given time in the reaction system can be simulated by simultaneously solving the final proton balance (**Equation 12**) and OPH rate equation (**Equation 13**).

5.3 MATERIALS AND METHODS

5.3.1 Materials

Urease from *Canavalia ensiformis* (jack bean) was purchased from Sigma (St. Louis, MO). Jack bean urease S, Lyo. SQ, a liquid stable industrial enzyme, was obtained as a gift from Roche Diagnostics GmbH (Basel, Switzerland). The *Klebsiella aerogenes* urease 9-1 mutant was expressed in *Escherichia coli* and purified by Drs. Ilona J. Fry and Joseph J. DeFrank at the US Army Edgewood Chemical Biological Center (Aberdeen Proving Ground, MD). OPH from *Pseudomonas diminuta* was kindly supplied by Dr. James R. Wild from the Department of Biochemistry and Biophysics at Texas A&M University. ADA from calf intestinal mucosa was purchased from Roche Diagnostics (Indianapolis, IN). All enzymes were used as received without further purification. The *Helicobacter pylori* urease gene cluster carried by the plasmid pHP8080 in *Escherichia coli* was generously provided by Dr. Harry L.T. Mobley from the University of Maryland School of Medicine. Fluoride standard solution (0.1 M) was purchased from Thermo Orion (Beverly, MA). Paraoxon employed in OPH activity assays and detoxification experiments was synthesized following the procedure described by Steurbaut et al.

(1975). All other reagents were purchased from Sigma or Aldrich (St. Louis, MO) and were of the highest purity available.

5.3.2 Methods

5.3.2.1 OPH Activity Assay

The initial rate of OPH-catalyzed hydrolysis of paraoxon was assayed spectrophotometrically using a Perkin-Elmer (Wellesley, MA) Lambda 2 UV/VIS spectrophotometer by continuously monitoring the release of *p*-nitrophenol over a range of pH's (6.5, 7.0, 7.5, 8.0 and 8.5) at 412 nm at room temperature. Briefly, enzyme was added to a solution of paraoxon (0.0 – 2.5 mM) in pH-adjusted buffer (50 mM Bis-Tris propane, 0.15 mM cobalt chloride). The extinction coefficient of *p*-nitrophenol at each pH was measured. Michaelis-Menten kinetic parameters (k_{cat} and K_M) were determined by non-linear regression while assuming a molecular weight of OPH of 39 kDa (Dumas et al., 1989). One unit of OPH was defined as the amount of enzyme that catalyzed the hydrolysis of 1 μmol of substrate per min at pH 8.0 when assayed with 0.8 mM paraoxon.

5.3.2.2 Urease Activity Assay

A pH-stat assay was employed to measure urease activity in the hydrolysis of urea as a function of pH (6.5, 7.0, 7.5, 8.0, 8.2). The generation of ammonia, a product of urea conversion, was titrated with hydrochloric acid (10 mM) using a Radiometer (Lyon, France) ABU901 autoburette and PHM290 pH-stat controller. At a set pH, the amount of acid required to neutralize the base formed was recorded and is proportional to enzyme activity. Reactions were initiated by the addition of enzyme to a non-buffered aqueous solution containing sodium

chloride (50 mM), cobalt chloride (0.15 mM) and urea (10 mM) and were carried out at room temperature. The pH electrode was pre-equilibrated at room temperature in the solution prior to adding the enzyme to obtain a stable baseline. Addition of titrant and pH were followed continuously for at least 15 min within the initial rate period, during which the reaction rate was linear. One unit of urease activity was defined as the amount of enzyme that catalyzed the hydrolysis of 1 μmol of substrate per min at pH 6.5 at the specified conditions.

5.3.2.3 Preparation of *Helicobacter Pylori* Urease

An overnight culture (200 mL) of *Escherichia coli* containing the plasmid pHP8080, which encodes the entire *H. pylori* gene cluster, was grown overnight at 37 °C in Luria broth supplemented with nickel chloride (100 μM). The bacteria were then centrifuged at 5000 rpm and 4 °C for 10 min in a Fisher Scientific (Pittsburgh, PA) Marathon 21000R centrifuge. The resulting pellet was washed and re-suspended in 5 mL of buffer (50 mM HEPES, pH 7.4) after which the bacteria were lysed via 4 passes through an AMINCO (Urbana, IL) French pressure cell equipped with a Carver (Wabash, IN) model C laboratory press. The cell lysate was centrifuged at 15,000 g for 30 mins at 4 °C and the resulting supernatant was stored frozen (-20 °C). In attempt to remove intracellular proteins or ions that may bind fluoride, the enzyme preparation was dialyzed against buffer (50 mM HEPES, pH 7.4) at 4 °C using a 5,000 MWCO membrane.

5.3.2.4 Fluoride Inactivation of Ureases

To determine the effect of fluoride on urease activity, progress curves of urea conversion were generated using the pH-stat titration assay. Enzyme was added to the unbuffered salt solution containing substrate (10 mM) and sodium fluoride (0 – 5 mM) to initiate the hydrolysis

reaction, which was titrated at pH 6.5 and room temperature. The reaction was monitored continuously until the rate of ammonia formation was linear, indicating a steady-state rate had been reached.

5.3.2.5 Use of Cationic Scavengers to Prevent Fluoride Inactivation of Urease

Progress curve analysis was employed to measure urease activity in the presence of sodium fluoride (0.2 mM) and either calcium chloride (0 – 750 mM), nickel chloride (0 – 1 mM), or lanthanum nitrate (0 – 0.15 mM) at pH 6.5 and room temperature. The cationic fluoride scavenger was added to the standard assay solution containing substrate (10 mM) and sodium fluoride immediately prior to initiation of the reaction with enzyme. In this method, the enzyme was not pre-incubated with fluoride or the scavenger.

5.3.2.6 ADA Activity Assay

The activity of ADA was assayed as a function of pH (6.0, 6.5, 7.0, 7.5, 8.0, 8.5) using a pH-stat titration method. To initiate the enzyme reaction, enzyme was added to a solution of sodium chloride (50 mM) and cobalt chloride (0.15 mM) containing adenosine (0.8 mM). The conversion of adenosine was monitored continuously for at lease 15 mins by recording the addition of titrant (10 mM hydrochloric acid) required to maintain the reaction pH at a set point. The rate at which titrant is added to the reaction is proportional to enzyme activity. All reactions were carried out at room temperature. The pH-electrode was pre-equilibrated in the solution pH prior to initiating the reaction in order to obtain a stable reading. One unit of ADA activity was defined as the amount of enzyme that catalyzed the hydrolysis of 1 μmol of substrate per min at pH 7.5 at the specified conditions.

The effect of fluoride on ADA activity was determined by adding sodium fluoride (0 – 200 mM final concentration) to the reaction solution. The order of addition of sodium fluoride and enzyme in the assay was such that the enzyme was not pre-incubated with fluoride.

5.3.2.7 Measurement of Nerve Agent Conversion and pH in Dynamic pH Controlled Reactions

Reactions in which urease-catalyzed hydrolysis of urea was employed to buffer the degradation of paraoxon by OPH were initiated by the addition of urease and OPH to a solution (40 mL) containing sodium chloride (50 mM), cobalt chloride (0.15 mM) and substrate (1 mM paraoxon, 10 mM urea). The reaction vessel was purged with nitrogen and subsequently sealed with rubber stoppers to prevent the absorption or evaporation of carbon dioxide to or from the reaction, which would alter the reaction pH. Paraoxon conversion was monitored by periodically assaying the amount of *p*-nitrophenol formed spectrophotometrically at 412 nm while the reaction pH was followed continuously using a pH electrode, which was pre-equilibrated in the salt solution with substrates for 30 min prior to the addition of enzyme. A range of urease-to-OPH ratios (0.3 – 31 urease units/OPH units) were employed in the detoxification reactions.

The simultaneous biocatalytic hydrolysis of DFP (0.5 mM initial concentration) and urea (10 mM initial concentration) was carried out in a similar reaction setup. DFP conversion was monitored by assaying residual butyrylcholinesterase (BChE) inhibition using the method described by Ellman et al. (1961). Complete conversion of DFP would result in 0 % relative BChE inhibition. To measure residual BChE inhibition, samples from the reaction solution were removed periodically and diluted 33-fold in ice cold deionized water. The diluted samples were subsequently diluted an additional 33-fold in buffer (1 mL; 50 mM sodium phosphate, pH 7.5) containing equine serum BChE (0.19 U/mL) and DTNB (5,5'-dithiobis(2-nitrobenzoic acid); 0.1

mM). The solution was incubated at room temperature for 3 mins after which the acetylthiocholine (0.5 mM) was added. BChE activity was subsequently followed spectrophotometrically at 412 nm for 30 sec.

A similar setup was also used for the carrying out reactions involving the simultaneous biocatalytic hydrolysis of adenosine and DFP. ADA (0.2 units/mL) and OPH (0.4 units/mL) were added to the reaction solution, which contained adenosine (25 mM) and DFP (5 mM). DFP conversion was monitored in the reaction by measuring the release of fluoride, a product of DFP hydrolysis, using a Hach (Loveland, CO) fluoride-ion sensitive electrode. Briefly, samples were periodically withdrawn from the reaction and diluted 40-fold in buffer (50 mM Bis-Tris propane, pH 8). The concentration of fluoride in the diluted samples was subsequently measured by using the electrode.

5.4 RESULTS AND DISCUSSION

5.4.1 Characterization of pH Buffering in OPH-Urease System and Experimental Validation of Predictive Model

Initially, the pH-dependence on urease (jack bean) activity (**Figure 15A**) and the kinetic parameters k_{cat} and K_M for the OPH-catalyzed hydrolysis of paraoxon were measured (**Figure 15B**). Because the optimum pH of urease activity was lower than that of OPH, the enzymes fit the general model depicted in **Figure 13**. This data was employed in developing the predictive model for describing the system pH and extent of paraoxon conversion.

The impact of the addition of urease and urea on pH in the hydrolysis of paraoxon was subsequently determined. With a ratio of urease-to-OPH activities of 31, the solution pH equilibrated to 8.1 within minutes (**Figure 16A**). The simulated pH and paraoxon conversion profiles generated by the model closely matched the experimentally measured values over the entire time course of the reaction. Given that the conversion of paraoxon and pH are intimately related in the model theory, significant differences between the simulated and experimental pH would cause the predicted conversion to deviate from its actual course. Since this was clearly not the case, a strong argument can be made for the high accuracy of the model. Control experiments showed that the solution pH rapidly decreases in the absence of the urease, resulting in the inactivation of OPH.

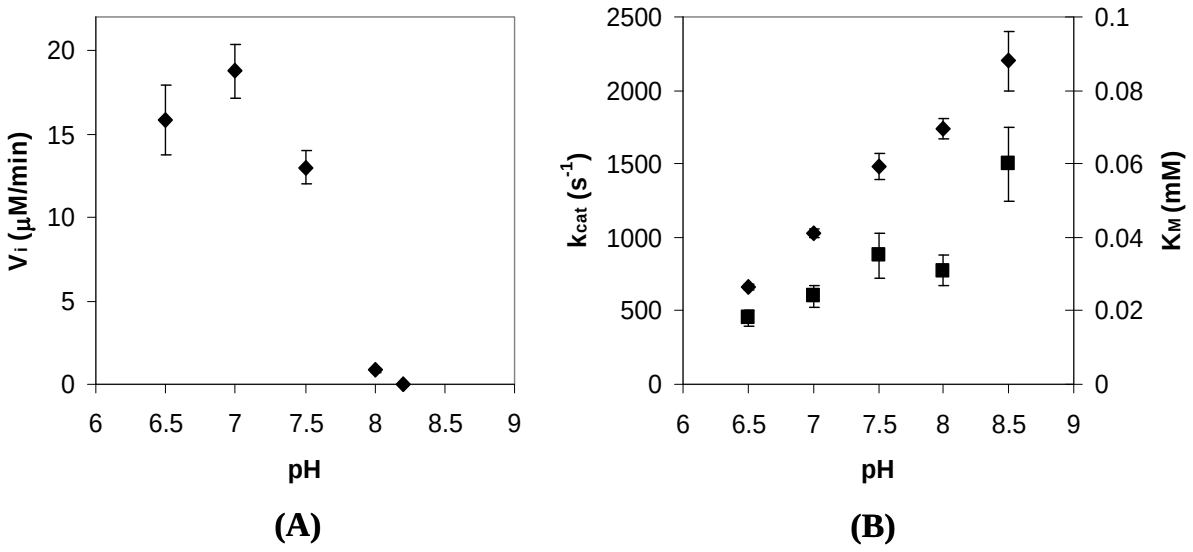

Figure 15. pH-Dependence of (A) urease (jack bean) activity and (B) the kinetic parameters k_{cat} (◆) and K_M (■) for paraoxon hydrolysis by OPH. Error bars are representative of standard deviations from the mean.

The complete degradation of paraoxon was achieved by increasing the concentrations of each enzyme 6-fold (**Figure 16B**). As one would expect, since the ratio of urease-to-OPH activities was not changed, the pH equilibrium point was the same. A gradual increase in the solution pH to 8.4 was observed as the conversion of paraoxon exceeded 60 %. The apparent pH shift is a response to the decrease in the rate of acid formation, which can be attributed to the consumption of substrate. As the conversion of paraoxon approaches 100 %, OPH activity becomes substrate concentration dependent, causing the rate at which OPH catalyzes the hydrolysis of paraoxon to decelerate. Urease activity becomes negligible at this pH and thus there was no further increase in the solution pH. Product inhibition, which was not accounted for in the predictive model, may also affect OPH activity beyond the initial rate period.

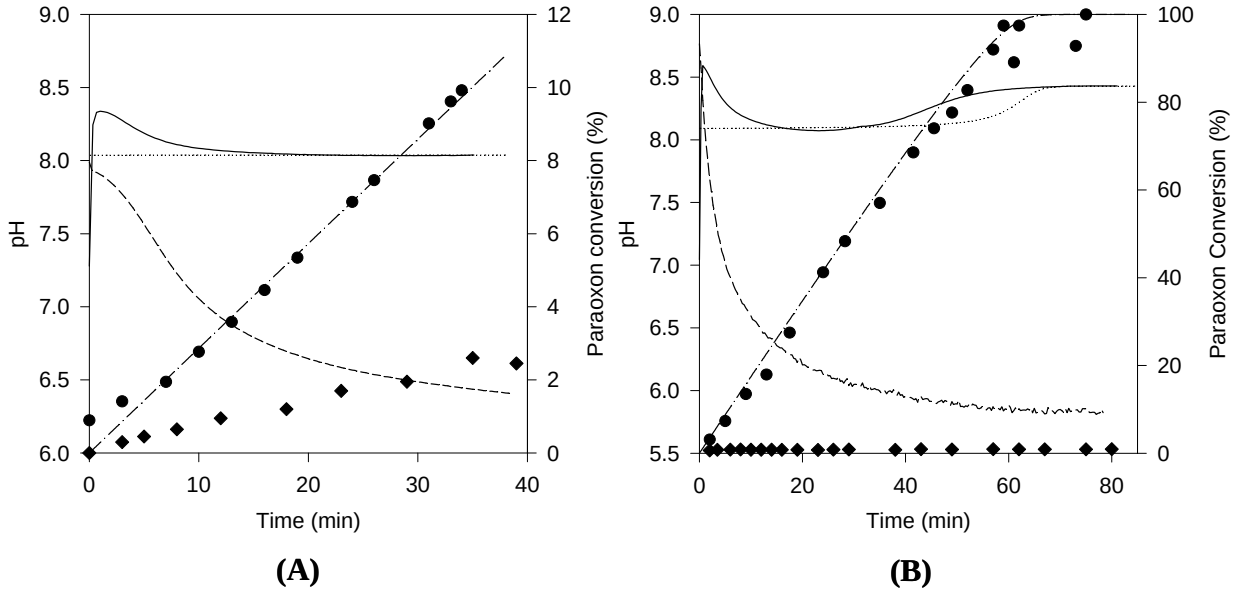

Figure 16. Dynamic pH buffer created by the simultaneous biocatalytic hydrolysis of paraoxon and urea. The solid line and closed circles represent the measured pH and paraoxon conversion profile respectively in the presence of urease (jack bean) and urea. The dotted and dash-dotted lines correspond to the model predicted pH and paraoxon conversion profile also in the presence of urease and urea. The dashed line and closed diamonds refer to the measured pH and paraoxon conversion profile in the absence of urease. The pH set-point remained constant as long as the ratio of activities of the enzymes was unchanged (A) [urease] = 0.081 units/mL and [OPH] = 0.0026 units/mL ([urease]/[OPH] = 31) (B) [urease] = 0.49 units/mL and [OPH] = 0.016 units/mL ([urease]/[OPH] = 31).

Further model validation was performed by comparing experimental and simulated results with different urease-to-OPH activity ratios. At a ratio of 0.54, the solution pH should equilibrate to a lower set-point than in the previously described experiments due to the greater relative activity of OPH. As anticipated, a pH equilibrium was established at 7.2 (**Figure 17**).

The model accurately predicted the change in the pH set-point of the reaction solution and the new paraoxon conversion profile. Additional experiments confirmed the predictability of the pH set-point and paraoxon conversion in the combined enzyme system at even lower urease-to-OPH activity ratios (**Figure 18**). In the present system, the range of achievable pH's is limited only by the difference in pH optima of the two enzymes (**Figure 19**). In all experiments, initiation of the enzyme reactions over on pH unit away from the set-point did not affect the equilibrium pH of the solution.

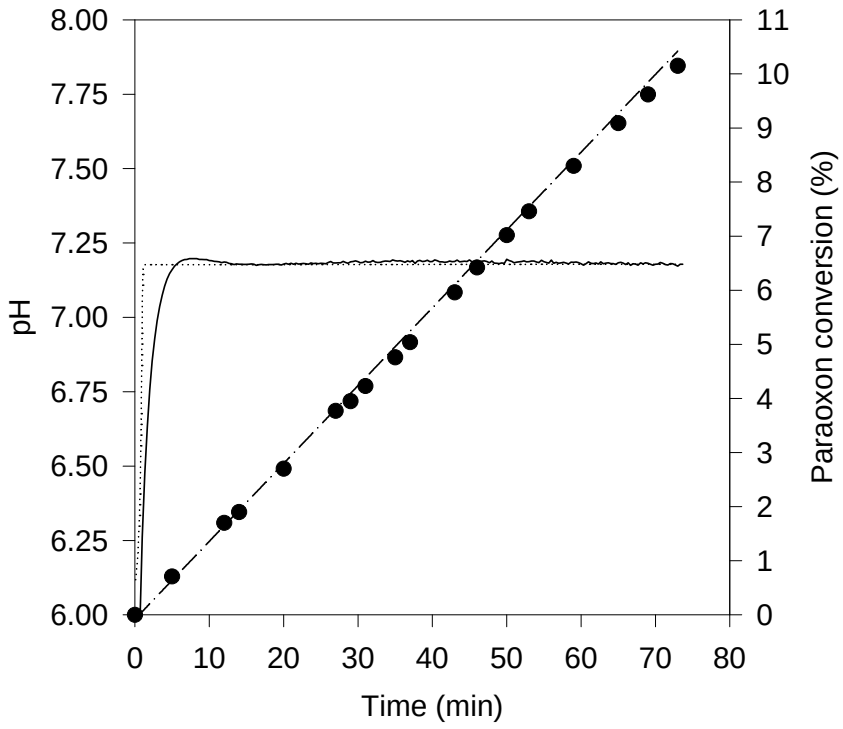

Figure 17. pH Buffering of paraoxon hydrolysis by OPH employing a ratio of jack bean urease-to-OPH activities of 0.54. The actual activities of urease and OPH were 0.0025 U/mL and 0.0047 U/mL respectively, resulting in a pH set-point of 7.20. The solid line and closed circles represent the measured pH and paraoxon conversion profile respectively in the presence of urease and urea.

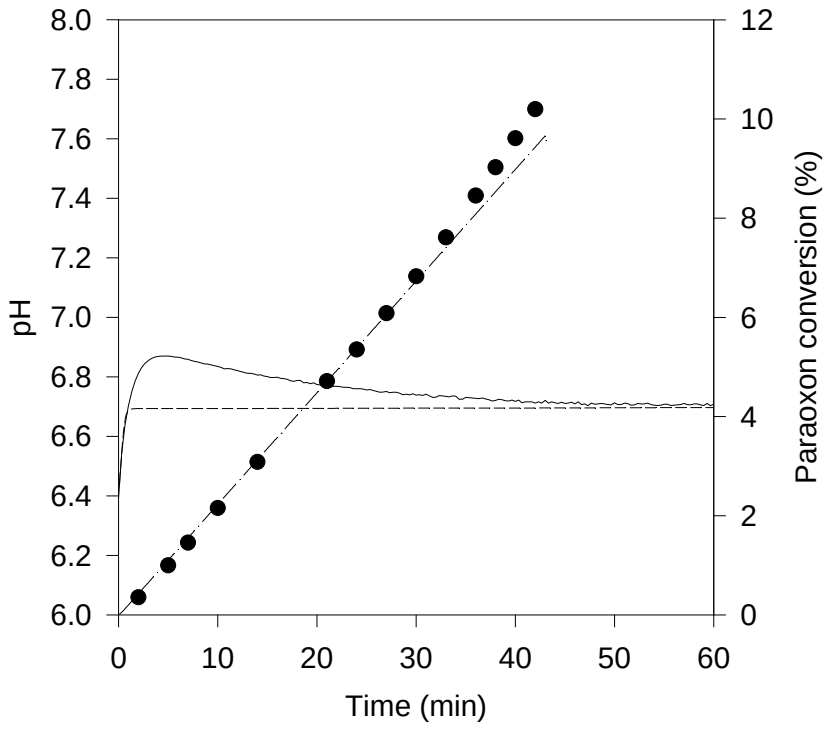

Figure 18. pH Buffering of paraoxon hydrolysis by OPH employing a ratio of jack bean urease-to-OPH activities of 0.30. The actual activities of urease and OPH were 0.0014 U/mL and 0.0048 U/mL respectively, resulting in a pH set-point of 6.71. The solid line and closed circles represent the measured pH and paraoxon conversion profile respectively in the presence of urease and urea.

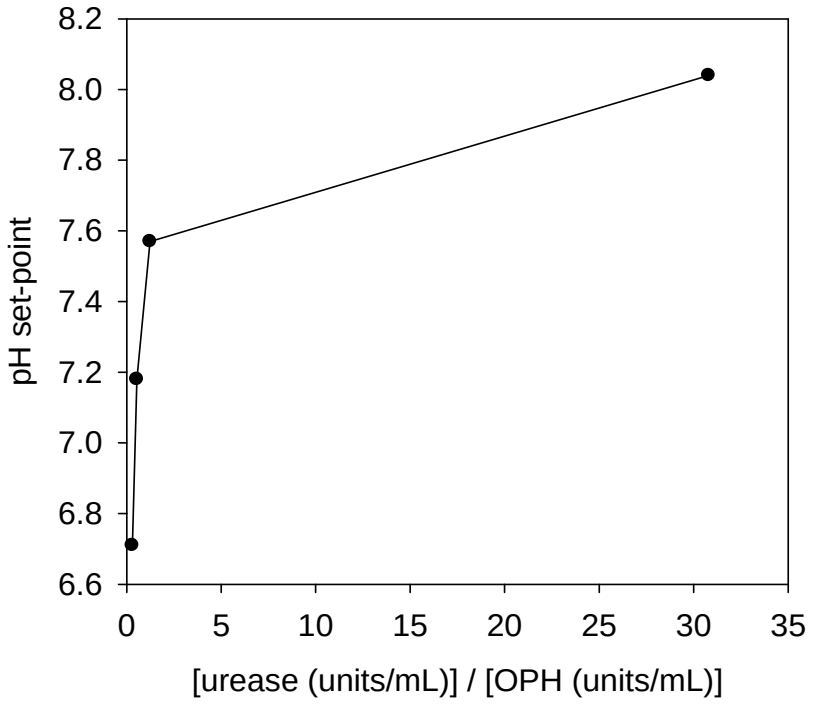

Figure 19. The impact of the ratio of jack bean urease-to-OPH activities on the pH set-point in the combined enzyme system.

5.4.2 Effect of Fluoride on Urease Activity

Inhibition of one or more of the enzyme reactions that constitute a biocatalytic buffer will alter the pH equilibrium created by the opposing reactions. The effects of inhibition in biocatalytic buffering were explored within the context of the OPH-urease system by considering the hydrolysis of diisopropylfluorophosphate (DFP), which is a surrogate for the G-type nerve agents sarin and soman (**Figure 20**). OPH as well as the other OP hydrolyzing enzymes diisopropylfluorophosphatase and organophosphorous acid anhydrolase catalyze the hydrolysis of the P-F bond in DFP.[131] The hydrolysis reaction results in the release of fluoride, which has

been shown to strongly inhibit most ureases.[132-135] Consequently, the key question thus becomes to what extent does the buildup of fluoride cause the pH equilibrium of the OPH-urease system to shift.

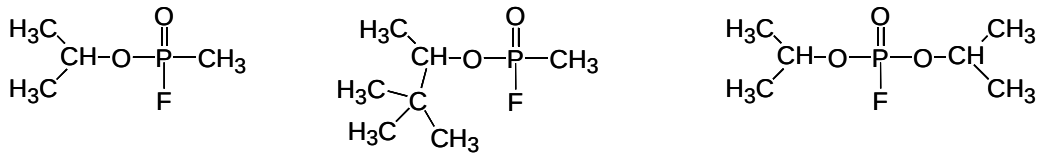

Sarin (GB) Soman (GD) Diisopropylfluorophosphate (DFP)

Figure 20. Chemical structures of organophosphate compounds that are degraded by hydrolysis of a P-F bond.

The mechanism of fluoride inhibition of ureases was elucidated by Todd and Hausinger.[133] A detailed kinetic analysis showed that fluoride inhibition of ureases follows an apparent uncompeptitive, slow-binding mechanism (**Figure 21**). Central to the mechanism of inhibition is a water molecule that bridges the two nickels in the enzyme's active site. This critical water molecule functions as a nucelophile in catalysis, attacking the carbonyl carbon of urea. Upon binding of urea, the water molecule is released, thereby enabling fluoride to bind reversibly to the active site nickels. Although the water molecule may release spontaneously with the enzyme in a resting state, the equilibrium between the native and structurally modified forms of the enzyme strongly favors the native state. The enzyme-inhibitor complex may further bind substrate, thus forming a ternary complex that is characteristic of classical uncompetitive inhibition. This ternary complex differs, however, from that in classical uncompetitive inhibition by the sequence in which it is formed. Specifically, in classical uncompetitive inhibition, the enzyme must initially bind substrate before binding the inhibitor.

The degree to which urease is inhibited by fluoride is greatly affected by the concentration of urea and pH.[132, 133] Because urea stabilizes the two forms of the enzyme-substrate complex (i.e. E-S and E*-S), fluoride binding is inhibited by increasing urea concentration. Additionally, by stabilizing the enzyme-inhibitor-substrate complex, urea also traps the enzyme in an inactive state. Changes in pH alter the rate of dissociation of fluoride from the enzyme, which increases linearly over the pH range 6.5 to 8.5. The observed sensitivity of fluoride dissociation to pH is presumably due to the ionization of an amino acid side chain group that is involved in fluoride binding. Further complicating the kinetics of inhibition, the dependence of the dissociation of fluoride on pH increases significantly in the presence of urea. This suggests that urea binding may alter the pKa of group or groups that are interact with fluoride.

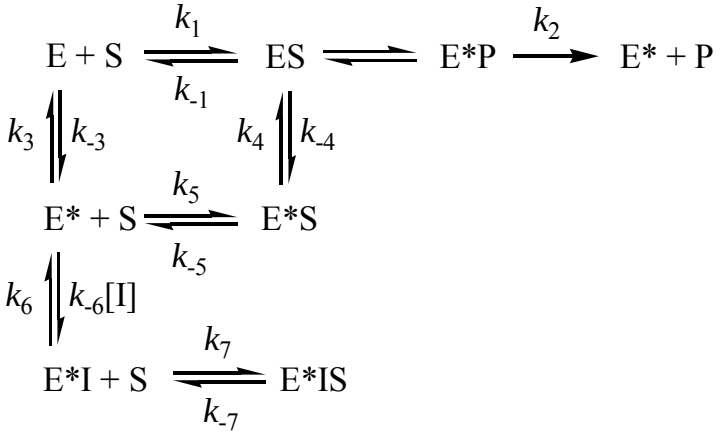

Figure 21. Mechanism of fluoride inhibition of urease. E and E* represent enzyme and a form of the enzyme that is missing a critical active site water molecule. Only E* can bind fluoride.

The impact of fluoride on jack bean urease, a commercially available enzyme that was used in the initial demonstration of biocatalytic buffering, was determined by monitoring the

production of ammonia in the presence of various amounts of the inhibitor. The rate of ammonia production was constant in the absence of fluoride (**Figure 22A**). Addition of fluoride to the enzyme assay did not affect the initial burst (v_o) of urease activity. However, in the presence of fluoride, the rate at which ammonia was liberated steadily decreased as the reaction progressed until attaining a final steady-state rate (v_f). Despite fluoride concentration having no effect on v_o, v_f and the rate at which v_o reached v_f were significantly impacted by the fluoride level in the reaction. An increase in fluoride concentration resulted in a decrease in v_f, which is characteristic of uncompetitive inhibition, and a marked increase in the rate at which v_o reached v_f. This data fits the apparent uncompetetive, slow-binding inhibition of *K. aerogenes* urease by fluoride observed by Todd and Hausinger.[133] The propensity of fluoride inhibition implies that in a combined reaction system, the hydrolysis of just micromolar levels of an organofluorphosphate substrate would inactive urease and in turn disable the buffer.

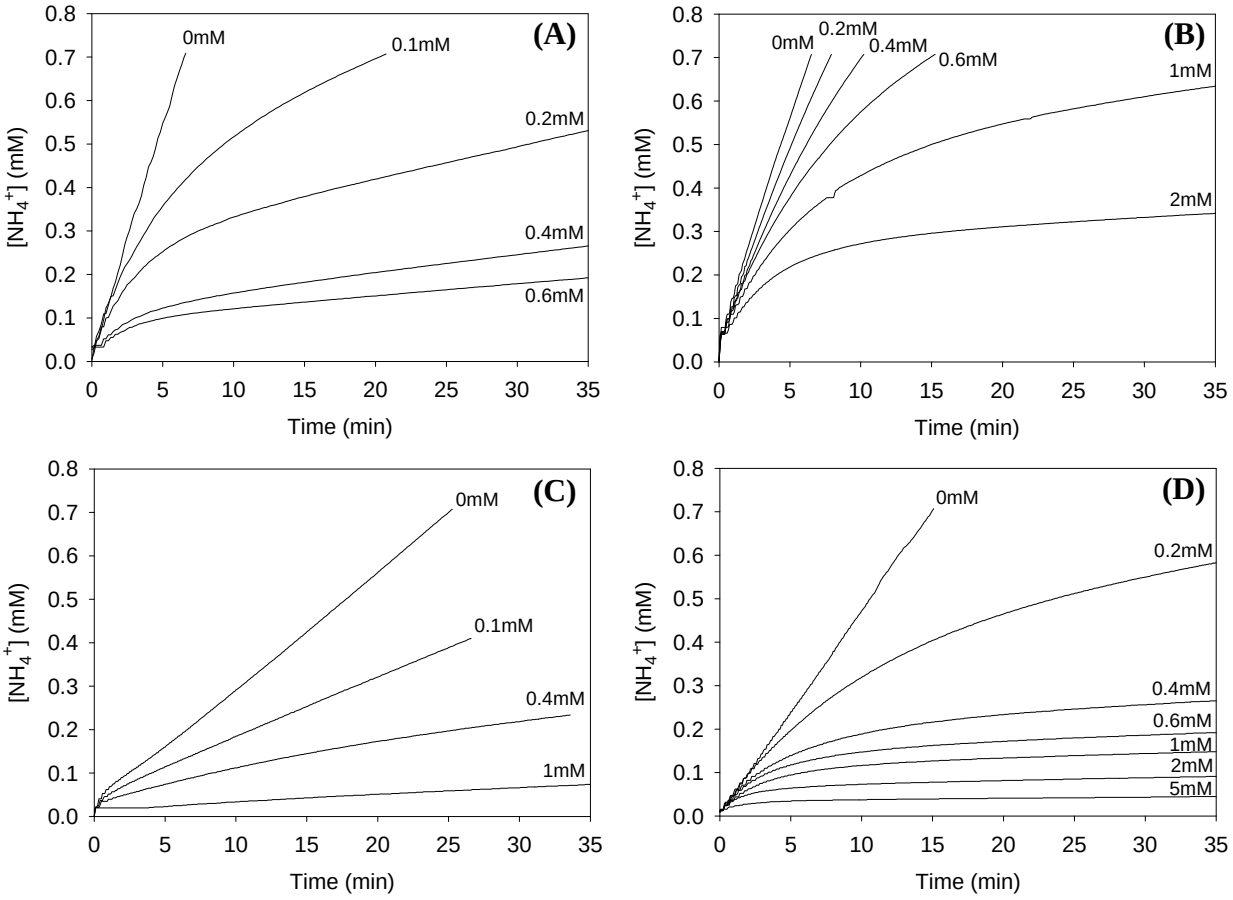

Figure 22. Fluoride inhibition of (A) jack bean urease, (B) *H. pylori* urease, (C) Roche liquid stable, industrial jack bean urease, and (D) *K. aerogenes* 9-1 mutant urease. The activity of the ureases in the presence of various concentrations of fluoride (denoted by the numbers in millimolar) was monitored by progress curves.

Several other ureases were subsequently screened for fluoride-resistant activity, which could be used in place of or as a supplement to jack bean urease to sustain the pH buffering effect in such reaction systems. The urease from *H. pylori*, a pathogenic bacterium that resides in the gastric mucosa in humans[136-140], was also inhibited by fluoride, although to a somewhat lesser degree (**Figure 22B**). In the presence of 0.6 mM fluoride, the bacterial urease liberated

approximately 5-fold more ammonia than jack bean urease after 15 mins. The reduced sensitivity of the *H. pylori* urease to fluoride is likely related to the acid-resistance of the enzyme, which stems from its unique supramolecular structure. The α and β subunits of the enzyme are tightly associated in such a way that shields the enzyme's active sites from the acidic environment.[138, 139] Nonetheless, with just 2 mM fluoride, *H. pylori* urease lost greater than 98 % of its initial activity in only 20 mins. A liquid stable urease, also from jack bean that is employed in industrial processes, and a mutant urease from *K. aerogenes*, which was engineered to have increased fluoride resistance by directed evolution, were even more strongly inhibited by fluoride than the jack bean and *H. pylori* enzymes (**Figure 22C and D**). The conserved sensitivity to fluoride may be attributed to the high degree of active site sequence homology among ureases.[141] Interestingly, inhibition of the liquid stable urease did not appear consistent with the slow-binding model. The progress curves show that the kinetics of the fluoride binding was significantly more rapid than in the case of the other ureases, with much of the loss of activity occurring in the initial 1 – 3 mins of the assay. The observed differences in the kinetics of inhibition may be attributed to the active site water molecule having an increased solvent accessibility.

5.4.3 Solution to the Fluoride Problem

To solve the fluoride problem presented by the hydrolysis of DFP, three different strategic approaches were explored. The first approach that was explored involved increasing the total activity of urease in the reaction system. The second strategy that was investigated entailed the use of cationic fluoride scavengers, which, in theory, would sequester the ions as they are generated. Lastly, alternative base-producing biocatalytic reactions that are resistant to

fluoride inactivation were considered for use as a supplment to or possible replacement for urease-catalyzed urea hydrolysis.

5.4.3.1 Impact of Urease Activity on Fluoride Inactivation of OPH-Urease Buffer

As expected, fluoride generated during the simultaneous biocatalytic hydrolysis of DFP and urea had a profound impact on buffering capacity of the OPH-urease system. In a reaction where the amounts of urease (*K. aerogenes* urease 9-1 mutant) and OPH present were 0.15 units/mL and 0.1 μg/mL respectively, the pH equilibrium was not stable over the time course of the reaction (**Figure 23A**). The solution pH dropped gradually, despite the total conversion of DFP being only 9 % at the end of the reaction. This result is consistent with the anticipated effect caused by the progressive inactivation of urease by fluoride. DFP conversion was determined by measuring the activity of the enzyme BChE upon its inhibition with residual DFP in the reaction solution. The inactivation of BChE and other cholinesterases, which regulate the transmission of nerve impulses, is the basis for the toxicity of OP substrates.[116, 120]

The observed effects of fluoride could be mitigated by increasing the activity of urease at the onset of the reaction. When the amount of urease activity was increased 3.33-fold, the solution pH was maintained at 7.25 for several minutes before rising (**Figure 23B**). The observed increase in pH is to be expected when the rate of DFP hydrolysis becomes substrate concentration dependent. Most importantly, DFP was degraded to completion (i.e. 0 % relative BChE inhibition) in the later reaction within the same time scale.

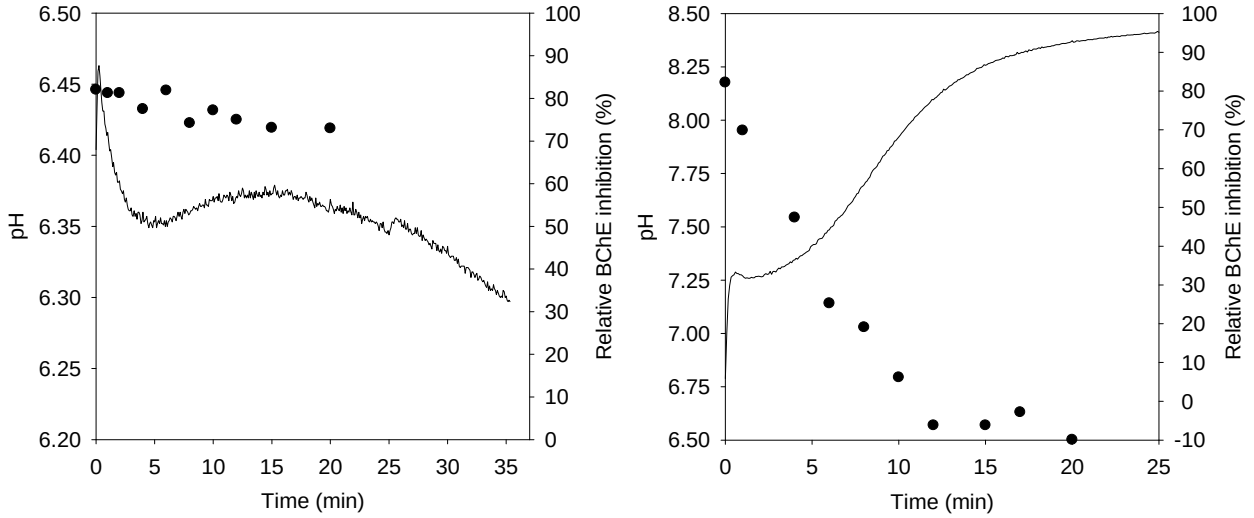

Figure 23. Simultaneous biocatalytic hydrolysis of DFP (0.5 mM) and urea by OPH and urease (*K. aerogenes* urease 9-1 mutant). The actual activities of urease and OPH were (A) [urease] = 0.15 units/mL and [OPH] = 0.1 μg/mL and (B) [urease] = 0.5 units/mL and [OPH] = 0.1 μg/mL. The solid line and closed circles represent the measured pH and conversion of DFP as a function of relative butyrlcholinesterase inhibition respectively.

By increasing the activity of urease, the added enzyme molecules presumably impact the reaction pH and subsequently the conversion of DFP by sequestering fluoride. In this way, the enzyme molecules likely protect the fraction of urease whose activity is critical to the buffering of the reaction solution. The stoichiometry of fluoride binding to ureases varies depending on the structure of the urease that is used. In the case of *K. aerogenes* urease, which has an $(\alpha\beta\gamma)_3$ quaternary structure containing two nickels per subunit, each molecule of enzyme can bind three fluoride ions.[126] Jack bean urease, which has an $(\alpha)_6$ quaternary structure also with two nickels per subunit, can sequester six fluoride ions per enzyme molecule.[142, 143] Although this method

was proved to be effective in overcoming the effects of fluoride, it may be impractical in cases where large amounts of decontamination materials are needed.

5.4.3.2 Cationic Fluoride Scavengers

Rather than sequestering the fluoride produced by DFP hydrolysis with excess urease, cationic fluoride scavengers may be added to reduce the concentration of fluoride to non-inhibitory levels. Cationic fluoride scavangers including calcium, magnesium, and lanthanum are routinely employed for removing fluoride from wastewater as well as for the treatment of acute fluoride poisoning.[144-149] Such scavangers are able to bind to fluoride resulting in the formation of an insoluble salt, although the extent of precipitation of the salt is dependent upon its solubility product constant (K_{sp}). The K_{sp} for several fluoride salts including calcium fluoride, magnesium fluoride, and lanthanum fluoride at ambient temperatures are 5.3×10^{-9}, 5.16×10^{-11}, and 7.0×10^{-17} respectively.[150] The use of cationic scavengers to protect urease from ion-induced inactivation is a novel concept.

The capacity of calcium, lanthanum, and nickel was determined by assaying urease activity in the presence of fluoride and the respective scavenger. Calcium and nickel are both divalent cations and thus can complex two fluoride ions per molecule of cation whereas lanthanum, which is trivalent, can bind three fluoride ions per cation molecule. To mimic the case in which the cation scavengers and urease would compete for fluoride as it is released by the hydrolysis of DFP, the cations in the form of inorganic salts were added to the fluoride-containing substrate solution immediately prior to the addition of enzyme. Progress curve analysis of urea hydrolysis indicates that fluoride inactivation of urease can be partially prevented by calcium when added in a large stoichiometric excess (**Figure 24A**). In the presence of calcium, the apparent rate of fluoride binding to the enzyme was markedly reduced, as is

evident by the increase in linearlity of the progress curves. Although progress curves in the presence with lanthanum were nearly linear over the time course of the assay, urease was considerably inhibited by the cationic scavenger (**Figure 24B**). The rate of conversion of urea decreased with increasing concentrations of lanthanum nitrate. To confirm that lanthanum and not the nitrate anion was inhibiting urease, control experiments were carried out with lanthanum chloride. Results of the control experiments showed that urease was also strongly inhibited lanthanum chloride. Similarly, the addition of nickel, which did not have any protective effect on the inactivation of urease by fluoride, significantly inhibited urease activity (**Figure 24C**).

Based on results of the urease protection assays, calcium ions appeared to be ideal fluoride scavengers for the OPH-urease system. Moreover, when assayed in the presence of calcium at concentrations as high as 0.5 M, the activities of urease and OPH were largely unaffected. The loss of activity at higher calcium concentrations is likely due to the associated change in ionic strength of the reaction solution. In the presence of 0.5 M calcium ions, DFP was degraded to completion in the combined OPH-urease system. Greater than 99.9 % conversion of the toxin was achieved in 24 mins. However, the same effect could be produced by using a sufficiently high enough urease concentration. Still, calcium ions may be of considerable utility in scavenging the initial burst of fluoride released such that significantly less urease may be needed for full decontamination. It is also conceivable that calcium ions may be effective in protecting urease in sensing applications, where it would be desireable for urease to remain active over long periods of time with potential exposure to low levels of fluoride.

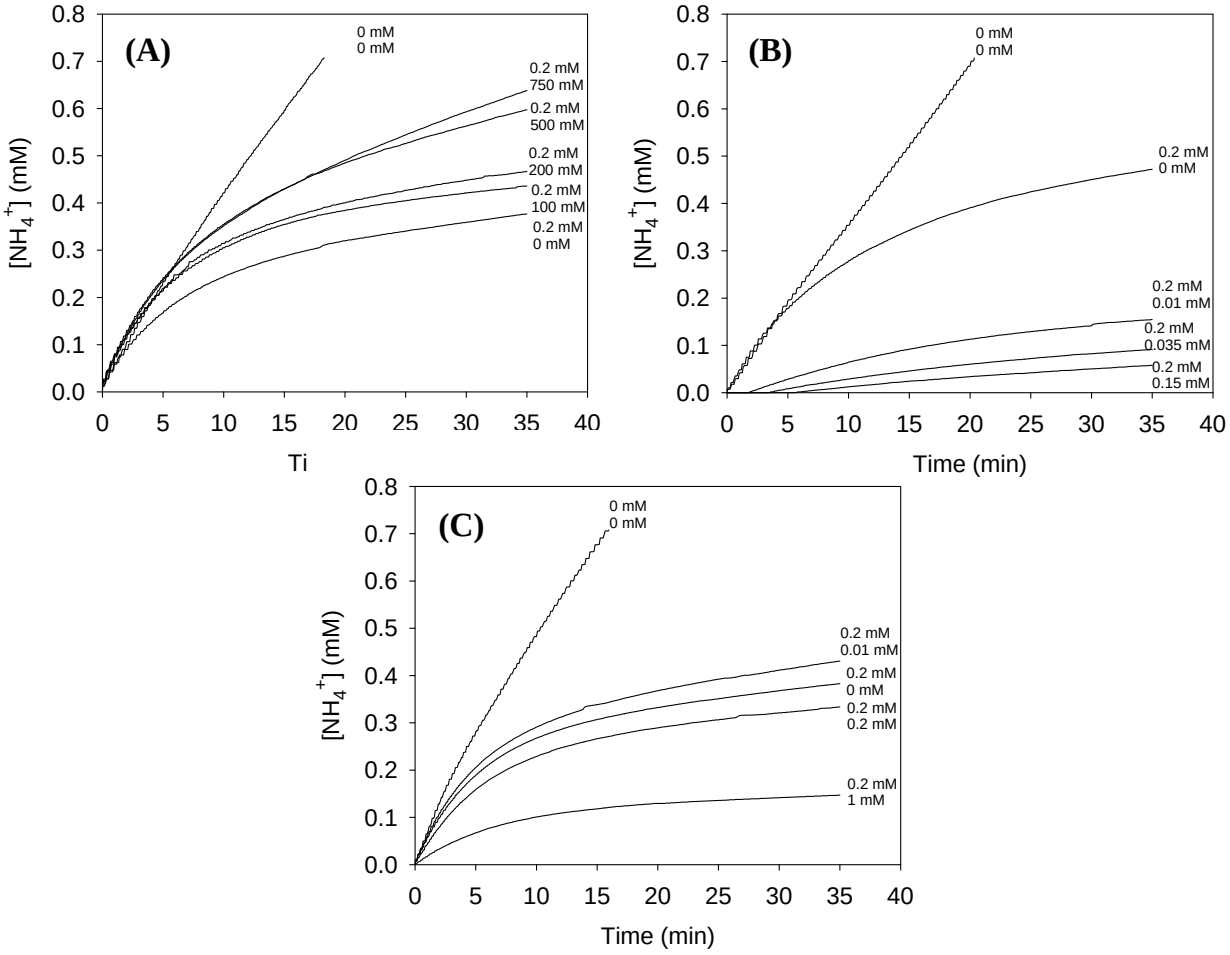

Figure 24. Protection of *K. aerogenes* urease mutant (9-1) from fluoride inactivation by the addition of (A) calcium chloride, (B) lanthanum nitrate, and (C) nickel chloride. Urease activity was monitored by progress curves in the presence of various concentrations of the cationic fluoride scavengers. For each assay, the concentrations of fluoride and cationic scavenger are inidicated as the top and bottom concentrations respectively.

5.4.3.3 Alternative Base-Producing Biocatalytic Reaction

The fluoride problem may also be solved through the use of alternative base-producing biocatalytic reactions that are insensitive to fluoride. Such reactions could potentially be used

either in place of or in addition to biocatlaytic urea hydrolysis in the OPH-urease combined enzyme system. One reaction that was identified as a possible candidate to mediate the impact of fluoride in dynamic pH buffering was the biocatalytic hydrolysis of adenosine. The zinc-containing enzyme ADA, which has been isolated from a wide range of organisims including bacteria, plants, vertebrates, invertebrates, mammals, and humans, catalyzes the hydrolysis of adenosine into inosine and ammonia (**Figure 25**).[151, 152] Although its exact physiological role has yet to be elucidated, loss of ADA activity has been implicated in the onset of severe combine immunodeficiency disease. Moreover, ADA activity has reportedly been linked to embryonic and fetal development as well as to a number of other pathologies such as, for example, tuberculosis, bacterial meningitis, multiple sclerosis, Down's syndrome, and Parkinson's disease.[151]

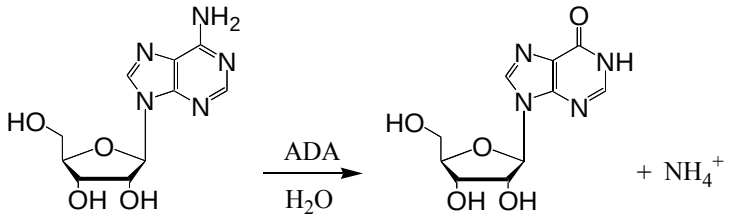

Figure 25. ADA-catalyzed hydrolysis of adenosine.

To determine the utility of ADA in dynamic pH control, the pH-dependence and fluoride sensitivity of ADA activity were measured. The apparent pH-activity profile of ADA was strikingly similar to that of urease (**Figure 26A**). The initial rate of adenosine hydrolysis, like the hydrolysis of urea by urease, was greatest at pH 7.0. Given this similarity, it is logical to expect that, in an unbuffered solution, the simultaneous biocatalytic hydrolysis of adenosine and DFP, or paraoxon, by ADA and OPH respectively will form a dynamic pH equilibrium

comparable to that observed in the OPH-urease system. Most significantly, ADA was largely uninhibited by fluoride compared to the different forms of ureases used in this study (**Figure 26B**). ADA retained considerable activity even when assayed in the presence of as much as 200 mM fluoride. Based on this, the biocatalytic hydrolysis of adenosine can presumably provide the necessary buffering means to enzymatically degrade near molar concentrations of organofluorophosphates.

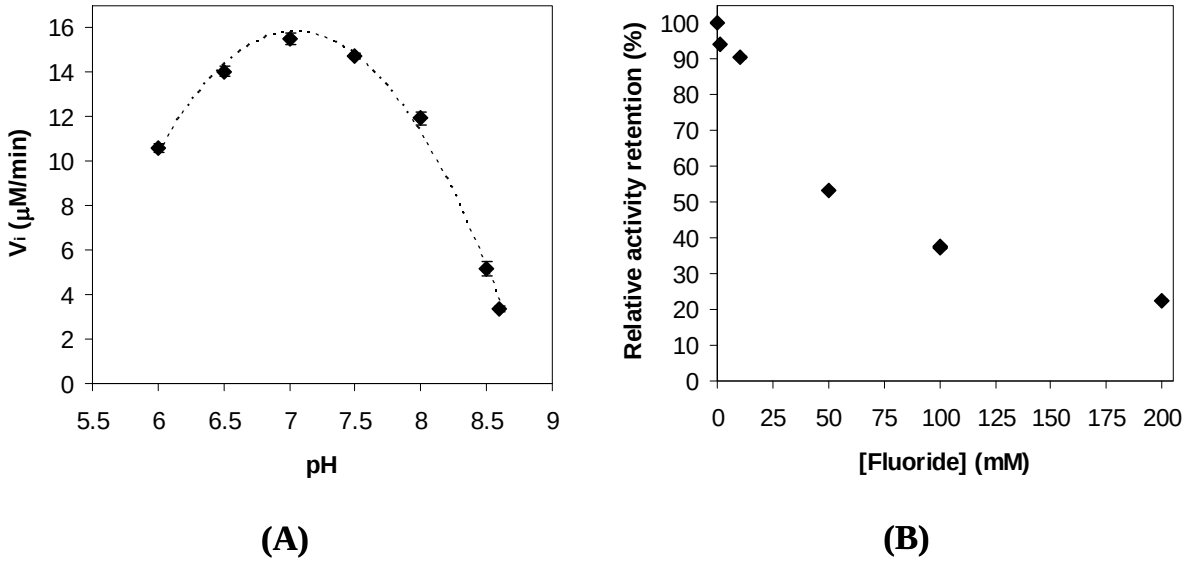

Figure 26. (A) pH-Dependence of ADA activity. (B) The effect of fluoride ions on ADA activity.

The fluoride resistant and pH-dependent properties of ADA make the biocatalytic hydrolysis of adenosine an attractive buffering agent for organofluorophosphate hydrolysis. Model decontamination reactions were subsequently carried out to verify if ADA-catalyzed adenosine hydrolysis could control pH over the course of DFP hydrolysis in an unbuffered solution. Using only the biocatalytic hydrolysis of adenosine as a buffering agent, solutions of DFP were fully decontaminated (**Figure 27**). The solution pH was dynamically controlled by

the rates of adenosine and DFP hydrolysis in a manner that closely resembled that in the OPH-urease combined enzyme system. A steady increase in the solution pH was observed as the conversion of DFP approached 100 %. Due to the pH-induced inactivation of ADA, the solution pH ultimately stopped increasing at 8.7. Additionally, there were no apparent effects of partial ADA inactivation on the pH or DFP conversion profiles over the course of the reaction.

Dynamic pH control involving the biocatalytic hydrolysis of adenosine, while effective in overcoming fluoride inactivation, has several drawbacks. One significant drawback is that the buffering capacity of adenosine on a per weight basis is lower than that of urea. Specifically, whereas between one and two moles of base are produced per mole of urea hydrolyzed at near neutral pH, the hydrolysis of a single mole of adenosine produces at most one mole of base. Thus, considerably more adenosine may be required to buffer a given amount of acid. The molecular mass of adenosine is also greater than 4-fold that of urea. This mass difference, combined with the need for more buffering agent, can potentially make the tactical transport of decontamination materials exceedingly difficult. Moreover, activity assays suggest that adenosine may partially inhibit OPH activity. Although this inhibition did not significantly impact DFP hydrolysis in model reactions in this study, it may introduce constraints in systems involving larger quantities of OP agents. To fully understand how this inhibition impacts the buffering capactivity of adenosine, the degree to which OPH is inhibited by adenosine must be fully characterized.

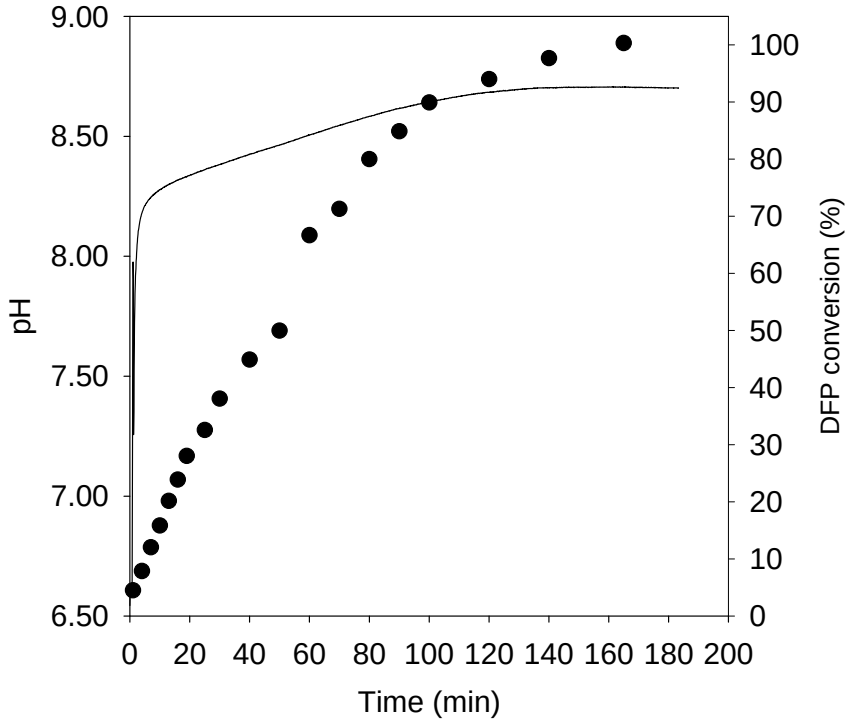

Figure 27. Simultaneous biocatalytic hydrolysis of DFP (5mM) and adenosine by OPH and ADA. The actual activities of adenosine deaminase and OPH were 0.2 units/mL and 0.4 units/mL respectively. The solid line and closed circles represent the measured pH and DFP conversion profile respectively.

5.5 CONCLUSIONS

In conclusion, the concept of biocatalytic pH control was demonstrated in solution by combining the biocatalytic hydrolysis of paraoxon and urea. The solution pH in the combined enzyme system, which remained constant over significant ranges of paraoxon conversion, was predictable. Furthermore, by altering the ratio of OPH-to-urease activities, it was possible to rationally control the dynamic pH equilibrium formed by the opposing acid and base generating reactions.

The use of DFP in place of paraoxon as the substrate for OPH offered a model reaction system for studying the impact of product inhibition on biocatalytic pH control. Fluoride released by the hydrolysis of fluorophosphates group of DFP was found to inactivate ureases from jack bean, *H. pylori*, and *K. aerogenes* at micromolar concentrations by an apparent uncompetitive, slow-binding mechanism. Fluoride inactivation of urease during the hydrolysis of DFP was mediated by increasing urease activity in the reaction system, enabling DFP to be degraded to completion. The use of cationic fluoride scavengers to improve the resistance of biocatalytic pH control in the OPH-urease system to fluoride inactivation was only partially successful. Addition of the scavangers prevented the loss of urease activity due to fluoride in kinetic assays. However, no significant enhancement in the rate of DFP hydrolysis was observed in biocatalytic pH control experiments containing the scavengers. The impact of fluoride in dynamic enzymatic buffers can also be overcome through the use of alternative enzymes for the biocatalytic formation of base. ADA, which is significantly less sensitive to fluoride relative to urease, was used to buffer the pH of the conversion of DFP by catalyzing the simultaneous hydrolysis of adenosine. Such use of different enzymes ultimately highlights the potential broader utility of this remarkable new approach to pH control.

6.0 REDUCING SCARRING IN LACERATED SKELETAL MUSCLE USING MATRIX METALLOPROTEINASE-1

6.1 INTRODUCTION

Formation of collagen (i.e. scar tissue), which is the result of the body's natural wound healing process, is a critical barrier in the regeneration of injured skeletal muscle.[153-155] Fibrotic tissue, which consists of predominately type III collagen in early stages of healing and type I collagen in later stages, is produced by fibroblasts that differentiate in response to injury.[156, 157] This phase of healing is referred to as the fibrosis phase and occurs after the initial clearing of damaged tissue and the onset of muscle phase.[158, 159] The collagen matrix blocks progenitor cells from infiltrating the site of injury where they can differentiate into new muscle tissue. Incomplete muscle regeneration due to scarring ultimately compromises the structural integrity of the tissue, prevents full recovery of function, and increases the likelihood of re-injury, thus having long-lasting effects.[154, 159, 160]

Several approaches aimed at improving muscle regeneration and functional recovery have been investigated. The growth factors insulin-like growth factor-1, basic fibroblast growth factor, and nerve growth factor improve regeneration when delivered to injured muscle by promoting myoblast proliferation and fusion.[161] Leukemia inhibitory factor, which induces the proliferation and subsequent differentiation of progenitor muscle cells, has also been shown to

enhance muscle healing in an animal model of Duchenne muscular dystrophy (a genetic disorder that causes myocyte death in conjunction with the progressive formation of fibrotic tissue in skeletal muscle).[162, 163] Moreover, drugs that inhibit or down-regulate expression of key fibrosis activators, such as transforming growth factor-β1, can enhance muscle regeneration. Suramin, decorin, and γ-interferon have been reported to reduce the extent of fibrosis in injured skeletal muscle *in vivo*, thus leading to improved regeneration.[164-167] Although these approaches have met with clinical success, related treatments are only effective if administered prior to scar formation.[168]

Because muscle injuries are often left untreated prior to scarring, a therapy that degrades scar tissue during or after completion of the normal healing process would be beneficial. The key to developing such a therapy may be an enzyme that targets and digests the fibrous scar tissue. Delivery of the exogenous enzyme to injured tissue could potentially degrade pre-existing scar, thereby mimicking natural tissue remodeling processes.

Tissue remodeling is driven by matrix metalloproteinases, a family of zinc and calcium-dependent endopeptidases that catalyze the hydrolysis of native and denatured extracellular matrix proteins.[169-172] The first member of this family, matrix metalloproteinase-1 (MMP-1), otherwise known as interstitial collagenase, was discovered in amphibian tissues, where its activity factilitates tissue resorption during metamorphosis.[173] Later, the same enzyme was found to be intimately involved in the remodeling of human tissues.[174] MMP-1 is expressed as a zymogen (proMMP-1), containing an N-terminal propeptide that must be cleaved for the enzyme to be catalytically active. Naturally, because of its specificity towards type I collagen, a major component of mature scar, MMP-1 may be effective in resolving scarring in injured muscle tissue.

The potential utility of MMP-1 in the treatment of fibrotic conditions was established by Iimuro and co-workers[175], who employed recombinant adenovirus expressing proMMP-1 to treat liver fibrosis in a rat model. More recently, we showed that direct injection of proMMP-1 into fibrotic skeletal muscle in mice resulted in the reduction of collagen content without adversely affecting the basal lamina of uninjured muscle.[176] However, by using the pro-form of MMP-1, it is difficult to determine the amount of enzyme that is activated in the scarred tissue prior to it being enzymatically degraded or diffusion of the enzyme from the tissue. A more efficient approach to using MMP-1 may be to deliver the pre-activated enzyme, which would allow for direct control over the activity of MMP-1 administered. Moreover, the required treatment time may be reduced using active MMP-1 since the enzyme would begin to work immediately.

In this study, we have compared the efficacy of three different forms of recombinant human MMP-1 in resolving muscle fibrosis in a laceration model in mice including proMMP-1 and active MMP-1 (rhMMP-1). The active form of the enzyme (43 kDa) was produced by expressing cDNA that encodes for residues 101 – 469 of the full-length enzyme. Additionally, a poly(ethylene glycol)-modified form of the rhMMP-1 (PEG-rhMMP-1), which was prepared by reacting the enzyme with an amine-reactive PEG (PEG-SPA; 5000 M_w), was also employed in the *in vivo* model. The covalent attachment of PEG may improve the enzyme's *in vivo* stability and thus effectiveness in degrading interfibrillar collagen at the site of laceration.

6.2 MATERIALS AND METHODS

6.2.1 Materials

Recombinant MMP-1 was produced and purified by Aldevron, LLC (Fargo, ND) using cDNA from human fibroblasts from American Type Culture Collection (Manassas, VA). Latent full-length human MMP-1 was purchased from Sigma (St. Louis, MO). Trypsin employed in peptide fingerprinting analysis of native and PEGylated rhMMP-1 was purchased from Promega (mass spectrometry grade, Madison, WI). The enzymes were used without further purification. PEG-succinimidyl propionate (PEG-SPA) was purchased from Nektar Therapeutics (San Carlos, CA). Electrophoresis reagents were purchased from Bio-Rad (Hercules, CA) and Pierce Biotechnology (Rockford, IL). The MMP-1 colorimetic substrate Acetyl-Pro-Leu-Gly-[2-mercapto-4-methyl-pentanoyl]-Leu-Gly-OC_2H_5 was obtained from Biomol International (Plymouth Meeting, PA). Type I acid soluble, lyophilized collagen from calf skin was purchased from Elastin Products (Owensville, MO). All other reagents were purchased from Sigma (St. Louis, MO) and were of the highest purity available.

6.2.2 Methods

6.2.2.1 PEGylation of rhMMP-1

Native rhMMP-1 was diluted to a concentration of 1.5 mg/mL in buffer (50 mM HEPES, 5 mM calcium chloride, pH 7.5). PEG-SPA was added in excess to the enzyme solution at a PEG-to-protein molar ratio of 1000:1 and the reaction solution was vigorously mixed at room temperature for 1 hr. Residual free PEG was removed using a centrifugal filtration device

(Millipore, Billerica, MA) with a nominal molecular weight limit of 10,000 Da. The protein concentration of PEGylated rhMMP-1 was quantified via measuring the absorbance of the sample at 280 nm (ε = 66,810 $M^{-1}cm^{-1}$).

6.2.2.2 Muscle Laceration Model

A lacerated muscle model was created in NOD.CB17-Prkdcscid/J mice from Jackson Laboratories (Bar Harbor, ME) as described previously by Menetrey and co-workers.[177] The mice were cared for and used in accordance with protocols approved by the University of Pittsburgh Institutional Animal Care and Use Committee (IACUC #25-03).

Initially, the mice were anesthetized via isofluorane inhalation. A posterior longitudinal incision was made in the skin to expose the right and left gastrocnemius muscle (GM) in the hind limbs of the mice. The GMs were subsequently lacerated bilaterally such that the injury spanned 50 % of the width and 100 % of the thickness of the muscle. Following the laceration, the skin at the wound site was sutured closed and the mice were allowed to recover while housed in cages with unrestricted movement.

To determine the effectiveness of proMMP-1, rhMMP-1, and PEG-rhMMP-1, an initial study was carried out using 30 female mice, which had an average age of 9 weeks at the time of laceration. A suture was inserted in muscle adjacent to the site of laceration in order to mark the wound site. At 33 days post-laceration, 0.4 mU or 0.8 mU of proMMP-1, rhMMP-1, or PEG-rhMMP-1 was injected (10 μL volume) at the site of injury using the suture as a point of reference. Both injured muscles in each animal received the same treatment. The amount of proMMP-1 required to deliver the specified dose was determined based on the specific activity of the enzyme when fully activated by trypsin (**Figure 28**). An equal volume of buffer (50 mM

HEPES, 5 mM calcium chloride, pH 7.5) was injected in the lacerated GM of control mice. The animals were sacrificed 14 days post-treatment after which tissue from the laceration site was collected and subsequently fixed in 10 % neutral buffered formalin.

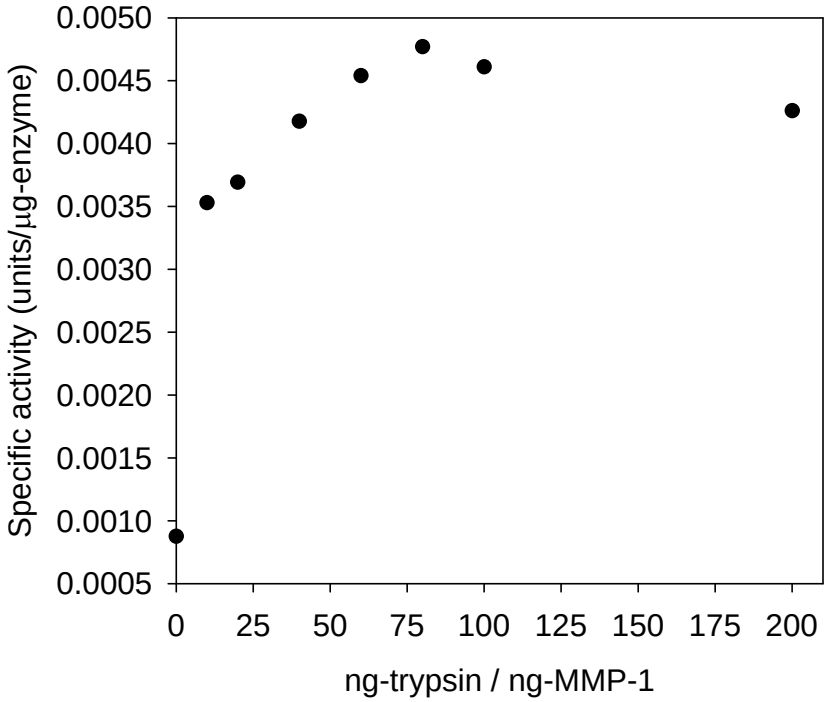

Figure 28. Specific activity of proMMP-1 upon activation of the full-length enzyme with varying mass ratios of trypsin-to-enzyme. When fully activated, proMMP-1 had a specific activity of 0.0047 units/µg-enzyme when assayed with a thioester substrate.

A follow-up study, which was carried out to confirm the *in vivo* results, involved a total of 17 mice, also female, that were, on average, 10 weeks of age. To more accurately mark the site of injury, blue tissue marking dye (Thermo Electron Corporation, Pittsburgh, PA) was applied across the wound site in place of the suture marker. Native or PEGylated rhMMP-1 was injected (10 µL volume) at a single dose of 0.8 mU at the site of injury in the right leg of the

mice at 23 days post-laceration. Concomitantly, the left legs of all mice were treated with an equal volume of buffer. Green fluorescent microspheres (0.5 μm; Molecular Probes, Eugene, OR) were co-injected at a concentration of 2 x 10^4 microspheres/μL with the enzyme or buffer to confirm delivery of treatment to the scarred muscle. At 11 days-post injection, the mice were sacrificed and rear legs were removed by cutting across the tibia at the proximal metaphysic and across the distal joint. The legs were immediately fixed in toto in 10 % neutral buffered formalin upon removal.

6.2.2.3 Histological Analysis

Fixed specimens from the initial study were embedded in paraffin blocks from which 5 μm sections were cut. The extent of fibrosis in muscle tissue adjacent to the laceration site was quantified in brightfield images of picrosirius red-stained sections at low power by measuring the distance between regenerating myofibers in selected 400 x 400 pixel areas (5.08 x 10^5 μm^2). Images were captured using a 4x objective on a Nikon TE2000 inverted phas-fluorescence microscope with a 12 bit 1600 x 1200 pixel CCD detector (Spot; Diagnostic Instruments, Sterling Heights, MI, USA) and a color wheel for color imaging. Digital analysis was performed using Adobe Photoshop 7.0 (Adobe Systems, San Jose, CA, USA).

In the follow-up study, the fixed tissue was cut to the bone, longitudinally across the incision site, orthogonally to the bone, using the blue tissue marking dye as a guide, separating the medial 1/4 of the tissue from the lateral 3/4. The medial 1/4 section was embedded in paraffin for sectioning, with the cut surface up, to demonstrate the relationship between the laceration and skin to the deep tissues and to show the labeling of the healed laceration site. The lateral 3/4 section was cut across the laceration and 2 mm proximal and distal to the incision.

These sections were also embedded in paraffin, with the incision sites up, to provide cross-sections of muscle proximal to the healed laceration for the quantification of muscle fibrosis in tissue adjacent to the injured muscle fibers. Ten-6 μm sections were then cut in paraffin ribbons with three unstained sections on one slide and three sections on a second slide stained with Masson's trichrome to label collagen blue and muscle red.

The healed laceration site was identified using the blue tissue marking dye in unstained sections. Fluorescent images were acquired at an excitation wavelength in the rage of 450 – 490 nm, a 510 dichroic mirror, and a 520 barrier filter in order to determine the distribution of microspheres, and thus enzyme or buffer, at the site of injury.

Cross-sections of muscle at the laceration site were imaged using a 10x plan apochromatic objective on the same inverted phase-fluorescence microscope and camera employed in the initial *in vivo* study. Selected areas of muscle, approximately 200 μm away from the blue tissue marking dye and fluorescent microspheres, were selected from the main images using Adobe Photoshop 7.0 for digital analysis of muscle and collagen content.

Transmitted light photographs, using the color wheel to record in separate channels, blue, green and red images, were used for image analysis of the selected areas. Specifically, blue and red filters, with 10 % cutoffs of approximately 390 – 520 nm and 620 – 680 nm and essentially no overlap between these channels were used for digital quantification of collagen content. The red image was digitally subtracted from the blue image, using each image expressed as a grayscale 8-bit file. Following this, the collagen signal (dark area) was separated from the background (light area) with a threshold levels filter (Fovea Pro 1.0, Reindeer Graphics, Asheville, NC, USA), yielding 2-bit images in which collagen appeared black and all other tissue

white. The relative area of collagen is reported as the percent area of the image that was black after setting threshold levels. Threshold levels were set by a blind observer.

Statistical analysis comparing the amount of muscle fibrosis between treatment groups in both the initial and follow-up studies was performed using the Student's t-test.

6.2.2.4 MMP-1 Activity Assay Using Thioester Substrate

The rate of MMP-1 catalyzed hydrolysis of the thioester substrate Acetyl-Pro-Leu-Gly-[2-mercapto-4-methyl-pentanoyl]-Leu-Gly-OC_2H_5 was assayed spectrophotometrically using a Molecular Devices (Sunnyvale, CA, USA) SpectraMax 340PC^{384} microplate spectrophotometer by continuously monitoring the release of free thiols in the presence of excess 5,5'-dithiobis(2-nitrobenzoic acid) (DTNB) at 412 nm at 37 °C over 5 mins. Briefly, native or PEG-modified rhMMP-1 (0 – 0.55 μg) was added to buffer (50 mM HEPES, 5 mM calcium chloride, pH 7.5) and DTNB (1 mM) in a 96-well polystyrene microplate. The solution was pre-incubated at 37 °C for 3 mins after which the reaction was initiated by the addition of substrate (100 μM final concentration). The total reaction volume was 100 μL. One unit of MMP-1 activity was defined as the amount of enzyme required to catalyze substrate hydrolysis at a rate of 1 OD per sec.

To assay the activity of proMMP-1, the enzyme was first activated proteolytically by incubation with trypsin (0 – 200 ng-trypsin/ng-proMMP-1) in assay buffer in a 37 °C water bath. After 1 hr, trypsin was fully inactivated by the addition of soybean trypsin inhibitor at a mass ratio of inhibitor-to-trypsin of 4:1 or greater and subsequent incubation of the reaction solution at room temperature for 10 mins.

6.2.2.5 Collagen Degradation Assay

Type I collagen scaffolds were incubated in buffer (10.3 mL, 50 mM HEPES, 5 mM calcium chloride, pH 7.5) containing native or PEG-modified rhMMP-1 (3 mg/mL) in 15-ml conical tubes in a constant temperature shaker set at 37 °C and 250 rpm. The dry weight of the collagen-containing tubes was recorded prior to the addition of buffer and enzyme. The tubes were periodically removed from the shaker and the remaining collagen scaffolds were washed repeatedly with water. Without being removed from the tube, the scaffolds were subsequently dried by lyophilization. The final weight of the collagen-containing tubes was measured to determine the relative mass of collagen remaining.

6.2.2.6 Stability of Native and PEG-Modified rhMMP-1

Enzyme was incubated in buffer (50 mM HEPES, 5 mM calcium chloride, pH 7.5) at a concentration of 0.1 mg/mL at 65 °C. Thermoinactivation was followed by removing aliquots periodically and assaying residual enzyme activity using the thioester substrate assay.

The thermostability of native and PEG-modified rhMMP-1 at 37 °C and 50 °C was also measured in the presence of varying amounts of trypsin (0 – 1 mg/mL) and substilisn (0.0 – 0.1 mg/mL) respectively. In these experiments, trypsin or subtilisin was fully inactivated prior assaying MMP-1 activity by incubating the enzyme samples with soybean trypsin inhibitor or phenylmethylsulfonyl fluoride respectively.

6.2.2.7 Computation of Solvent Accessibilities of Lysines

The solvent accessible surfaces of lysines in rhMMP-1 were determined using the Swiss-Pdb viewer (http://expasy.org/spdbv).[178] The size of the probe used to determine the solvent accessibility of each residue was equal in size to that of a water molecule, which has radius of

1.4 Å. Solvent accessibility is reported as a percentage of the accessible surface of the residue relative to the accessible surface of the residue in the extended conformation of a standard peptide (GGXGG). A residue that is fully exposed has a solvent accessibility of 100 % whereas a residue that is completely buried has a solvent accessibility of 0 %. The crystal structure of the active form of MMP-1 employed for the calculations, which was solved for by Iyer et al.[179], was acquired from the Protein Data Bank (PDB accession code: 2CLT).

6.2.2.8 Computation of Lysine pKa Values

The theoretical pKa values of all lysines in rhMMP-1 were predicted using the H++ server (http://biophysics.cs.vt.edu/H++/index.php), which employs a standard continuum electrostatics methodology.[180]

6.2.2.9 SDS-PAGE of Native and PEG-Modified rhMMP-1

Native and PEG-modified rhMMP-1 samples were separated on 10 % linear or 4 – 20 % gradient polyacrylamide gels with tris-glycine-SDS running buffer. The enzymes were subsequently stained for using the SilverSNAP Stain Kit II from Pierce (Rockford, IL). A staining time of 3.5 mins was used in order to enhance the intensity of protein bands corresponding to PEG-rhMMP-1.

6.2.2.10 Matrix Assisted Laser Desorption/Ionization Time-of-Flight (MALDI-TOF) Mass Spectrometry

MALDI-TOF analysis of proMMP-1 in addition to native and PEG-modified rhMMP-1 was carried out using an Applied Biosystems PerSeptive STR Mass Spectrometer (Foster City, CA). Enzyme samples were mixed at a 1:1 v/v ratio with a saturated solution of sinapinic acid

(0.5 mL water, 0.5 mL acetonitrile, 1 μL of 1 % v/v trifluoracetic acid) and subsequently spotted on the sample plate where the enzyme was co-crystallized with the matrix solution at room temperature. After complete evaporation of the matrix solution, MALDI-TOF spectra were recorded in positive-ion linear mode.

The peptide fingerprint of trypsin-digested native and PEG-modified rhMMP-1 was also analyzed by MALDI-TOF. Briefly, the enzymes were initially resolved by SDS-PAGE using a 10 % polyacrylamide gel, which was subsequently stained with silver. The enzyme bands were carefully excised, transferred to 1.5-mL microcentrifuge tubes, and destained in sodium thiosulphate (50 mM) and potassium ferricyanide (15 mM) for 20 mins at room temperature. This was followed by repeated washings of the gel pieces in ammonium bicarbonate buffer and acetonitrile at 37 °C, reduction and alkylation of the enzyme in the presence of dithiothreitol (10 mM) and iodoacetamide (55 mM) respectively, and tryptic digestion. The digestion step was carried out by incubating the gel pieces with typsin (25 ng/μL) in buffer (25 mM ammonium bicarbonate) overnight at 37 °C. Peptide fragments were subsequently extracted by washing the gel pieces three times with a solution of formic acid (5 % v/v) and acetonitrile (50 % v/v) at 37 °C for 15 mins with constant shaking. The rinse from each wash was collected and the peptide fragments were concentrated by vacuum centrifugation. The peptide fragments were then desalted using Millipore C18 Ziptips (Bedford, MA) and eluted into a solution of acetonitrile (50 % v/v) and α-cyano-4-hydroxycinnamic acid and trifluoroacetic acid (0.1 % v/v), which was spotted on the MALDI-TOF sample plate. Low mass peptides (≤ 10 kDa) were analyzed in positive reflector mode whereas high mass peptides (10 - 30 kDa) were analyzed in positive-ion linear mode.

6.2.2.11 Analytical Ultracentrifugation Analysis of Native and PEG-Modified rhMMP-1

The sedimentation behavior of native or PEG-modified rhMMP-1 was determined via analytical ultracentrifugation using a Beckman-Coulter (Fullerton, CA) XL-A ultracentrifuge. Sedimentation velocity analysis was determined at 18,000 rpm at a fixed temperature of 20 °C using enzyme solutions that were prepared in buffer (50 mM HEPES, 5 mM calcium chloride, pH 7.5). Optical scans were generated by recording the absorption of the enzyme samples at 280 nm.

6.3 RESULTS AND DISCUSSION

6.3.1 Rapid Assessment of Potential Therapuetic Efficacy of proMMP-1, rhMMP-1, and PEG-rhMMP-1 in Laceration Model

Morphometric analysis showed a statistically significant ($p < 0.05$) reduction in interfibrillar collagen in the lacerated GMs of mice treated with proMMP-1, rhMMP-1, and PEG-rhMMP-1 relative to those treated with buffer (**Figures 29A and B**). This reduction was greatest in lacerated GMs treated with 0.8 mU rhMMP-1 (51 %) and slightly less so in lacerated GMs treated with 0.4 mU proMMP-1 (40 %) and with 0.4 mU (41 %) and 0.8 mU PEG-rhMMP-1 (30 %). However, the effects of the enzyme treatments were not dose-dependent in the range of enzyme concentrations studied. This suggests that the efficacy of muscle remodeling does not increase linearly with the rate of collagen degradation. Rather, there is likely a critical point at which the rate of remodeling becomes limiting and any subsequent increase in the rate of

collagen degradation has a negligible impact on muscle regeneration. It is thus conceivable that the efficacy of remodeling in the lacerated muscle was maximal upon delivery of 0.4 mU of collagenase activity. Additionally, it is noteworthy that SDS-PAGE indicated a significant fraction of the proMMP-1 preparation had undergone autolytic activation and thus any effect caused by the injection of proMMP-1 may be partially attributed to this faction of the enzyme.

Excessive fibrosis in many pathologies is linked to changes in relative levels of matrix metalloproteinases to tissue inhibitors of matrix metalloproteinases (TIMPs).[170, 175, 181, 182] Delivery of MMP-1 to pre-existing scar in skeletal muscle may shift the balance of MMP-1-to-TIMP activity to facilitate collagen degradation. Assuming this to be the case, small molecules that inhibit TIMPs and thus alter the balance of endogenous collagenase-to-TIMP activity could also potentially be used to treat muscle fibrosis.

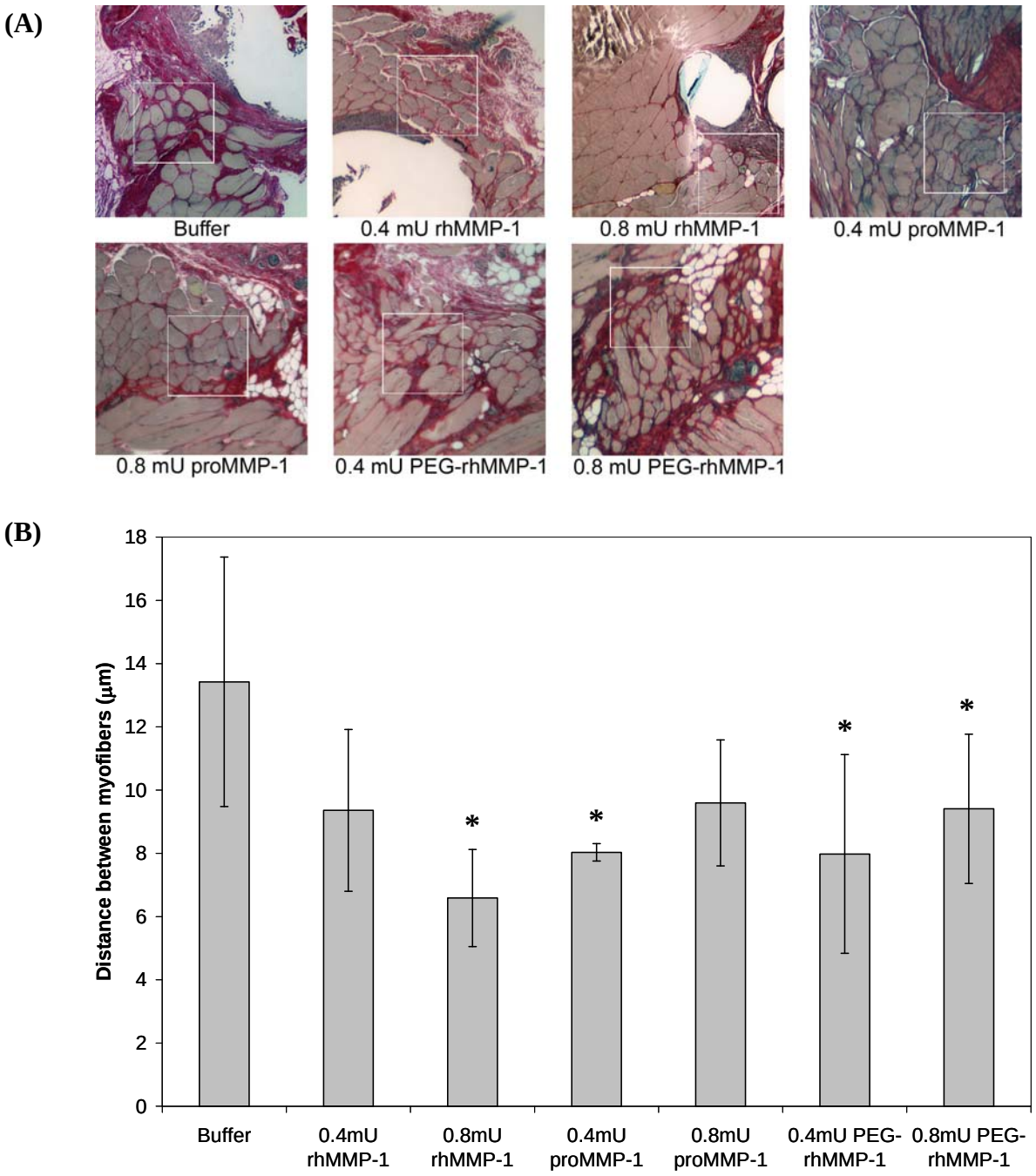

Figure 29. Histological analysis of muscle adjacent to the laceration site 14 d after treatment. (A) Images of tissue stained with picrosirius red acquired with a 4x objective. (B) Comparison of interfibrillar collagen in control and treatment groups (∗ $p < 0.05$). The boxed areas represent the fields in which the amount of connective collagen was quantified. Error bars represent the standard deviation from the mean for each treatment group.

6.3.2 Quantitative Comparison of Efficacies of Native and PEG-Modified rhMMP-1 in Reducing Muscle Scarring in Laceration Model

In attempt to improve the *in vivo* stability of rhMMP-1, and thus its efficacy as a scar reducing agent, we covalently modified the enzyme with PEG-SPA. PEG-modification, commonly referred to as PEGylation, is an often effective strategy for reducing the clearance of therapeutic proteins.[51-53] The attachment of PEG can render a protein less immunogenic and prevent proteolysis and autolysis, when the target protein is itself a protease, through steric effects and by altering residue charge.

A follow-up *in vivo* study was carried out to quantifiably compare the effects of native and PEG-modified rhMMP-1 on muscle fibrosis in the laceration model. To accurately identify the laceration site in tissue sections, blue tissue marking dye was applied to the wound site after injury. Additionally, green fluorescent microspheres were co-injected with the enzymes or buffer to label the injection site in relation to the site of injury. Fluorescent images showed the co-localization of the microspheres with the tissue marking dye at the laceration site, thereby verifying delivery of the enzymes or buffer to the fibrotic tissue (**Figure 30**). Hemosiderin deposits were also observed in muscle at the laceration site, which are the result of hematoma formation in the muscle tissue.

Compared to in lacerated GMs treated with buffer, the GMs of mice injected with a single dose of rhMMP-1 (0.8 mU) contained 30 % less interfibrillar collagen (**Figure 31**). While the effect of rhMMP-1 was statistically significant ($p < 0.05$), GMs treated with the active enzyme still contained on average 5-fold more interfibrillar collagen than normal (i.e. uninjured) GMs. Direct injection of PEG-modified rhMMP-1 did not, however, yield a significant effect on the interfibrillar collagen in the lacerated GMs of mice. The key question thus becomes why is

the activity of PEG-modified rhMMP-1 in the laceration model significantly lower than that of the native enzyme.

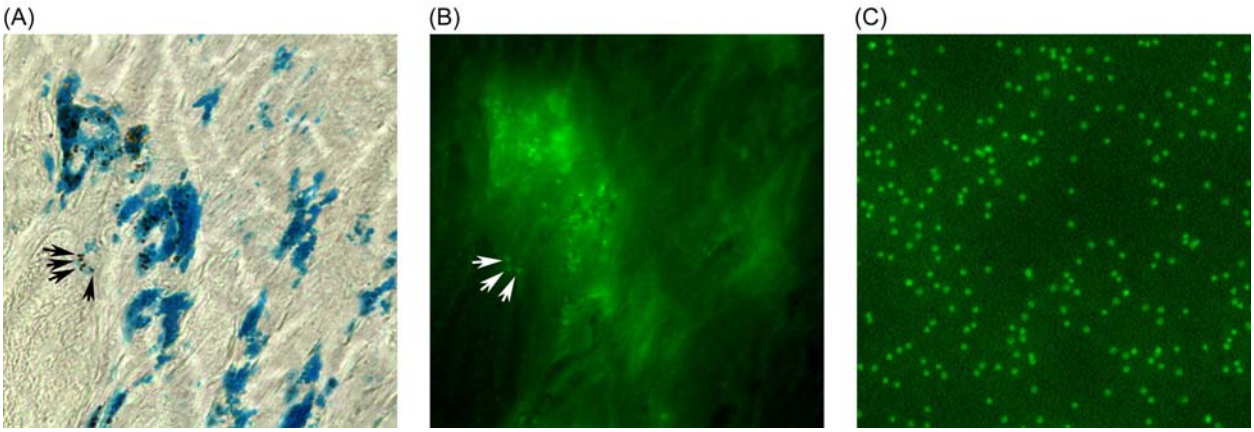

Figure 30. (A) Brightfield image of blue tissue marking dye at laceration site acquired with 100x objective. The arrows indicate the presence of hemosiderin, the brown pigment, at the site of injury. (B) Fluorescent image of the equivalent field showing co-localization of green fluorescent microspheres with the tissue marking dye at the laceration site. The arrows point to examples of individual microspheres in the captured field. (C) Control image showing the size of the green fluorescent microspheres prepared on a blank glass slide at the same magnification.

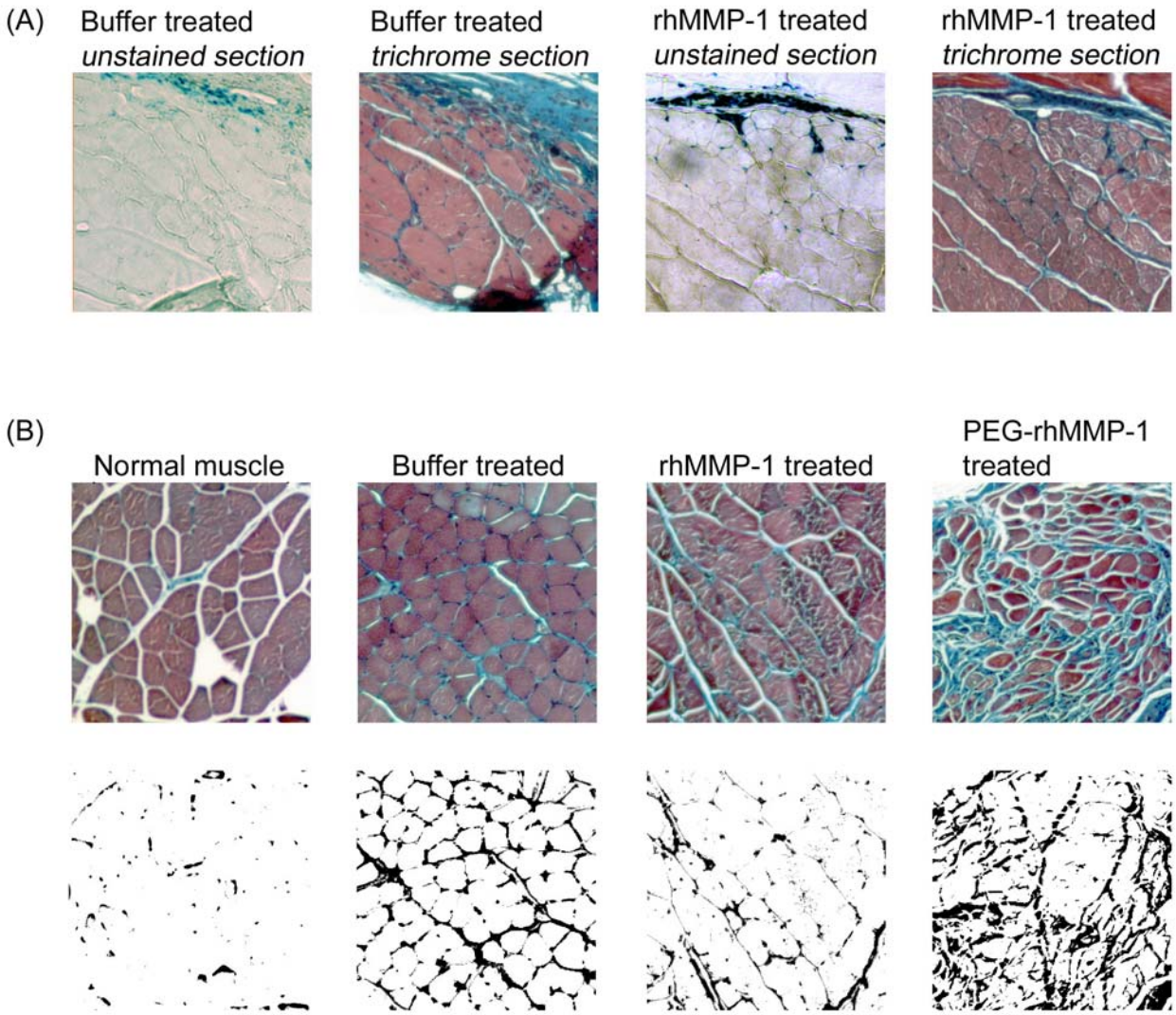
(A)
Buffer treated
unstained section
Buffer treated
trichrome section
rhMMP-1 treated
unstained section
rhMMP-1 treated
trichrome section
(B)
Normal muscle
Buffer treated
rhMMP-1 treated
PEG-rhMMP-1
treated

(C)

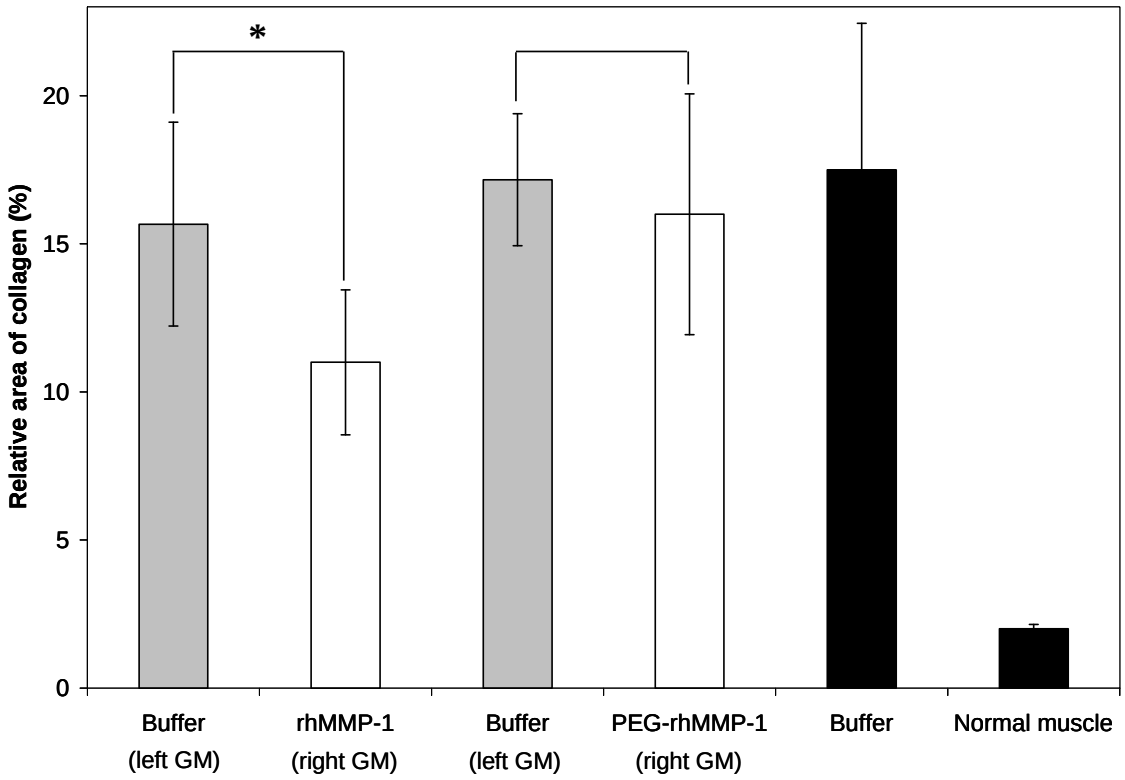

Figure 31. Results of histological analysis from follow-up *in vivo* study at 11 d post-treatment of lacerated GMs with rhMMP-1 (0.8 mU) or PEG-rhMMP-1 (0.8 mU). (A) Images of unstained sections showing tissue marking dye at site of laceration and matching area in Masson's trichrome stained specimens (10x objective). (B) Selected fields from Masson's trichrome stained specimens used for quantification of interfibrillar collagen and below, corresponding thresholded areas. (C) Comparison of interfibrillar collagen in the left and right GMs of mice within the same treatment group (∗ $p < 0.05$). The level of fibrosis in the GMs of mice treated with buffer only and in the GM of uninjured mice are also shown. Error bars represent the standard deviation from the mean for each treatment group.

6.3.3 Effect of PEGylation on rhMMP-1 *In Vitro* Activity and Stability

To determine if PEG-attachment effected the activity of rhMMP-1, the kinetic parameters (k_{cat} and K_M) of native and PEG-modified rhMMP-1 were determined using a thioester peptide substrate (**Table 4**). Differences in k_{cat}, K_M, and k_{cat}/K_M of rhMMP-1 versus PEG-rhMMP-1 were minimal, suggesting that PEG-attachment does not drastically affect the catalytic efficiency of rhMMP-1. The intrinsic activity and specificity of the recombinant human active MMP-1 may have been subtly affected by the presence of a hexahistidine tag and differences in glycosylation levels of proMMP-1 and rhMMP-1.

Table 4. Kinetic parameters for native and PEG-modified rhMMP-1 catalyzed degradation of thioester peptide substrate.

Enzyme	**k_{cat} (s^{-1})**	**K_M (mM)**	**k_{cat}/K_M ($s^{-1}mM^{-1}$)**
rhMMP-1	7.3 ± 0.4	0.87 ± 0.14	8.4 ± 1.8
PEG-rhMMP-1	5.9 ± 0.1	0.98 ± 0.05	6.0 ± 0.4

The error associated with the catalytic efficiency (k_{cat}/K_M) was calculated as follows:

$$\Delta\left(\frac{k_{cat}}{K_M}\right)=\left(\frac{k_{cat}}{K_M}\right)\times\left(\frac{\Delta k_{cat}}{k_{cat}}+\frac{\Delta K_M}{K_M}\right)$$

The impact of PEGylation on the activity of rhMMP-1 towards type I collagen, the natural substrate of MMP-1 in scar, was also investigated via assaying the rate of enzymatic hydrolysis of collagen scaffolds (**Figure 32**). Collagen is a much larger substrate molecule than

the thioester peptide, although since the substrates share a common target cleavage site, the mechanism of catalysis of collagen and thioester peptide is presumably similar. Incubation of collagen scaffolds with native rhMMP-1 over the course of 14 days resulted in an approximate 29 % reduction scaffold mass. Conversely, the rate of hydrolysis of collagen scaffolds in the presence of equivalent amounts of PEG-rhMMP-1 was comparable to that of the scaffold in buffer. A plausible explanation for this is the modification of a residue that is critical to the catalytic mechanism of the enzyme. The rather large error in the assay results is intrinsic in the measurement of scaffold weights.

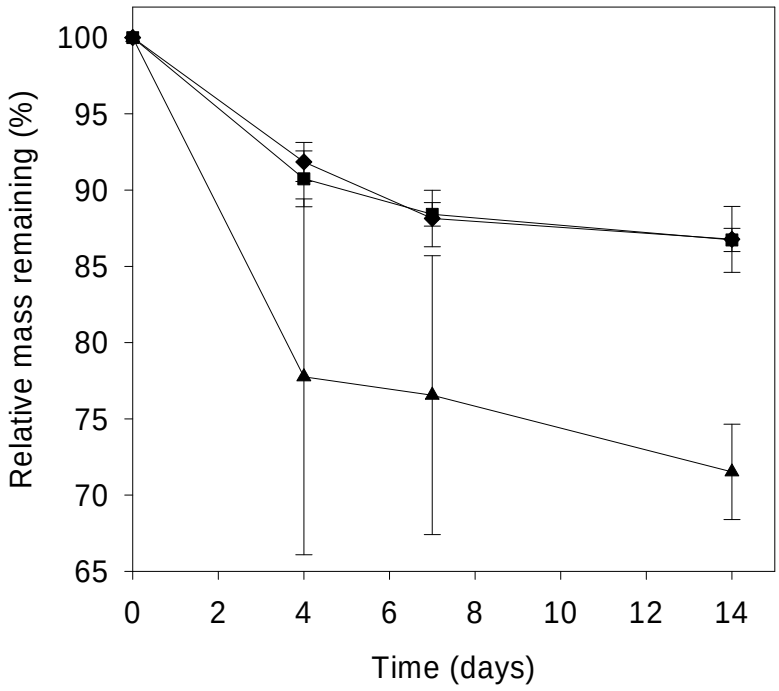

Figure 32. Degradation of lyophilized type I collagen scaffolds by native rhMMP-1 (▲), PEG-rhMMP-1 (■), and buffer (◆). Error bars represent the standard deviation from the mean for three separate experiments.

To determine if PEG-attachment enhanced the overall stability of rhMMP-1, the stability of native and PEG-modified rhMMP-1 at elevated temperature and in the presence of proteolytic enzymes was assayed. Enzyme inactivation in these studies was determined by measuring residual activity over time using the thioester peptide substrate. Modification of rhMMP-1 with PEG resulted in a marked thermostability enhancement (a 60-fold increase in half-life) at 65 °C (**Figure 33**). The thermostability of rhMMP-1 when incubated at the same temperature in the presence of 10 % (w/v) free PEG (5000 M_w) was greater than that of the native enzyme alone, but significantly less than that of the modified enzyme. When incubated with trypsin or subtilisin, native and PEG-modified rhMMP-1 were inactivated at comparable rates, independent of the concentration of the added protease (**Figure 34**). These results suggest that PEGylation does not mask the susceptibility of rhMMP-1 to proteolytic digestion. Hence, the attachment of PEG would presumably have little effect on the *in vivo* half-life of rhMMP-1 in the laceration model.

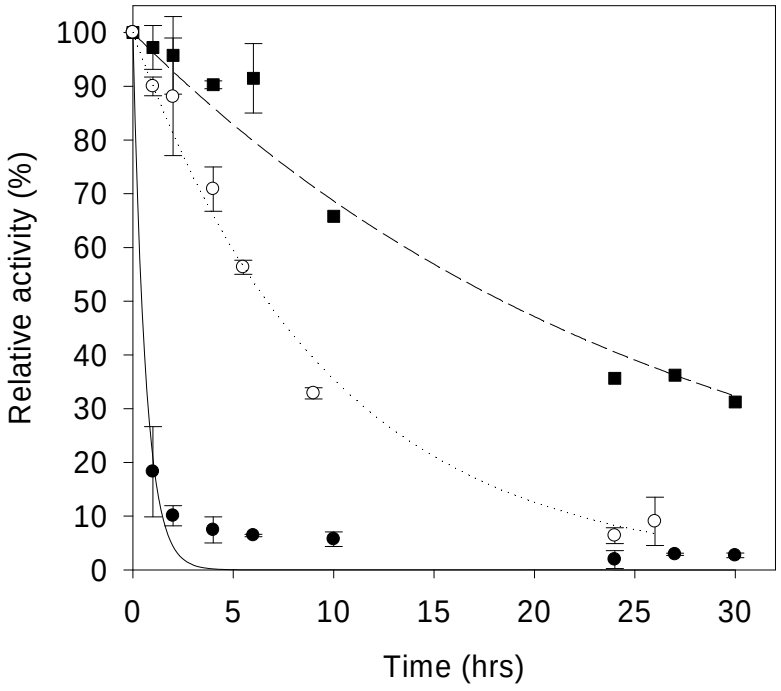

Figure 33. Thermostability of native (●) and PEGylated rhMMP-1 (■) at 65 °C. The stability of rhMMP-1 in the presence of 10 % (w/v) fully hydrolyzed PEG-SPA (M_w 5000) was also measured (○). Error bars represent the standard deviation from the mean for two separate experiments.

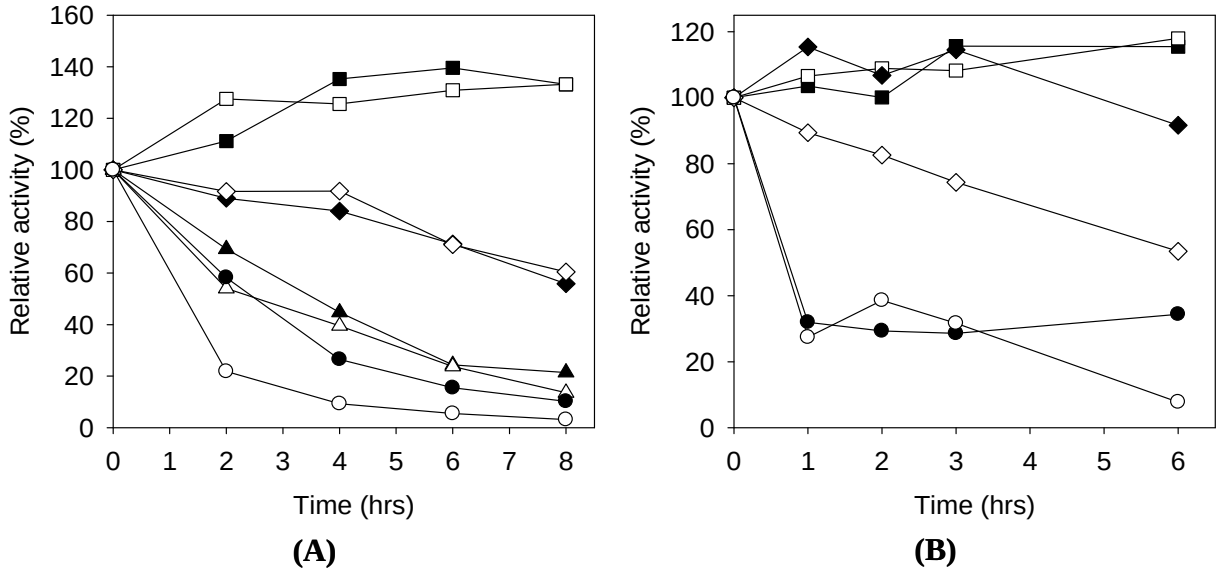

Figure 34. (A) Stability of native and PEGylated rhMMP-1 in the presence of trypsin at 50 °C. Native rhMMP-1 (closed symbols) and PEG-rhMMP-1 (open symbols) were incubated with varying amounts of trypsin (0.0 mg/mL (squares), 0.1 mg/mL (diamonds), 0.5 mg/mL (triangles), 1.0 mg/mL (circles)). (B) Stability of native and PEGylated rhMMP-1 in the presence of subtilisin Carlsberg at 37 °C. Native rhMMP-1 (closed symbols) and PEG-rhMMP-1 (open symbols) were incubated with varying amounts of substilisin (0.0 mg/mL (squares), 0.001 mg/mL (diamonds), 0.1 mg/mL (circles)).

6.3.4 Prediction of Reactivity of Modification Sites in rhMMP-1

Modification with PEG resulted in the inactivation of rhMMP-1 towards collagen and was ineffective in enhancing the enzyme's stability under near physiological conditions. As a result, with the ultimate aim of determining the structural basis for the apparent deactivation of

rhMMP-1, we predicted the most likely sites of PEG-attachment by means of computational analysis.

Given the reactivity of PEG-SPA towards primary amines, the principal sites for rhMMP-1 modification are the ε-amino groups of lysines and the N-terminal α-amino group (**Figure 35**). The relative reactivity of these sites can be modeled by computing their respective pKa values and solvent accessibilities, enabling the most probable sites of PEG-attachment to be predicted. Generally, the most reactive sites are those that are on the enzyme's surface, and thus solvent accessible. These sites also typically have low pKa values, which are characteristic of strong nucelophiles.[73, 183-185] Potential modification sites that are largely inaccessible, such as those in the active cleft of an enzyme, for example, may still be highly reactive if their pKa values are unusually low. Therefore, the pKa value of a potential modification site can have a larger influence on reactivity than solvent accessibility when it is buried in the core of an enzyme.[183]

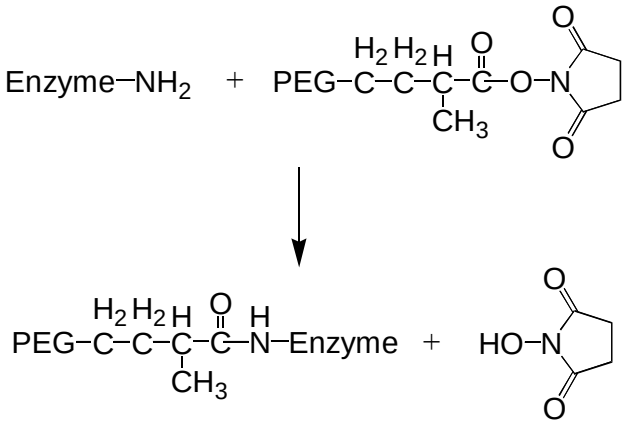

Figure 35. Schematic of rhMMP-1 PEGylation with PEG-SPA.

The pKa and solvent accessibility values of the lysines in rhMMP-1 and of the N-terminal α-amino group, which were calculated from the crystal structure of the enzyme using

H++ server and Swiss-PdB Viewer respectively, are summarized in **Table 5** Out of the possible modification sites, Lys459 is presumably the most reactive since it has the lowest pKa (9.54) and moderately high accessibility (31.14 %). Another probable site for PEG-attachment is Lys432 since it too has a comparatively low pKa (10.19), although it is largely inaccessible to solvent (9.89 %). Among the other sites in rhMMP-1 that may potentially be modified based on pKa and solvent accessibility include Lys362, 281, and 347.

Interestingly, Lys459, 432, 362, 281, and 347 are all in the C-terminal hemopexin domain of the enzyme (**Figure 36**). This 183 residue segment, which is tethered to the catalytic domain of MMP-1 by a short hinge, plays a critical role in the enzyme's ability to bind collagen as demonstrated by mutation deletion studies [186-189]. Modification of a lysine in the hemopexin domain or other proximal lysines would be expected to impact collagen binding. Moreover, modification at these sites may not fully shield the catalytic domain from attack of proteases. It may be possible to prevent deactivation of rhMMP-1 and protect the enzyme from proteolytic degradation through site-specific modifications. A reversible inhibitor or substrate may also be used to shield critical residues in the enzyme during modification to prevent deactivation.

Table 5. Theoretical pKa and solvent accessibility values of the N-terminal α-amino group and lysines in rhMMP-1. The residue number corresponds to that of the residue in the sequence of full-length proMMP-1.

Residue	pKa	Solvent accessibility (%)
F81(α-NH_2)	11.87	33.68
K136	10.67	19.41
K151	11.23	27.84
K276	11.31	44.69
K281	10.36	47.99
K298	13.55	16.85
K344	11.95	18.32
K347	10.37	34.80
K362	10.20	25.27
K375	10.52	55.68
K388	15.62	13.19
K396	10.66	29.30
K404	10.79	46.89
K413	10.87	26.37
K425	14.35	29.67
K432	10.19	9.89
K446	10.75	14.65
K450	10.88	64.10
K452	11.72	38.46
K459	9.54	31.14

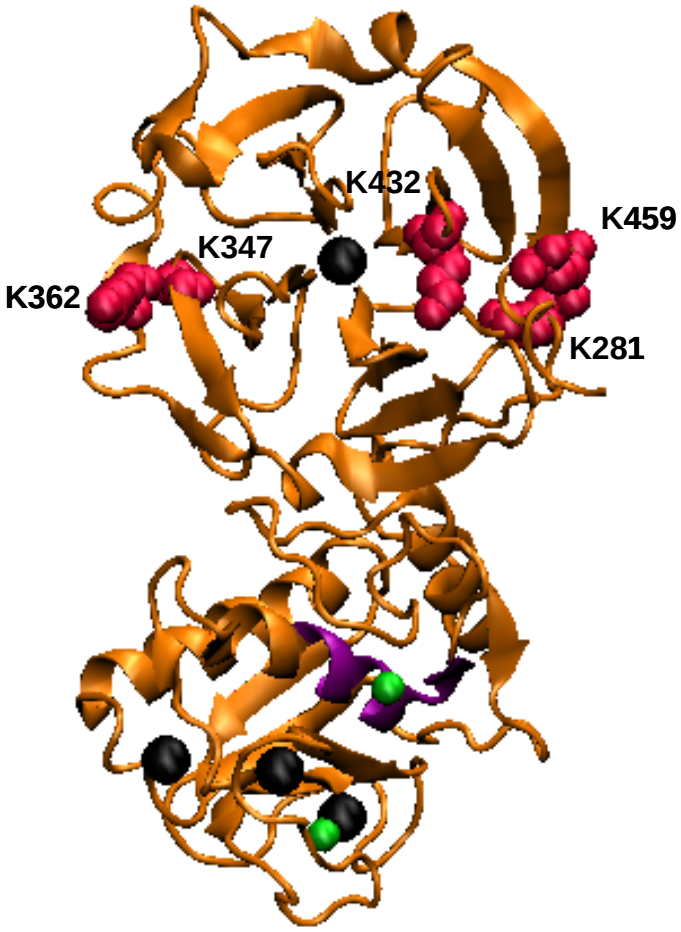

Figure 36. Ribbon diagram of rhMMP-1 showing the most likely sites of PEG-attachment (red). The active site residues H_{218}ALGHSLGLSH (purple) and the enzyme-associated zinc (green) and calcium (black) ions are also highlighted.

In attempt to experimentally determined the number and sites of modification, PEG-rhMMP-1 was further characterized using a variety of analytical and biophysical techniques. When separated by SDS-PAGE, PEG-rhMMP-1, prepared using a 1000:1 molar ratio of PEG -to-protein, resolved into several species (**Figure 37**). These species, ranging in molecular weight from 43 kDa to greater than 250 kDa, are presumably representative of rhMMP-1 modified with increasing number of PEGs, including a small fraction of residual unmodified enzyme. The

average number of attached PEGs per enzyme molecule could not be determined, however, since the migration of PEG-modified proteins is not consistent with that of native proteins of equilivalent mass. Such differences in the migration of native and PEGylated proteinas are likely due to entanglement of the PEG chains and may reflect differences in SDS binding.[190, 191] Autolytic peptide fragments, which were apparent in native rhMMP-1, were presumably also modified, thereby complicating the analysis of PEG-rhMMP-1.

Analytical ultracentrifugation was also employed to quantitatively determine the extent of PEG-attachment to rhMMP-1. In analytical ultracentrifugation analysis, the absolute molecular weight and conformation of proteins can be ascertained based on their sedimentation behavior.[192] Native rhMMP-1 sedimented as a single species in sedimentation velocity analysis whereas multiple sedimenting species were observed in the analysis of PEG-rhMMP-1. This serves as additional evidence that PEG-rhMMP-1 was indeed modified with multiple PEGs and that the distribution in number of attached PEGs varied. However, due to error associated with obtaining a stable baseline signal, the average molecular weight, and thus number of attached PEGs per enzyme molecule, of the modified enzyme could also not be determined using this method. Such error, which may be due to autolytis of the modified enzyme over the course of analysis, may potentially be prevented in future studies by the addition of MMP-1 inhibitior or zinc chelating agents.

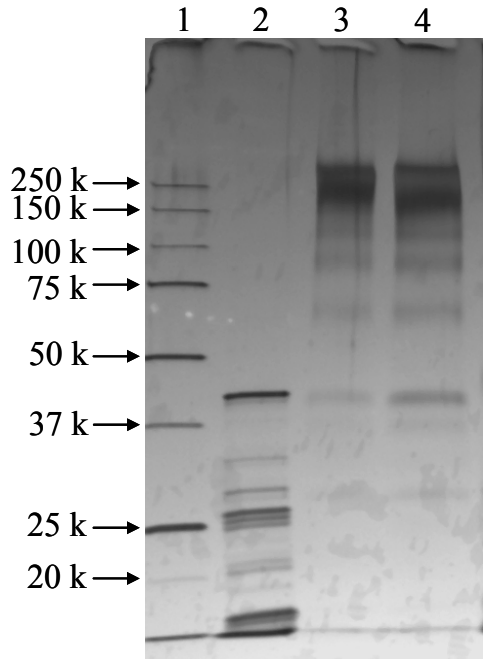

Figure 37. SDS-PAGE of native and PEGylated rhMMP-1. Lanes: (1) protein molecular weight markers, (2) native rhMMP-1 (0.5 μg), (3) PEG-rhMMP-1 (M_w 5000; 1 μg), and (4) PEG-rhMMP-1 (M_w 5000; 2 μg).

A peptide mapping approach was used to pinpoint the modified sites and thus confirm modification of a critical lysine in the hemopexin domain. PEG-rhMMP-1 was initially subjected to in-gel tryptic digestion after which the mass of the resulting peptide fragments were analyzed by MALDI-TOF. A lysine that is modified with PEG will, in theory, be shielded from tyrpsin, thereby resulting in a shift in the expected mass of the peptide fragment containing this lysine. However, the peptide fingerprint of PEG-rhMMP-1 was not detectable by MALDI-TOF, thereby preventing the successful identification of the modified sites in the enzyme. The method settings used for MALDI-TOF analysis including the laser intensity, accelerating voltage, grid voltage, guide wire voltage and delay time were varied and different matricies were used in attempt to improve the signal of the peptide fragments. Similarly, intact native and PEGylated

rhMMP-1 were also not amenable to MALDI-TOF analysis, suggesting that the enzymes and tryptic peptide fragments are not readily ionizable.

6.4 CONCLUSIONS

In our earlier work, we have demonstrated the feasibility of using proMMP-1 to reduce the extent of interfibrillar collagen in lacerated skeletal muscle. The objective of this study was to examine the impact of pre-activation and PEG-modification on the therapeutic efficacy of MMP-1 in the treatment of scarred muscle. A rapid assessment of the efficacy of proMMP-1, rhMMP-1, and PEG-rhMMP-1 in an *in vivo* murine model of lacerated muscle found the pre-activated enzyme to be most effective in resolving fibrotic tissue. However, the enzyme treatments did not show a dose-dependent effect, suggesting the rate of muscle remodeling was limiting relative to that of collagen degradation. A quantitative comparison of scar degrading activities of rhMMP-1 and PEG-rhMMP-1 in the laceration model confirmed that the modified form of the enzyme was significantly less effective than rhMMP-1 in digesting pre-existing scar. It was found that PEG-modification resulted in the loss of collagenase activity in *in vitro* activity assays, thereby presumably explaining the inability of PEG-rhMMP-1 to effectively degrade fibrotic tissue in the laceration model. Stability studies also indicate that the covalent attachment of PEG did not increase the half-life of rhMMP-1 when incubated in the presence of trypsin or subtilisin. Computational modeling of the reactivity of potential modification sites in rhMMP-1 suggest that one or more critical lysines in the hemopexin domain of the enzyme are covalently modified, which would likely block collagen docking. Accordingly, the impact of PEGylation on the activity and stability of rhMMP-1 may be dramatically improved through site-specific modifications.

Overall, these results provide valuable insight into the development of a novel strategy for treating fibrotic pathologies based on the use of MMP-1. Further studies are required to characterize the effect of MMP-1 treatment on the physiological function of fibrotic muscle.

These along with additional studies that examine the impact of multiple MMP-1 injections and different dosing regimens will be reported in a subsequent communication.

APPENDIX

SOURCECODE

MATLAB Model of pH and Paraoxon Conversion in OPH-Urease System

Main Program:

```
%Clear workspace
clear;

%Define enzyme concentrations:
urease = (5.1/1000)*22.45;                          %in U/mL
oph_units = (0.001/1000)*2624.898;                  %in U/mL

%Define unit definitions of enzymes:
%1 unit of jack bean urease activity = 1 micromole of urea hydrolyzed per min (micromol/min)
%at pH 6.5, T=25C, and [urea]=10mM in 50mM NaCl, 0.15mM CoCl2
%Activity determined using pH-stat method
%
%1 unit of Pseudomonas diminuta OPH activity = 1 micromole of paraoxon hydrolyzed per min
(micromol/min)
%at pH 8, T=25C, and [paraoxon]=1mM in 50mM bis-tris propane, 0.15mM CoCl2
%Activity determined spectroscopically by monitoring p-nitrophenol generation at 412nm

%Convert concentration of OPH from activity units to molar basis using Michaelis-Menten rate
%equation and empirical kinetic parameters (kcat and KM) at pH 8:
kmunit = 0.031;                                     %in mM
kcatunit = 1740;                                    %in s-1
oph =(oph_units)*1000*(10^(-6))*((kmunit/1000)+(1/1000))/((kcatunit)*60*1/1000);      %in M


%Define initial conditions for ode solver:
```

```
%y0(1) = Initial paraoxon concentration (M)
%y0(2) = Initial system pH
y0=[0.001; 6];

%Define time step:
tspan = [0; 100];
refine = 500;

%Call ode solver:
%ode15s is required due to stiffness of problem
%solver calls on function “stifffun”
options = odeset('BDF','on','Refine', refine);
[t,y] = ode15s(@stifffun, tspan, y0, options, urease, oph);

%Generate plot of pH and paraoxon conversion as a function of time:
plot(t,y(:,2),'b');

%Write time, pH, and paraoxon conversion to data.txt (data file):
fid = fopen('data.txt','w+');
[size1, size2]=size(y);
for i=1:size1
   paraoxon_conversion=(y(1,1)-y(i,1))./y(1,1)*100;
   ret2 = fprintf(fid, '%f %2.5f %f\n', t(i), y(i,2), paraoxon_conversion);
end
status = fclose(fid);
```

Function “stifffun”:

```
function [dydt]=stifffun(t, y, urease, oph);
dydt = zeros(2,1);

%Calculate pH-dependent kinetic constants for OPH against paraoxon:
km = (0.001)*(-0.01*((y(2))^2) + 0.155*(y(2)) - 0.568);      %in M
kcat = -6720*((y(2))^2) + 141600*(y(2)) - 597780;            %in min-1

%Calculate rate of paraoxon hydrolysis:
Voph = (kcat)*(oph)*(y(1))/(km+(y(1)));                      %in M/min

%Define acid/base dissociation constants:
pkaPNP = 7.1;                                                %p-nitrophenol
kaNH4 = 5.6E-10;                                             %ammonium
pkaH2CO3 = 6.352;                                            %carbonic acid
pkaHCO3 = 10.329;                                            %bicarbonate
```

```
%Compute proportionality factors as a function of pH:
%Generation of protons per mol of p-nitrophenol as a function of pH:
alpha = 1 + 1/(1 + 10^(pkaPNP-(y(2))));

%Generation of hydroxide ions per mol of bicarbonate as a function of pH:
factorA = 10^(pkaH2CO3-(y(2)));
factorB = 10^((y(2))- pkaHCO3);
beta = 2/(1+(kaNH4/(10^(-(y(2))))))-((1/(1+factorA))-(factorB/(1+factorA))*(1/(1+factorB)))-
2*((factorB/(1+factorA))*(1/(1+factorB)));

%Conversion of d[H+]/dt to dpH/dt:
gamma = 1/(-2.302585*(10^(-(y(2)))));

%Calculate rate of urea hydrolysis
Vurease = (10^(-6))*((-15.047*((y(2))^2) + 208.016*(y(2)) - 700.421))*(urease/0.01585);  %in
M/min

%Michaelis-Menten rate equation (dydt(1)) for monitoring rate of change of paraoxon
%concentration:
dydt(1) = -(kcat)*(oph)*(y(1))/((km)+(y(1)));    %in M/min

%Differential equation for monitoring rate of change of system pH (dydt(2)):
dydt(2) = (gamma)*(alpha*(Voph) - beta*(Vurease));
```

BIBLIOGRAPHY

1. Rozzell JD. Commercial scale biocatalysis: Myths and realities. *Bioorg Med Chem.* Oct 1999;7(10):2253-2261.

2. Liang JF, Li YT, Yang VC. Biomedical application of immobilized enzymes. *J Pharm Sci.* Aug 2000;89(8):979-990.

3. Koeller KM, Wong CH. Enzymes for chemical synthesis. *Nature.* Jan 11 2001;409(6817):232-240.

4. Alcalde M, Ferrer M, Plou FJ, Ballesteros A. Environmental biocatalysis: from remediation with enzymes to novel green processes. *Trends Biotechnol.* Jun 2006;24(6):281-287.

5. Russell AJ, Fersht AR. Rational modification of enzyme catalysis by engineering surface charge. *Nature.* Aug 6-12 1987;328(6130):496-500.

6. Bloom JD, Meyer MM, Meinhold P, Otey CR, MacMillan D, Arnold FH. Evolving strategies for enzyme engineering. *Curr Opin Struct Biol.* Aug 2005;15(4):447-452.

7. Dordick JS. Enzymatic catalysis in monophasic organic solvents. *Enzyme Microb Technol.* 1989;11:194-211.

8. Russell AJ, Chatterjee S, Bambot S. Mechanistic Enzymology in Nonaqueous Media. *Pure & Appl Chem.* Aug 1992;64(8):1157-1163.

9. Kibanov AM. Improving enzymes by using them in organic solvents. *Nature.* Jan 11 2001;409(6817):241-246.

10. Mesiano AJ, Beckman EJ, Russell AJ. Supercritical biocatalysis. *Chem Rev.* Feb 1999;99(2):623-633.

11. Erbeldinger M, Mesiano AJ, Russell AJ. Enzymatic catalysis of formation of Z-aspartame in ionic liquid - An alternative to enzymatic catalysis in organic solvents. *Biotechnol Prog.* Nov-Dec 2000;16(6):1129-1131.

12. Zaks A, Klibanov AM. Enzyme-catalyzed processes in organic solvents. *Proc Natl Acad Sci U S A.* May 1985;82(10):3192-3196.

13. Volkin DB, Klibanov AM. Minimizing protein inactivation. In: Creighton TE, ed. *Protein Function: A Practical Approach*. Oxford: IRL Press; 1989:1-24.

14. Fersht A, Winter G. Protein Engineering. *Trends Biochem Sci.* Aug 1992;17(8):292-294.

15. Yang Z, Russell AJ. Fundamentals of non-aqueous enzymology. In: Koskinen AMP, Klibanov AM, eds. *Enzymatic reactions in organic media*. London: Chapman and Hall; 1996:43-69.

16. Klibanov AM. Enzymatic catalysis in anhydrous organic solvents. *Trends Biochem Sci.* Apr 1989;14(4):141-144.

17. Anthonsen T, Sjursnes B. Importance of water activity for enzyme catalysis in non-aqueous organic systems. In: Gupta MN, ed. *Methods in non-aqueous enzymology*. Basel: Birkhauser; 2000:14-35.

18. Halling P. What can we learn by studying enzymes in non-aqueous media? *Philos Trans R Soc Lond B Biol Sci.* 2004;359:1287-1297.

19. Carrea G, Riva S. Properties and synthetic applications of enzymes in organic solvents. *Angewandte Chemie-International Edition.* 2000;39(13):2226-2254.

20. Ke T, Klibanov AM. On enzymatic activity in organic solvents as a function of enzyme history. *Biotechnol Bioeng.* Mar 20 1998;57(6):746-750.

21. Chatterjee S, Russell AJ. Determination of Equilibrium and Individual Rate Constants for Subtilisin-Catalyzed Transesterification in Anhydrous Environments. *Biotechnol Bioeng.* Nov 1992;40(9):1069-1077.

22. Fitzpatrick PA, Steinmetz AC, Ringe D, Klibanov AM. Enzyme crystal structure in a neat organic solvent. *Proc Natl Acad Sci U S A.* Sep 15 1993;90(18):8653-8657.

23. Yennawar NH, Yennawar HP, Farber GK. X-ray crystal structure of gamma-chymotrypsin in hexane. *Biochemistry.* Jun 14 1994;33(23):7326-7336.

24. Halling PJ. Thermodynamic predictions for biocatalysis in nonconventional media: theory, tests, and recommendations for experimental design and analysis. *Enzyme Microb Technol.* Mar 1994;16(3):178-206.

25. Kamat S, Barrera J, Beckman EJ, Russell AJ. Biocatalytic Synthesis of Acrylates in Organic-Solvents and Supercritical Fluids .1. Optimization of Enzyme Environment. *Biotechnol Bioeng.* Jun 5 1992;40(1):158-166.

26. Alston MJ, Freedman RB. The water-dependence of the catalytic activity of bilirubin oxidase suspensions in low-water systems. *Biotechnol Bioeng.* 2002;77(6):651-657.

27. Halling PJ. Salt hydrates for water activity control with biocatalysts in organic media. *Biotechnol Tech.* 1992;6:271-276.

28. Kvittingen L, Sjursnes B, Anthonsen T, Halling P. Use of Salt Hydrates to Buffer Optimal Water Level during Lipase Catalyzed Synthesis in Organic Media - a Practical Procedure for Organic Chemists. *Tetrahedron.* Mar 27 1992;48(13):2793-2802.

29. Zacharis E, Omar IC, Partridge J, Robb DA, Halling PJ. Selection of salt hydrate pairs for use in water control in enzyme catalysis in organic solvents. *Biotechnol Bioeng.* Jul 20 1997;55(2):367-374.

30. Yang L, Dordick JS, Garde S. Hydration of enzyme in nonaqueous media is consistent with solvent dependence of its activity. *Biophys J.* Aug 2004;87(2):812-821.

31. Laane C, Boeren S, Vos K, Veeger C. Rules for optimization of biocatalysis in organic solvents. *Biotechnol Bioeng.* 1987;30:81-87.

32. Reichardt C. Solvatochromic dyes as solvent polarity indicators. *Chem Rev.* 1994;94(8):2319-2358.

33. Gordon CM. New developments in catalysis using ionic liquids. *App Catal A Gen.* 2001;222:101-117.

34. Brennecke JF, Maginn EJ. Ionic liquids: Innovative fluids for chemical processing. *AIChE J.* Nov 2001;47(11):2384-2389.

35. Cull SG, Holbrey JD, Vargas-Mora V, Seddon KR, Lye GJ. Room-temperature ionic liquids as replacements for organic solvents in multiphase bioprocess operations. *Biotechnol Bioeng.* Jul 20 2000;69(2):227-233.

36. Lau RM, van Rantwijk F, Seddon KR, Sheldon RA. Lipase-catalyzed reactions in ionic liquids. *Org Lett.* Dec 28 2000;2(26):4189-4191.

37. Laszlo JA, Compton DL. alpha-chymotrypsin catalysis in imidazolium-based ionic liquids. *Biotechnol Bioeng.* Oct 20 2001;75(2):181-186.

38. Yang FX, Russell AJ. The role of hydration in enzyme activity and stability .1. Water adsorption by alcohol dehydrogenase in a continuous gas phase reactor. *Biotechnol Bioeng.* Mar 20 1996;49(6):700-708.

39. Yang FX, Russell AJ. The role of hydration in enzyme activity and stability .2. Alcohol dehydrogenase activity and stability in a continuous gas phase reactor. *Biotechnol Bioeng.* Mar 20 1996;49(6):709-716.

40. Yang F, Wild JR, Russell AJ. Nonaqueous biocatalytic degradation of a nerve gas mimic. *Biotechnol Prog.* 1995;11:471-474.

41. Dunn RV, Daniel RM. The use of gas-phase substrates to study enzyme catalysis at low hydration. *Philos Trans R Soc Lond B Biol Sci.* Aug 29 2004;359(1448):1309-1320.

42. LeJeune KE, Dravis BC, Yang F, Hetro AD, Doctor BP, Russell AJ. Fighting nerve agent chemical weapons with enzyme technology. *Ann N Y Acad Sci.* Dec 13 1998;864:153-170.

43. Hwang SO, Park YH. Gas phase ethyl acetate production in a batch bioreactor. *Bioprocess Engineering.* Jun 1997;17(1):51-54.

44. Fersht A. The pH-dependence of enzyme catalysis. *Structure and mechanism in protein science: a guide to enzyme catalysis and protein folding*. New York: Freeman; 1999:169-190.

45. Fersht A. Protein stability. *Structure and mechanism in protein science: a guide to enzyme catalysis and protein folding*. New York: Freeman; 1999:508-539.

46. Gaertner HF, Puigserver AJ. Increased activity and stability of poly(ethylene glycol)-modified trypsin. *Enzyme Microb Technol.* 1992;14:150-155.

47. Tyagi R, Gupta MN. Chemical modification and chemical crosslinking for enhancing thermostability of enzymes. In: Gupta MN, ed. *Thermostability of enzymes*. Berlin: Springer-Verlag; 1993:146-160.

48. Yang Z, Domach M, Auger R, Yang FX, Russell AJ. Polyethylene glycol-induced stabilization of subtilisin. *Enzyme Microb Technol.* 1996;18:82-89.

49. Yang F, Williams D, Russell AJ. Synthesis of protein-containing polymers in organic solvents. *Biotechnol Bioeng.* 1995;45:10-17.

50. Roberts MJ, Harris JM. Attachment of degradable poly(ethylene glycol) to proteins has the potential to increase therapeutic efficacy. *J Pharm Sci.* Nov 1998;87(11):1440-1445.

51. Sheffield WP. Modification of clearance of therapeutic and potentially therapeutic proteins. *Curr Drug Targets Cardiovasc Haematol Disord.* Jun 2001;1(1):1-22.

52. Caliceti P, Veronese FM. Pharmacokinetic and biodistribution properties of poly(ethylene glycol)-protein conjugates. *Adv Drug Deliv Rev.* Sep 26 2003;55(10):1261-1277.

53. Veronese FM, Pasut G. PEGylation, successful approach to drug delivery. *Drug Discov Today.* Nov 1 2005;10(21):1451-1458.

54. Vellard M. The enzyme as drug: application of enzymes as pharmaceuticals. *Curr Opin Biotechnol.* 2003;14:444-450.

55. Gray CJ. Stabilisation of enzymes with soluble additives. In: Gupta MN, ed. *Thermostability of enzymes*. Berlin: Springer-Verlag; 1993:124-143.

56. Xie GF, Timasheff SN. Mechanism of the stabilization of ribonuclease A by sorbitol: Preferential hydration is greater for the denatured than for the native protein. *Protein Sci.* Jan 1997;6(1):211-221.

57. Kaushik JK, Bhat R. Thermal stability of proteins in aqueous polyol solutions: Role of the surface tension of water in the stabilizing effect of polyols. *J Phys Chem B.* Sep 3 1998;102(36):7058-7066.

58. Fields PA, Wahlstrand BD, Somero GN. Intrinsic versus extrinsic stabilization of enzymes - The interaction of solutes and temperature on A(4)-lactate dehydrogenase orthologs from warm-adapted and cold-adapted marine fishes. *Euro J Biochem.* Aug 2001;268(16):4497-4505.

59. O'Fagain C. Enzyme stabilization - recent experimental progress. *Enzyme Microb Technol.* Aug 13 2003;33(2-3):137-149.

60. Bolen DW. Effects of naturally occurring osmolytes on protein stability and solubility: issues important in protein crystallization. *Methods.* Nov 2004;34(3):312-322.

61. Arakawa T, Timasheff SN. Mechanism of poly(ethylene glycol) interaction with proteins. *Biochemistry.* Nov 19 1985;24(24):6756-6762.

62. Hermanson GT. Functional targets. *Bioconjugate techniques*. San Diego: Academic Press; 1996:3-136.

63. Mattson G, Conklin E, Desai S, Nielander G, Savage MD, Morgensen S. A practical approach to crosslinking. *Mol Biol Rep.* Apr 1993;17(3):167-183.

64. Ertan H, Kazan D, Erarslan A. Cross-linked stabilization of Escherichia coli penicillin G acylase against pH by dextran-dialdehyde polymers. *Biotechnol Tech.* Apr 1997;11(4):225-229.

65. DeSantis G, Jones JB. Chemical modification of enzymes for enhanced functionality. *Curr Opin Biotechnol.* Aug 1999;10(4):324-330.

66. Lele BS, Russell AJ. Enhancing enzyme stability against TiO2-UV induced inactivation. *Biomacromolecules.* Jan-Feb 2005;6(1):475-482.

67. Cupo P, El-Deiry W, Whitney PL, Awad WM, Jr. Stabilization of proteins by guanidination. *J Biol Chem.* Nov 25 1980;255(22):10828-10833.

68. Turunen O, Vuorio M, Fenel F, Leisola M. Engineering of multiple arginines into the Ser/Thr surface of Trichoderma reesei endo-1,4-beta-xylanase II increases the thermotolerance and shifts the pH optimum towards alkaline pH. *Protein Eng.* Feb 2002;15(2):141-145.

69. Walsh S, Shah A, Mond J. Improved pharmacokinetics and reduced antibody reactivity of lysostaphin conjugated to polyethylene glycol. *Antimicrob Agents Chemother.* 2003;47(2):554-558.

70. Inada Y, Furukawa M, Sasaki H, Kodera Y, Hiroto M, Nishimura H, Matsushima A. Biomedical and biotechnological applications of PEG- and PM-modified proteins. *TIBTECH.* 1995;13:86-91.

71. Werle M, Bernkop-Schnurch A. Strategies to improve plasma half life time of peptide and protein drugs. *Amino Acids.* Jun 2006;30(4):351-367.

72. Maneepun S, Klibanov AM. Stabilization of microbial proteases against autolysis using acylation with dicarboxylic acid anhydrides. *Biotechnol Bioeng.* 1982;24:483-486.

73. Berberich JA, Yang LW, Madura J, Bahar I, Russell AJ. A stable three-enzyme creatinine biosensor. 1. Impact of structure, function and environment on PEGylated and immobilized sarcosine oxidase. *Acta Biomater.* 2005;1:173-181.

74. Siddiqui KS, Loviny-Anderton T, Rangarajan M, Hartley BS. Arthrobacter D-xylose isomerase: chemical modification of carboxy groups and protein engineering of pH optimum. *Biochem J.* Dec 15 1993;296 (Pt 3):685-691.

75. Yamashita H, Nakatani H, Tonomura B. Change of substrate specificity by chemical modification of lysine residues of porcine pancreatic alpha-amylase. *Biochim Biophys Acta.* Sep 3 1993;1202(1):129-134.

76. Klibanov AM. Immobilized enzymes and cells as practical catalysts. *Science.* 1983;219(4585):722-727.

77. Cabral JMS, Kennedy JF. Immobilization techniques for altering thermal stability of enzymes. In: Gupta MN, ed. *Thermostability of enzymes*. Berlin: Springer-Verlag; 1993:162-179.

78. Polizzi KM, Bommarius AS, Broering JM, Chaparro-Riggers JF. Stability of biocatalysts. *Curr Opin Chem Biol.* Apr 2007;11(2):220-225.

79. Zhao XS, Bao XY, Guo WP, Lee FY. Immobilizing catalysts on porous materials. *Materials Today.* Mar 2006;9(3):32-39.

80. LeJeune KE, Russell AJ. Covalent binding of a nerve agent hydrolyzing enzyme within polyurethane foams. *Biotechnol Bioeng.* Aug 20 1996;51(4):450-457.

81. Drevon GF, Danielmeier K, Federspiel W, Stolz DB, Wicks DA, Yu PC, Russell AJ. High-activity enzyme-polyurethane coatings. *Biotechnol Bioeng.* 2002;79(7):785-794.

82. Leatherbarrow RJ, Fersht AR. Protein engineering. *Protein Eng.* Oct-Nov 1986;1(1):7-16.

83. Shaw WV. Protein engineering. The design, synthesis and characterization of factitious proteins. *Biochem J.* Aug 15 1987;246(1):1-17.

84. Nosoh Y, Sekiguchi T. Protein enginerring for thermostabilization. In: Gupta MN, ed. *Thermostability of enzymes*. Berline: Springer-Verlag; 1993:183-203.

85. Eijsink VGH, Bjork A, Gaseidnes S, Sirevag R, Synstad B, van den Burg B, Vriend G. Rational engineering of enzyme stability. *J Biotechnol.* Sep 30 2004;113(1-3):105-120.

86. Fersht A. Protein engineering. *Structure and mechanism in protein science: a guide to enzyme catalysis and protein folding*. New York: Freeman; 1999:420-456.

87. Arnold FH. Design by directed evolution. *Acc Chem Res.* Mar 1998;31(3):125-131.

88. Arnold FH. Unnatural selection: molecular sex for fun and profit. *Eng Sci.* 1999;62(1&2):40-50.

89. Eijsink VG, Gaseidnes S, Borchert TV, van den Burg B. Directed evolution of enzyme stability. *Biomol Eng.* Jun 2005;22(1-3):21-30.

90. Otten LG, Quax WJ. Directed evolution: selecting today's biocatalysts. *Biomol Eng.* Jun 2005;22(1-3):1-9.

91. Chirumamilla RR, Muralidhar R, Marchant R, Nigam P. Improving the quality of industrially important enzymes by directed evolution. *Mol Cell Biochem.* 2001;224:159-168.

92. Bornscheuer UT, Pohl M. Improved biocatalysts by directed evolution and rational protein design. *Curr Opin Chem Biol.* 2001;5(2):137-143.

93. Holbrey JD, Seddon KR. Ionic liquids. *Clean Products and Processes.* 1999;1:223-236.

94. Lozano P, De Diego T, Carrie D, Vaultier M, Iborra JL. Over-stabilization of Candida antarctica lipase B by ionic liquids in ester synthesis. *Biotechnol Lett.* Sep 2001;23(18):1529-1533.

95. Kaftzik N, Wasserscheid P, Kragl U. Use of ionic liquids to increase the yield and enzyme stability in the beta-galactosidase catalysed synthesis of N-acetyllactosamine. *Org Process Res Dev A.* Jul-Aug 2002;6(4):553-557.

96. Eckstein M, Sesing M, Kragl U, Adlercreutz P. At low water activity alpha-chymotrypsin is more active in an ionic liquid than in non-ionic organic solvents. *Biotechnol Lett.* Jun 2002;24(11):867-872.

97. Leo A, Hansch C, Elkins D. Partition coefficients and their uses. *Chem Rev.* 1971;71(6):525-616.

98. Anthony JL, Maginn EJ, Brennecke JF. Solution thermodynamics of imidazolium-based ionic liquids and water. *J Phys Chem B.* 2001;105(44):10942-10949.

99. Fletcher KA, Storey IA, Hendricks AE, Pandey S, Pandey S. Behavior of the solvatochromic probes Reichardt's dye, pyrene, dansylamide, Nile Red and 1-pyrenecarbaldehyde within the room-temperature ionic liquid bmimPF6. *Green Chem.* Oct 2001;3(5):210-215.

100. Drevon GF, Hartleib J, Scharff E, Ruterjans H, Russell AJ. Thermoinactivation of diisopropylfluorophosphatase-containing polyurethane polymers. *Biomacromolecules.* Fal 2001;2(3):664-671.

101. Cedergren A. Reaction rates between water and Karl Fischer reagent. *Talanta.* 1974;21(4):265-271.

102. Kamat S, Critchley G, Beckman EJ, Russell AJ. Biocatalytic Synthesis of Acrylates in Organic-Solvents and Supercritical Fluids .3. Does Carbon-Dioxide Covalently Modify Enzymes. *Biotechnol Bioeng.* Jun 20 1995;46(6):610-620.

103. Pogorevc M, Stecher H, Faber K. A caveat for the use of log P values for the assessment of the biocompatibility of organic solvents. *Biotechnol Lett.* Jun 2002;24(11):857-860.

104. Huddleston JG, Willauer HD, Swatloski RP, Visser AE, Rogers RD. Room temperature ionic liquids as novel media for 'clean' liquid-liquid extraction. *Chem Commun.* Aug 21 1998(16):1765-1766.

105. Muldoon MJ, Gordon CM, Dunkin IR. Investigations of solvent-solute interactions in room temperature ionic liquids using solvatochromic dyes. *J Chem Soc Perkin Trans.* Apr 2001(4):433-435.

106. Baker SN, Baker GA, Bright FV. Temperature-dependent microscopic solvent properties of 'dry' and 'wet' 1-butyl-3-methylimidazolium hexafluorophosphate: correlation with ET(30) and Kamlet-Taft polarity scales. *Green Chem.* 2002;4(2):165-169.

107. Aki SNVK, Brennecke JF, Samanta A. How polar are room-temperature ionic liquids? *Chem Commun.* 2001(5):413-414.

108. Dzyuba SV, Bartsch RA. Expanding the polarity range of ionic liquids. *Tetrahedron Lett.* Jun 24 2002;43(26):4657-4659.

109. Carmichael AJ, Seddon KR. Polarity study of some 1-alkyl-3-methylimidazolium ambient-temperature ionic liquids with the solvatochromic dye, Nile Red. *J Phys Org Chem.* Oct 2000;13(10):591-595.

110. Sheldon RA, Lau RM, Sorgedrager MJ, van Rantwijk F, Seddon KR. Biocatalysis in ionic liquids. *Green Chem.* 2002;4(2):147-151.

111. Arroyo M, Sanchez-Montero JM, Sinisterra JV. Thermal stabilization of immobilized lipase B from Candida antarctica on different supports: Effect of water activity on enzymatic activity in organic media. *Enzyme Microb Technol.* Jan-Feb 1999;24(1-2):3-12.

112. Inada Y, Takahashi K, Yoshimoto T, Ajima A, Matsushima A, Saito Y. Application of polyethylene glycol-modified enzymes in biotechnological processes: organic solvent-soluble enzymes. *Trends Biotechnol.* 1986;4:190-194.

113. Drevon GF, Russell AJ. Irreversible immobilization of diisopropylfluorophosphatase in polyurethane polymers. *Biomacromolecules.* Win 2000;1(4):571-576.

114. Eckstein M, Wasserscheid P, Kragl U. Enhanced enantioselectivity of lipase from Pseudomonas sp at high temperatures and fixed water activity in the ionic liquid, 1-butyl-3-methylimidazolium bis[(trifluoromethyl)sulfonyl]amide. *Biotechnol Lett.* May 2002;24(10):763-767.

115. Chamouleau F, Coulon D, Girardin M, Ghoul M. Influence of water activity and water content on sugar esters lipase-catalyzed synthesis in organic media. *J Mol Cat B: Enzym.* Jan 22 2001;11(4-6):949-954.

116. Grimsley JK, Rastogi VK, Wild JR. Biological detoxification of organophosphorous neurotoxins. In: Sikdar SK, LIrvine RL, eds. *Bioremediation: Principles and Practice*. Lancaster, PA: Technomic Publ; 1999.

117. Di Sioudi BD, Miller CE, Lai K, Grimsley JK, Wild JR. Rational design of organophosphorus hydrolase for altered substrate specificities. *Chem Biol Interact.* May 14 1999;119-120:211-223.

118. DeFrank JJ. Organophosphorus cholinesterase inhibitors: detoxification by microbial enzymes. In: Kelly JW, Baldwin TO, eds. *Applications of Enzyme Biotechnology*. New York: Plenum Press; 1991:165-180.

119. Di Sioudi BD, Grimsley JK, Lai K, Wild JR. Modification of near active site residues in organophosphorus hydrolase reduces metal stoichiometry and alters substrate specificity. *Biochemistry.* 1999;38:2866-2872.

120. Russell AJ, Berberich JA, Drevon GF, Koepsel RR. Biomaterials for mediation of chemical and biological warfare agents. *Annu Rev Biomed Eng.* 2003;5:1-27.

121. Cheng TC, Calomiris JJ. A cloned bacterial enzyme for nerve agent decontamination. *Enzyme Microb Technol.* Jun 1996;18(8):597-601.

122. Zhang Y, Autenrieth RL, Bonner JS, Harvey SP, Wild JR. Biodegradation of neutralized sarin. *Biotechnol Bioeng.* 1999;64:221-231.

123. McKone TE, Huey BM, Downing E, Duffy LM. *Strategies to Protect the Health of Deployed U.S. Forces: Detecting, Characterizing, and Documenting Exposures*. Washington, D.C.: Nat Acad Press; 2000.

124. Gestrelius S, Mattiasson B, Mosbach K. Studies on pH-activity profiles of an immobilized two-enzyme system. *Biochim Biophys Acta.* Aug 28 1972;276(2):339-343.

125. Qin Y, Cabral JM. Kinetic studies of the urease-catalyzed hydrolysis of urea in a buffer-free system. *Appl Biochem Biotechnol.* Dec 1994;49(3):217-240.

126. Mobley HL, Island MD, Hausinger RP. Molecular biology of microbial ureases. *Microbiol Rev.* Sep 1995;59(3):451-480.

127. Ciurli S, Benini S, Rypniewski WR, Wilson KS, Miletti S, Mangani S. Structural properties of the nickel ions in urease: novel insights into the catalytic and inhibition mechanisms. *Coord Chem Rev.* Sep 1999;192:331-355.

128. Krajewska B, Chudy M, Drozdek M, Brzozka Z. Potentiometric study of urease kinetics over pH 5.36-8.21. *Electroanal.* 2003;15(5-6):460-466.

129. Sanyo H, Noriko S. Inclusion effects of cyclomaltohexa- and heptose (a- and b-cyclodextrins) on the acidities of several phenol derivatives. *Carbohydr Res.* 1997;304:229-238.

130. Galkin VI, Sayakhov RD, Garifzyanov AR, Cherkasov RA, Pudivok AN. Laws governing the dissociation of dialkylphosphoric, -phosphonic and -phosphinic acids in water and in aqueous ethanol. *Dokl Chem Eng Transl En.* 1991;318:114-116.

131. Landis WG, DeFrank JJ. Enzymatic hydrolysis of toxic organofluorophosphate compounds. *Adv Appl Biotechnol Ser.* 1990;4:183-201.

132. Dixon NE, Blakeley RL, Zerner B. Jack bean urease (EC 3.5.1.5). III. The involvement of active-site nickel ion in inhibition by beta-mercaptoethanol, phosphoramidate, and fluoride. *Can J Biochem.* Jun 1980;58(6):481-488.

133. Todd MJ, Hausinger RP. Fluoride inhibition of Klebsiella aerogenes urease: mechanistic implications of a pseudo-uncompetitive, slow-binding inhibitor. *Biochemistry.* May 9 2000;39(18):5389-5396.

134. Krajewska B, Zaborska W, Leszko M. Inhibition of chitosan-immobilized urease by slow-binding inhibitors: Ni2+, F- and acetohydroxamic acid. *J Mol Cat B: Enzym.* Jul 6 2001;14(4-6):101-109.

135. Saboury AA, Moosavi-Movahedi AA. A simple novel method for determination of an inhibition constant by isothermal titration microcalorimetry. The effect of fluoride ion on urease. *J Enzyme Inhib.* 1997;12:273-279.

136. Bauerfeind P, Garner R, Dunn BE, Mobley HLT. Synthesis and activity of Helicobacter pylori urease and catalase at low pH. *Gut.* 1997;40(1):25-30.

137. Weeks DL, Eskandari S, Scott DR, Sachs G. A H+-gated urea channel: The link between Helicobacter pylori urease and gastric colonization. *Science.* Jan 21 2000;287(5452):482-485.

138. Dunn BE, Grutter MG. Helicobacter pylori springs another surprise. *Nat Struct Biol.* Jun 2001;8(6):480-482.

139. Ha NC, Oh ST, Sung JY, Cha KA, Lee MH, Oh BH. Supramolecular assembly and acid resistance of Helicobacter pylori urease. *Nat Struct Biol.* Jun 2001;8(6):505-509.

140. Hong W, Sano K, Morimatsu S, Scott DR, Weeks DL, Sachs G, Goto T, Mohan S, Harada F, Nakajima N, Nakano T. Medium pH-dependent redistribution of the urease of Helicobacter pylori. *J Med Microbiol.* Mar 2003;52(3):211-216.

141. Tanaka T, Kawase M, Tani S. alpha-hydroxyketones as inhibitors of urease. *Bioorg Med Chem.* Jan 15 2004;12(2):501-505.

142. Lee MH, Mulrooney SB, Hausinger RP. Purification, characterization, and in vivo reconstitution of Klebsiella aerogenes urease apoenzyme. *J Bacteriol.* Aug 1990;172(8):4427-4431.

143. Alagna L, Hasnain S, Piggott B, Williams DJ. The nickel ion environment in jack bean urease. *Biochem* 1984;220:591-595.

144. Yang M, Hashimoto T, Hoshi N, Myoga H. Fluoride removal in a fixed bed packed with granular calcite. *Wat Res.* 1999;33(16):3395-3402.

145. Carney SA, Hall M, Lawrence JC, Ricketts CR. Rationale of the treatment of hydrofluoric acid burns. *Br J Ind Med.* 1974;31:317-321.

146. Greco RJ, Hartford CE, Haith LR, Patton ML. Hydrofluoric acid-induced hypocalcemia. *j Trauma.* 1988;28(11):1593-1596.

147. Heard K, Hill RE, Cairns CB, Dart RC. Calcium neutralizes fluoride bioavailabilty in a lethal model of fluoride poisoning. *Clin Toxicol.* 2001;39(4):349-353.

148. Bruckenstein S. Process for purifying waste water containing fluoride ion. US patent 4145282, 1979.

149. Harrison JP. Process for calcium fluoride production from industrial waste waters. US patent 4414185, 1983.

150. Dean JA. *Lange's Handbook of Chemistry*. 15th edition ed. New York: McGraw-Hill; 1999.

151. Cristalli G, Costanzi S, Lambertucci C, Lupidi G, Vittori S, Volpini R, Camaioni E. Adenosine deaminase: functional implications and different classes of inhibitors. *Med Res Rev.* 2001;21(2):105-128.

152. Kinoshita T, Nakanishi I, Terasaka T, Kuno M, Seki N, Warizaya M, Matsumura H, Inoue T, Takano K, Adachi H, Mori Y, Fujii T. Structural basis of compound recognition by adenosine deaminase. *Biochemistry.* 2005;44:10562-10569.

153. Li Y, Cummins J, Huard J. Muscle injury and repair. *Curr Opin Orthop.* 2001;12(5):409-415.

154. Huard J, Li Y, Fu FH. Muscle injuries and repair: current trends in research. *J Bone Joint Surg Am.* May 2002;84-A(5):822-832.

155. Sato K, Li Y, Foster W, Fukushima K, Badlani N, Adachi N, Usas A, Fu FH, Huard J. Improvement of muscle healing through enhancement of muscle regeneration and prevention of fibrosis. *Muscle Nerve.* Sep 2003;28(3):365-372.

156. Lehto M, Duance VC, Restall D. Collagen and fibronectin in a healing skeletal muscle injury. An immunohistological study of the effects of physical activity on the repair of injured gastrocnemius muscle in the rat. *J Bone Joint Surg Br.* Nov 1985;67(5):820-828.

157. Hurme T, Kalimo H, Sandberg M, Lehto M, Vuorio E. Localization of type I and III collagen and fibronectin production in injured gastrocnemius muscle. *Lab Invest.* Jan 1991;64(1):76-84.

158. Kaariainen M, Jarvinen T, Jarvinen M, Rantanen J, Kalimo H. Relation between myofibers and connective tissue during muscle injury repair. *Scand J Med Sci Sports.* Dec 2000;10(6):332-337.

159. Jarvinen TA, Jarvinen TL, Kaariainen M, Kalimo H, Jarvinen M. Muscle injuries: biology and treatment. *Am J Sports Med.* May 2005;33(5):745-764.

160. Taylor DC, Dalton JD, Jr., Seaber AV, Garrett WE, Jr. Experimental muscle strain injury. Early functional and structural deficits and the increased risk for reinjury. *Am J Sports Med.* Mar-Apr 1993;21(2):190-194.

161. Menetrey J, Kasemkijwattana C, Day CS, Bosch P, Vogt M, Fu FH, Moreland MS, Huard J. Growth factors improve muscle healing in vivo. *J Bone Joint Surg Br.* Jan 2000;82(1):131-137.

162. Kurek J, Bower J, Romanella M, Austin L. Leukaemia inhibitory factor treatment stimulates muscle regeneration in the mdx mouse. *Neurosci Lett.* Jul 19 1996;212(3):167-170.

163. White JD, Bower JJ, Kurek JB, Austin L. Leukemia inhibitory factor enhances regeneration in skeletal muscles after myoblast transplantation. *Muscle Nerve.* May 2001;24(5):695-697.

164. Fukushima K, Badlani N, Usas A, Riano F, Fu F, Huard J. The use of an antifibrosis agent to improve muscle recovery after laceration. *Am J Sports Med.* Jul-Aug 2001;29(4):394-402.

165. Foster W, Li Y, Usas A, Somogyi G, Huard J. Gamma interferon as an antifibrosis agent in skeletal muscle. *J Orthop Res.* Sep 2003;21(5):798-804.

166. Chan YS, Li Y, Foster W, Fu FH, Huard J. The use of suramin, an antifibrotic agent, to improve muscle recovery after strain injury. *Am J Sports Med.* Jan 2005;33(1):43-51.

167. Chan YS, Li Y, Foster W, Horaguchi T, Somogyi G, Fu FH, Huard J. Antifibrotic effects of suramin in injured skeletal muscle after laceration. *J Appl Physiol.* 2003;95(2):771-780.

168. Huard J, Li Y, Peng H, Fu FH. Gene therapy and tissue engineering for sports medicine. *J Gene Med.* Feb 2003;5(2):93-108.

169. Dioszegi M, Cannon P, Van Wart HE. Vertebrate collagenases. *Methods Enzymol.* 1995;248:413-431.

170. Visse R, Nagase H. Matrix metalloproteinases and tissue inhibitors of metalloproteinases - Structure, function, and biochemistry. *Circ Res.* 2003;92(8):827-839.

171. Pardo A, Selman M. MMP-1: the elder of the family. *Int J Biochem Cell Biol.* 2005;37(2):283-288.

172. Yong VW. Metalloproteinases: mediators of pathology and regeneration in the CNS. *Nat Rev Neurosci.* 2005;6(12):931-944.

173. Gross J, Lapiere CM. Collagenolytic activity in amphibian tissues: a tissue culture assay. *Proc Natl Acad Sci U S A.* Jun 15 1962;48:1014-1022.

174. Evanson JM, Jeffrey JJ, Krane SM. Human collagenase: identification and characterization of an enzyme from rheumatoid synovium in culture. *Science.* Oct 27 1967;158(800):499-502.

175. Iimuro Y, Nishio T, Morimoto T, Nitta T, Stefanovic B, Choi SK, Brenner DA, Yamaoka Y. Delivery of matrix metalloproteinase-1 attenuates established liver fibrosis in the rate. *Gastroenterology.* 2003;124:445-458.

176. Bedair H, Liu TT, Kaar JL, Badlani N, Russell AJ, Li Y, Huard J. Matrix metalloproteinase-1 therapy improve muscle healing. *J Appl Physiol.* 2007;102:2338-2345.

177. Menetrey J, Kasemkijwattana C, Fu FH, Moreland MS, Huard J. Suturing versus immobilization of a muscle laceration. A morphological and functional study in a mouse model. *Am J sports Med.* 1999;27(2):222-229.

178. Guex N, Peitsch MC. SWISS-MODEL and the Swiss-PdbViewer: an environment for comparative protein modeling. *Electrophoresis.* Dec 1997;18(15):2714-2723.

179. Iyer S, Visse R, Nagase H, Acharya KR. Crystal structure of an active form of human MMP-1. *J Mol Biol.* Sep 8 2006;362(1):78-88.

180. Gordon JC, Myers JB, Folta T, Shoja V, Heath LS, Onufriev A. H++: a server for estimating pKas and adding missing hydrogens to macromolecules. *Nucleic Acids Res.* Jul 1 2005;33(Web Server issue):W368-371.

181. Kossakowska A, Edwards DR, Lee SS, Urbanski LS, Stabbler AL, Zhang CL, Phillips BW, Zhang Y, Urbanski SJ. Altered balance between matrix metalloproteinases and their inhibitors in experimental biliary fibrosis. *Am J Pathol.* 1998;153(6):1895-1902.

182. Iredale JP. Models of liver fibrosis: exploring the dynamic nature of inflammation and repair in a solid organ. *J Clin Invest.* 2007;117(3):539-548.

183. Glocker MO, Borchers C, Fiedler W, Suckau D, Przybylski M. Molecular characterization of surface topology in protein tertiary structures by amino-acylation and mass spectrometric peptide mapping. *Bioconjugate Chem.* 1994;5:583-590.

184. Scaloni A, Ferranti P, Simone GD, Mamone G, Sannolo N, Malorni A. Probing the reactivity of nucleophilie residues in human 2,3-diphosphoglycerate/deoxy-hemoglobin complex by aspecific chemical modifications. *FEBS.* 1999;452:190-194.

185. O'Brien AM, O'Fagain C, Nielsen PR, Welinder KG. Location of crosslinks in chemically stabilized horseraish peroxidase: implications for design of crosslinks. *Biotechnol Bioeng.* 2001;76:277-284.

186. Murphy G, Allan JA, Willenbrock F, Cockett MI, O'Connell JP, Docherty AJP. The role of the C-terminal domain in collagenase and stromelysin specificity. *J Biol Chem.* 1992;267:9612-9618.

187. Gomis-Ruth FX, Gohlke U, Betz M, Knauper V, Murphy G, Lopez-Otin C, Bode W. The helping hand of collagenase-3 (MMP-13): 2.7 A crystal structure of its C-terminal haemopexin-like domain. *J Mol Biol.* 1996;264(3):556-566.

188. Murphy G, Knauper V. Relating matrix metalloproteinase structure to function: why the "hemopexin" domain? *Matrix Biol.* 1997;15(8-9):511-518.

189. Jozic D, Bourenkov G, Lim NH, Visse R, Nagase H, Bode W, Maskos K. X-ray structure of human proMMP-1: new insights into procollagenase activation and collagen binding. *J Biol Chem.* 2005;280(10):9578-9585.

190. McGoff P, Baziotis AC, Maskiewicz R. Analysis of polyethylene glycol modified superoxide dismutase by chromatographic, electrophoretic, light scattering, chemical and enzymatic methods. *Chem Pharm Bull.* 1988;36(8):3079-3091.

191. Kurfurst MM. Detection and Molecular-Weight Determination of Polyethylene Glycol-Modified Hirudin by Staining after Sodium Dodecyl-Sulfate Polyacrylamide-Gel Electrophoresis. *Anal Biochem.* Feb 1 1992;200(2):244-248.

192. Lebowitz J, Lewis MS, Schuck P. Modern analytical ultracentrifugation in protein science: a tutorial review. *Protein Sci.* 2002;11:2067-2079.